Upgrade and Design of Coastal Structures Exposed to Climate Changes

Upgrade and Design of Coastal Structures Exposed to Climate Changes

Revised Version

PhD Thesis
Defended in public at Aalborg University
September 23, 2013

Jørgen Quvang Harck Nørgaard

Department of Civil Engineering,
The Faculty of Engineering and Science,
Aalborg University, Aalborg, Denmark

River Publishers
Aalborg

ISBN 978-87-93102-51-4 (e-book)

Published, sold and distributed by:
River Publishers
Niels Jernes Vej 10
9220 Aalborg Ø
Denmark

Tel.: +45369953197
www.riverpublishers.com

Contents

Chapter 1: ***Introduction and Background to Thesis***
1.1 General Introduction 14
1.2 Climate Change Predictions 14
1.2.1 Influence from Climate Changes on Global SWL 14
1.2.2 Influence from Climate Changes on Future Regional Extreme Events 16
1.3 Strategies for Protection of Coasts against Climate Changes 16
1.4 Focus of the Study 17
1.5 Thesis Outline 17

Part 1: Evaluation and Modification of Existing Tools for Design of Coastal Structures in Deep and Shallow-Water Wave Conditions

Chapter 2: ***Distribution of Wave Heights and Wave Run-Up Levels in Shallow-Water Wave Conditions***
2.1 Transformation of Waves in Shallow Water 22
2.2 Existing Wave Height Distributions in Deep and Shallow-Water Conditions 23
2.2.1 Rayleigh-distribution 23
2.2.2 Glukhovskii-distribution 23
2.2.3 Battjes & Groenendijk-distribution 24
2.2.4 Modified Battjes & Groenendijk-distribution 24
2.2.5 Goda Breaker Index Method 25
2.3 Influence from Wave Height, Wave Period, and Bed Slope on Low Exceedance Wave Heights 25
2.4 Evaluation of State-of-the-art Wave Height Distributions against New Model Tests 26
2.5 Existing Wave Run-Up Formulae 28
2.6 Extension of Deep-Water Wave Run-Up Formulae to Shallow-Water Wave Conditions 29
2.7 Scale and Model Effects on Wave Run-Up Levels in Small Scale Model Tests 30
2.8 Summary of Findings in Chapter 30

Chapter 3: ***Wave Loads on Crown Walls***
3.1 Stability of Crown Walls 34
3.1.1 New Tests 34
3.2 Evaluation of Existing Formulae for Horizontal Wave Loads 35
3.3 New Formulae for Wave Loads on Crown Walls in Shallow-Water Wave Conditions 35
3.4 Correlation between Horizontal and Vertical Loads 37
3.5 Structural Response of Crown Walls Subjected to Impulsive Wave Loading 38
3.6 Summary of Findings in Chapter 40

Chapter 4: ***Single Wave Overtopping Volumes on Rubble Mound Breakwater Crown Walls***
4.1 Wave Overtopping on Rubble Mound Breakwaters in Deep and Shallow-Water Wave Conditions 44
4.2 Average Overtopping Discharge in Deep and Shallow-Water Wave Conditions 44
4.3 Number of Overtopping Waves on Rubble Mound Breakwaters in Deep and Shallow-Water Wave Conditions 45
4.3.1 New Correction Factor 45
4.4 Individual Wave Overtopping Volumes on Rubble Mound Breakwaters in Deep and Shallow-Water Wave Conditions 46
4.4.1 New Shape Factor 47
4.5 Summary of Findings in Chapter 48

Chapter 5: ***Overtopping Flow Parameters on Sea Dikes***
5.1 Overtopping Flow Parameters on Sea Dikes 50
5.2 Existing Knowledge on Influence from Oblique and Short Crested Waves on Sea Dikes in 3-D 50
5.3 Existing Knowledge on Overtopping Flow Parameters in 2-D 51
5.4 New Investigations on Overtopping Flow on Sea Dikes in Oblique and Short-Crested Waves 52
5.4.1 New Measurement Procedure for Flow Velocities on Sea Dike Crests in Oblique and Short Crested Waves 52
5.4.2 New Investigations on Overtopping Flow Directions on Dike Crest in Oblique and Short Crested Waves 53
5.4.3 New Suggested Reduction Factor for Flow Parameters in Oblique and Short-Crested Waves 53
5.4.4 New Investigations on Distribution of Individual Flow Parameters in Oblique and Short Crested Waves 54
5.5 Summary of Findings in Chapter 56

Part 2: Case Studies

Chapter 6: *Dike Case Study*
6.1 Resilience of Sea Dikes against Wave Overtopping and Experience from In-Situ Tests 60
6.2 Case Example on Influence from Oblique and Short-Crested Waves and SWL-rise on Flow Parameters 61
6.2.1 Influence from Oblique and Short-Crested Waves on Flow Parameters 62
6.2.2 Influence from SWL-rise on Flow Parameters 62
6.3 Summary of Findings in Chapter 63

Chapter 7: *Rubble Mound Breakwater Case Study*
7.1 Design of Rubble Mound Breakwaters 66
7.2 Deep and Shallow Water Examples 66
7.3 Stability of Armor Layer in Deep and Shallow Water-Wave Conditions 66
7.4 Wave Overtopping on Rubble Mound Breakwaters in Deep and Shallow-Water Wave Conditions 67
7.5 Wave Loads on Crown Walls in Deep and Shallow Water Wave Conditions 68
7.6 Summary of Findings in Chapter 69

Chapter 8: *Dampening of Waves by Wave Energy Converters*
8.1 Wave Energy Converters for Coastal Protection 72
8.2 Existing Studies on Wave Height Reduction behind WECs 72
8.3 Present Study on Use of WECs for Coastal Protection 73
8.3.1 Wave Dragon Device 73
8.3.2 Physical Investigation of Wave Transmission from Wave Dragon Devices 73
8.3.3 Calibration of Numerical Wave Propagation Model 74
8.3.4 Single and Multiple Device Transmission 75
8.3.5 Case Application using Calibrated Numerical Model 76
8.4 Summary of Findings in Chapter 79

Chapter 9: *Dampening of Storm Surges and Improvement of Water Exchange by Barrier*
9.1 Multipurpose Storm Surge Barriers 82
9.2 Case Application of Storm Surge Barrier for Flood Protection and Improvement of Water Exchange in the Limfjord 82
9.3 Summary of Findings in Chapter 86

Part 3: Conclusions

Chapter 10: *Conclusions and Discussion*
10.1 General Findings in Thesis 90
10.1.1 Wave Actions on Rubble Mound Breakwaters with Crown Walls in Deep and Shallow-Water Wave Conditions 90
10.1.2 Influence from Realistic Three-Dimensional Waves on Overtopping Flow Parameters on Sea Dikes 91
10.1.3 Innovative Multipurpose Structures for Coastal Protection 91
10.1.4 Specific Finding in Papers 92
10.2 Discussion of Findings in Thesis 93
10.3 Recommendations for Supplementary Studies 93

Bibliography 95

Summary in English

This thesis *"Upgrade and Design of Coastal Structures Exposed to Climate Changes"* evaluates the performance of existing types of structures when exposed to climate changes. This includes also the potential of using cost-sharing multipurpose structures for protection against the effects of future climate changes.

The thesis consists of three parts. The first part evaluates the performance of existing design formulae for estimation of wave actions on structures, especially in shallow water since these structures are most vulnerable to the rising sea water levels caused by climate changes. Existing design formulae for estimation of wave loads and single overtopping wave volumes on rubble mound breakwater crown walls are considered too conservative in cases with shallow-water wave conditions where highest waves are limited by depth. The formulae are thus modified to include the effects of non-Rayleigh distributed wave heights. Additionally, an extension of existing formulae for estimation of wave overtopping flow parameters on sea dikes is performed to include the effects of oblique and short-crested waves. The general outcome of the first part of the thesis are tools for design of selected types of coastal protection structures, which are extended to a wider range of wave conditions, and which can be used to more accurately estimate the influence from climate changes.

In the second part of the thesis, the extended and modified formulae are used in case studies to evaluate the influence from climate changes on a typical sea dike structure and typical rubble mound breakwaters positioned in deep and shallow waters. Additionally, two case examples are evaluated on the use of cost-sharing multipurpose structures for coastal protection. The first case example evaluates the potential of using wave energy converters for coastal protection in Santander, Spain. The second case example evaluates the potential of using a barrier for protection against storm surges and for improvement of water exchange in the Limfjord, Denmark.

The third and last part summarizes and discusses the conclusions in the thesis. Moreover, it gives suggestions for future complementary work. The conclusions provide an overview of some of the most important topics in relation to design of coastal protection structures in deep and shallow water and in relation to evaluation of impact from climate changes. Additionally, the conclusion presents an evaluation of the use of new types of innovative multipurpose structures for coastal protection against future climate changes.

Dansk resume

Denne PhD-afhandling *"Opgradering og design af kystbeskyttelseskonstruktioner udsat for klimaændringer"* evaluerer indflydelsen fra klimaændringer på udvalgte typer af kystbeskyttelses-konstruktioner på dybt og lavt vand. Dette inkluderer desuden en analyse af muligheden for brug af innovative multifunktionskonstruktioner til beskyttelse af kyster mod klimaændringer.

Afhandlingen er opdelt i tre overordnede dele. I den første del evalueres brugen af eksisterende designformler til vurdering af bølgelaster og bølgeoverskyld på kystbeskyttelseskonstruktioner specielt på lavt vand, da disse er særligt udsatte for påvirkning af klimaændringer. Eksisterende designformler som oprindeligt er baserede på bølger på dybt vand giver konservative estimater på f.eks. bølgelaster på konstruktioner på lavt vand. Derfor er formlerne i denne afhandling modificeret, således at de også inkluderer effekterne fra bølgebrydning på lavt vand. Herudover er eksisterende formler til estimering af flowparametre fra bølgeoverskyld på diger modificeret således at de ud over vinkelrette langkammede bølger også inkluderer effekterne fra mere realistiske skråt-indkomne og kortkammede bølger. Produktet af den første del af afhandlingen er designformler som er mere generelt anvendelige i et bredere spektrum af bølgeforhold og som kan give mere præcise estimater på indflydelse fra klimaændringer på udvalgte typer af kystbeskyttelseskonstruktioner.

I den anden del af afhandlingen benyttes de modificerede formler i udvalgte casestudier til at evaluere indflydelsen fra skråt-indkomne kortkammede bølger og klimaændringer på et typisk dige samt til at evaluere indflydelsen fra klimaændringer på typiske stenkastningsmoler på dybt og lavt vand. Herudover er der konstrueret to case-eksempler til evaluering af brugen af multifunktionskonstruktioner til kystbeskyttelse. I det første eksempel benyttes såkaldte Wave Dragon bølgeenergimaskiner til dæmning af bølger i Santander, Spanien. I det andet eksempel benyttes en barriere til beskyttelse mod stormfloder samt forøgelse af vandgennemstrømning i Limfjorden, Danmark.

I den tredje og sidste del af afhandlingen opsamles konklusioner fra de forskellige kapitler og der gives anbefalinger til fremtidige studier. Konklusionerne i afhandlingen belyser nogle af de vigtige forhold der skal tages hensyn til ved evaluering af indflydelse fra klimaændringer på kystbeskyttelseskonstruktioner på dybt og lavt vand. Herudover belyses nye muligheder for at benytte nye innovative typer af konstruktioner til beskyttelse af kyster mod klimaændringer.

List of abbreviations

2-D	Two-dimensional
3-D	Three-dimensional
AAU	Aalborg University
AR4	Fourth Assessment Report
Calc.	Calculated
Dist.	Distance
Geom.	Geometry
IPCC	Intergovernmental Panel on Climate Change
JONSWAP	Joint North Sea Wave Observation Project
Meas.	Measured
Mod.	Modified
Sim.	Simulated
SRES	Special Report on Emissions Scenarios
SWL	Sea Water Level
Tot.	Total
Triang.	Triangular
WAB	Wave Activated Bodies
WD	Wave Dragon
WEC	Wave Energy Converter
WT	Work Task

List of appended papers

The thesis is presented as a collection of nine research-papers, which are summarized in this thesis introduction. The papers are not included in this summary due to copyright agreements but the most important findings from the papers are summarized in this document with references to the papers (referred to as paper 1, 2, 3, etc.).

Thesis title: *Upgrade and Design of Coastal Structures Exposed to Climate Changes*
Name of PhD student: Jørgen Quvang Harck Nørgaard
Supervisor: Thomas Lykke Andersen

List of papers:

Paper 1: Nørgaard, J. H., Lykke Andersen, T., & Kofoed, J. P. (2011). *"Wave Dragon Wave Energy Converters Used as Coastal Protection".* Proceedings of the sixth Coastal Structures Conference, 2011, Yokohama, Japan.

Paper 2: Nørgaard, J. H., & Lykke Andersen, T. (2012). *"Investigation of Wave Transmission from a Floating Wave Dragon Wave Energy Converter"*. Proceedings of the Twenty-second International Offshore and Polar Engineering Conference (ISOPE), p. 509-516, Rhodes, Greece. June 17–22, 2012.

Paper 3: Nørgaard, J. Q. H., & Lykke Andersen, T. (2013). *"Investigation of Wave Height Reduction behind the Wave Dragon Wave Energy Converters and Application in Santander, Spain"*. To be submitted to a conference.

Paper 4: Nørgaard, J. Q. H., Bentzen T. R, Larsen, T., Lykke Andersen, T., & Kvejborg, S. (2013). *Influence of Closing Storm Surge Barrier on Extreme Water Levels and Water Exchange; The Limfjord, Denmark"*. In review in Coastal Engineering Journal (World Scientific).

Paper 5: Nørgaard, J. Q. H., Lykke Andersen, T., Burcharth, H. F., & Steendam, G. J. (2013). *"Analysis of Overtopping Flow on Sea Dikes in Oblique and Short-Crested Waves".* Coastal Engineering (Elseveir) Vol. 76, 2013, p. 43-54, http://dx.doi.org/10.1016/j.coastaleng.2013.01.012

Paper 6: Lykke Andersen, T., Nørgaard, J. H., & Burcharth, H. F. (2011). *"A Least Square Method for Determination of Front Velocities in Run-Up Events on Dikes in Oblique and Short-Crested Waves".* Proceedings of the sixth Coastal Structures Conference, Yokohama, Japan, 2011.

Paper 7: Nørgaard, J. Q. H., Lykke Andersen, T., & Burcharth, H. F. (2014). *"Distribution of individual wave overtopping volumes in shallow water wave conditions".* Coastal Engineering (Elseveir) Vol. 83, January 2014, Pages 15–23, ISSN 0378-3839, http://dx.doi.org/10.1016/j.coastaleng.2013.09.003.

Paper 8: Nørgaard, J. Q. H., Lykke Andersen, T., & Burcharth, H. F. (2013). *"Wave Loads on Rubble Mound Breakwater Crown Walls in Deep and Shallow-water wave Conditions".* , Coastal Engineering, Volume 80, October 2013, Pages 137-147, ISSN 0378-3839, http://dx.doi.org/10.1016/j.coastaleng.2013.06.003.

Paper 9: Nørgaard, J. Q. H., Andersen, L. V., Lykke Andersen, T., & Burcharth, H. F. (2012). *"Displacement of Monolithic Rubble-Mound Breakwater Crown-Walls".* Proceedings of the Thirty-third International Conference on Coastal Engineering (ICCE), Santander, Spain, July 1-6, 2012.

Other relevant publications to the thesis (project reports and research papers), which are made during the same period but are not included in appendix, are:

Andersen, T. L., Martinelli, L., Zanuttigh, B., Nørgaard, J. H., Silva, R., & Roul, P. (2010). *"Barriers for wave energy conversion: Part B"*. THESEUS Deliverable OD 2.1. (p. 7-22). European Commission.

Nørgaard, J. Q. H., Bentzen, T. R., & Larsen, T. (2012). *"Vandstande og saltholdighed i Limfjorden ved lukket Thyborøn Kanal."* (danish paper) Aalborg Universitet. Institut for Byggeri og Anlæg. (DCE Technical Memoranda; Nr. 27).

Vicinanza, D., Contestabile, P., Ferrante, V., Stagonas, D., Müller, G., Lykke Andersen, T., Nørgaard, J. H., & Frigaard, P. (2012*a*). *"Innovative Seawalls and Rubble Mound Breakwater Design for Wave Energy Conversion."* 33 Conference of Hydraulics and Hydraulic Engineering, Brescia, Italy, 2012.

Vicinanza, D., Stagonas, D., Müller, G., Nørgaard, J. H., & Lykke Andersen, T. (2012*b*). *"Innovative Breakwaters Design for Wave Energy Conversion."* Coastal Engineering conference, Santander, Spain, 2012. American Society of Civil Engineers. (Proceedings of the International Conference on Coastal Engineering; 33).

Vicinanza, D., Nørgaard, J. H., Contestabile, P., & Lykke Andersen, T. (2013). *"Wave loadings acting on Overtopping Breakwater for Energy Conversion."* Proceedings of the 12th international coastal symposium, Plymouth, Great Britain.

Margheritini, L., & Nørgaard, J. H. (2012). *"Key Aspects of Wave Energy".* Proceedings of Sustainable Energy and Environmental Sciences (SEES 2012). Singapore.

Preface

This thesis "*Upgrade and Design of Coastal Structures Exposed to Climate Changes"* is the outcome of a PhD study within the period August 2010 to July 2013 at the Department of Civil Engineering, Aalborg University, Aalborg, Denmark. The thesis presents an introduction summary of a collection of papers presented at a number of international conferences and papers published or under review in scientific journals. It is recommendable to read the selected publications re-printed in Appendix. The thesis is defended in public at Aalborg University on 23 September 2013.

The PhD study is affiliated with the four-year research project THESEUS *"Innovative technologies for safer European coasts in a changing climate"* which is funded by the European Commission (grant 244104) and includes 31 partner institutes worldwide. The THESEUS project has the objective to study the application of innovative coastal mitigation and adaptation technologies generally aiming at delivering a safe (or low-risk) coast for human use/development and healthy coastal habitats as climate changes continues to evolve. The outcome of the THESUS project is general guidelines for integrated design and application of efficient, equitable, and sustainable coastal defense technologies. Moreover, the project aims at providing end-users, such as coastal managers and governments, with a software tool to support them in their decision making when planning for future protection against climate changes. The software tool will provide simple estimates on the influence of climate changes on hydraulic, environmental, social, and economic issues.

Aalborg University has delivered work within three engineering work tasks (WTs) in the THESEUS project; WT. 2.1 (*"Barriers for wave energy conversion"*), WT. 2.3 (*"Overtopping resistant dikes"*), and WT. 2.5 (*"Upgrade of existing defenses"*). The work has consisted mainly of numerical and physical model tests with the objective to deliver guidelines for the THESEUS reports and to provide simple tools for the decision-software. Key findings in the THESEUS project from the work by Aalborg University, carried out by the author of this PhD-study, form the present thesis.

Acknowledgements

I wish to thank the support of the European Commission through FP7.2009-1, Contract 244104 - THESEUS (*"Innovative technologies for safer European coasts in a changing climate"*) together with the support of the Department of Civil Engineering and the doctoral school.

I thank my supervisor Thomas Lykke Andersen for his large commitment to the project and for the fruitful discussions and co-operation we had during the project period. Additionally, I wish to thank Hans Burcharth for his useful input during the PhD-study, and I wish to thank the colleagues and the technical staff within the department for their support and assistance.

Finally yet importantly, I wish to thank my wife Maria for sharing both the burdens and the joys related to the PhD study these past three years.

Aalborg, June, 2013
Jørgen Quvang Harck Nørgaard

(http://www.earthtimes.org, 2013)

CHAPTER #1

INTRODUCTION AND BACKGROUND TO THESIS

This chapter presents an outline of the thesis and an introduction, background, motivation, and objectives of the work.

1.1 General Introduction

Typically, two solutions are distinguished when dealing with coastal protection structures. One solution is to protect the shoreline using so-called "hard" structures (groins, dikes, revetments, sea walls, rubble mounds). Hard protection structures, such as rubble mounds or sea walls, can be positioned both onshore and offshore for protection of coastlines against erosion and flooding. Additionally, hard protection structures are typically used for protection of areas and infrastructures, such as roads and harbours, against waves. Low-lying areas are typically protected against flooding using dikes and levees.

Another solution is to use so-called flexible "soft" methods for maintaining the shoreline, such as applying periodical nourishment and/or constructing artificial sand banks. Typically, smaller initial costs are required for soft protection methods but large long-term costs are required compared to hard structures due to periodic maintenance and nourishment.

The effect from climate changes on beach erosion and soft protection methods is in many studies related directly to the influence from Sea Water Level (SWL) rise or the storm surge residual such as in the studies by Bruun (1962), Zhang et al. (2004), FitzGerald et al. (2008), and Nicholls & Cazenave (2010). Moreover, Ranasinghe et al. (2004), Bryan et al. (2008), and Tamura et al. (2010) noted the influences from increasing wave celerity due to SWL-rise, which can alter the wave refraction and thereby cause changes in shorelines. Sheppard et al. (2005) and Gravelle & Mimura (2008) noted the damages on natural protective elements such as losses of coral reefs due to rising temperatures in the ocean.

For hard coastal protection structures, the impact from climate changes is more complex, since various factors are influenced, such as wave overtopping, wave loading, and consequently stability of foundation and structure material. As an example, Chini & Stansby (2012) evaluated the influence from SWL-rise on extreme overtopping events on a sea wall at Walcott, UK. They found that the average overtopping discharge rates with return periods of 100-years would increase by up to a factor 10 for an SWL-rise of 1 *m*.

Climate changes especially influence hard coastal structures in shallow-water areas, since the water depth limits the wave height due to wave breaking. This will lead to increased run-up levels and consequently increased wave overtopping and wave loading on the structures. Isobe (2013) investigated the influence from increased SWL and wind speed on the wave run-up level, wave overtopping, and stability of armor layers on coastal protection structures in shallow water. The study concluded that rising SWL had a significant effect on the wave run-up level. Lee et al. (2013) performed a reliability analysis on the influence on wave run-up and armor stability for various SRES-scenarios defined in (IPCC, 2000), and found that inside the surf-zone the probability of failure of the structure due to SWL-rise was increasing with decreasing water depth.

The present thesis focuses on the influence from climate changes on selected wave actions on selected types of hard protection structures especially in shallow waters. Soft solutions, such as beach nourishment and artificial sand banks, are not considered.

1.2 Climate Change Predictions

The air temperature has been increasing during the past century due to the so-called greenhouse effect, and forecasts predict that this tendency may even accelerate in the 21st century. A warmer climate will influence the safety in coastal areas, and areas that are safe at present may become more threatened in the future due to rising SWLs and increasing storminess.

1.2.1 Influence from Climate Changes on Global SWL

Two key factors contribute to SWL-rise. The first is the expansion of water due to rising temperatures. This effect is expected to be the largest contribution to the SWL-rise over the next hundred years (IPCC, 2007). The thermal expansion will also continue after the stabilization of greenhouse gasses, see Figure 1. Since warm water expands more than cold water, this effect can also lead to changes in ocean circulation and thus changes in wind speeds/directions and ocean water salinity. The second contribution to SWL-rise is melting glaciers.

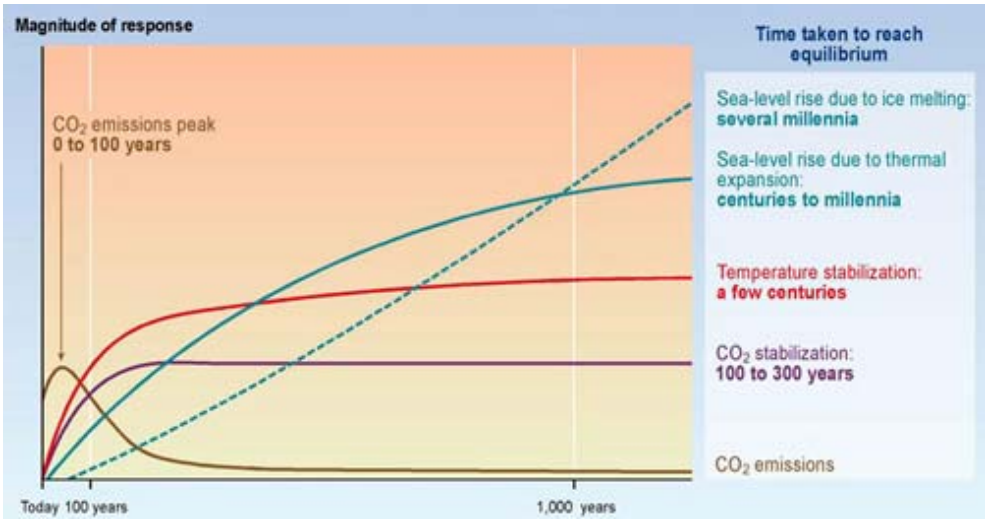

Figure 1. Future projections of SWL-rise, CO2 concentrations, and temperature rise, for the next 1000 years (IPCC, 2007).

The Fourth Assessment Report by the Intergovernmental Panel on Climate Changes (IPCC, 2007) presented climate changes observed in the past and recent time, and projected future changes, together with options for mitigation and adaption against climate changes. Over 6,000 peer-reviewed studies formed the basis for the assessment report and represented the most detailed summary on the situation of climate changes at the time of publishing. The Fifth Assessment Report by IPCC is expected to be completed in 2013/2014.

Figure 2 illustrates the projected global changes in SWL from IPCC (2007). The projections in Figure 2 are presented under different SRES-scenarios for the period 2090 - 2099 relative to the period 1980 - 1999.

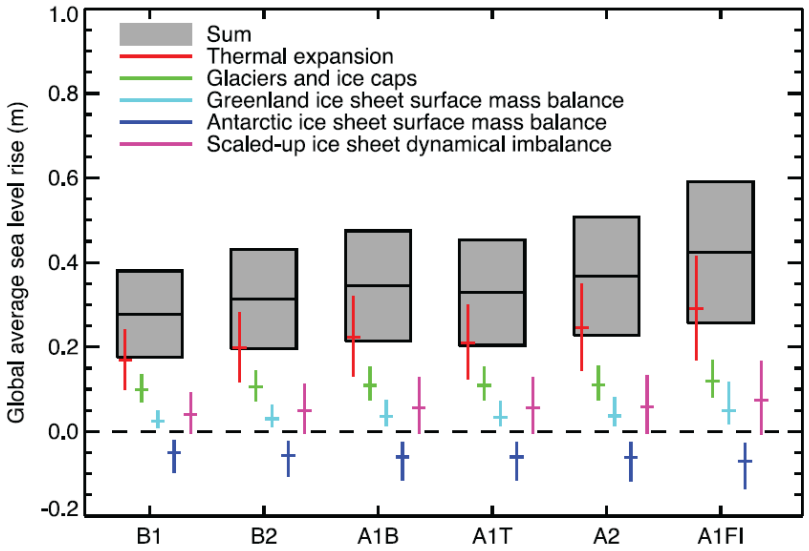

Figure 2. Projected changes in SWL for the period 2090 – 2099 relative to the period 1980 - 1999 (IPCC, 2007).

The newest report by the Intergovernmental Panel on Climate Changes (IPCC, 2012) has collected recent studies since the Fourth Assessment Report (IPCC, 2007). The studies in (IPCC, 2012) yield projections by year 2100 for various SRES-scenarios, which are even more extreme compared to the projections in Figure 2. Table 1 summarizes the recent projections on global SWL rise.

Table 1. Recent global SWL-rise projections since IPCC (2007).		
Author	**Evaluated scenario(s)**	**Projected global SWL rise (year 2100) [*m*]**
(Rahmstorf, 2007)	B1 to A1F1	0.50-1.40
(Horton et al., 2008)	B1 to A2	0.47-1.00
(Vermeer & Rahmstorf, 2009)	B1 to A1FI	0.75 to 1.90
(Grinsted et al., 2010)	A1B	0.90-1.30

It should be mentioned, that Church et al. (2011) noted non-linear effects such as the ocean-heat uptake and the reduction in glacial areas, which was not included in some of the summarized studies in (IPCC, 2012). These effects may reduce the projections from the models.

1.2.2 Influence from Climate Changes on Future Regional Extreme Events

Global and regional climate change effects may significantly differ due to altered astronomical tidal ranges at some coastlines (Mitrovica et al., 2010) and due to land subsidence and uplift from glacial isostatic adjustment at some locations (Lambeck et al.,2010).

Extreme regional events, such as extreme wave heights and extreme SWLs, are often associated with extreme wind events (except for tsunamis, which are not considered in the present thesis). Several studies discusses that there may be an increase in storminess due to climate changes, which will have an effect on the return periods for wind, wave heights, and water levels.

Haugen & Iversen (2008) concluded a future reduced return period for the present extreme winds. Furthermore, Grabemann & Weisse (2008) analyzed the influence from climate changes on extreme wave conditions in the North Sea where future sea states were simulated for a 30-year period (2071-2100). The analysis showed that the future annual 99% non-exceedance significant wave height and wind speeds would increase by up to 18% and 7%, respectively, compared to the reference period (1961-1990). The periods 1961-1990 and 2071-2100 were further considered by Debernard & Røed (2008) where the annual 99-percentiles of the significant wave height and storm surge residual in the North Sea were seen to increase by 6-8% and 8-10%, respectively. The recent study by Winter & Ruessink (2013) on wind extremes in the North Sea indicated that climate changes could lead to changes in wind directions and changes in wave directions during extreme wind events. Such altered wind and wave directions can have significant influence on the shoreline evolution along the North Sea coasts.

Worth et al. (2006) found indications of increased storm surge extremes along the North Sea coasts. They projected an increase of 0.6–0.7 *m* in the annual 99.5% storm surge water level exceedance percentile in the period 2071 – 2100 relatively to the period 1961 – 1990. Kont et al. (2008) reported increased beach erosion in Estonia, which is expected to be due to an increased storminess in the eastern Baltic Sea since 1954 and due to exposed coastlines from reduced sea ice cover during wintertime.

1.3 Strategies for Protection of Coasts against Climate Changes

Adoption of different strategies in the future can overcome the problems related to climate changes. One strategy is to leave the coastal protection structures as they presently are without performing any types of upgrade actions. Such strategy will change the reliability level of the structures and retreat may be needed in exposed coastal areas. An in-depth evaluation of the influence from climate changes on existing coastal protection structures is needed if applying such strategy, such as evaluation of the structure resilience against extra wave overtopping and extra wave loading.

A second strategy is to upgrade the existing defenses by changing the dimensions or by re-designing the structures to retain their functionality and safety. Rubble mound structures can be upgraded by heightening the crests and improving the stability of cover-layers and superstructures. Another solution can be to build submerged detached low-crested breakwaters in front of the existing structures to dampen the waves. As with breakwaters, dikes can also be upgraded by heightening the crests. However, there are also

other options than heightening the crest level in order to mitigate the effects of climate changes. One option is to create overtopping resistant dikes by reinforcing the crests and landward slopes so they can resist the erosive flow from a specific amount of wave overtopping.

Climate changes demands for innovative solutions, which can have a positive effect on the environment. The research project "THESEUS" (THESEUS, 2013) investigated the use of innovative solutions for wave dampening such as artificial reefs, bottom vegetation, and other types of submerged structures. Additionally, innovative multipurpose coastal protection structures with low or no environmental impact have recently gained an increasing attention. The main advantage of multi-purpose structures is the sharing of costs between different functions, which can help introduce more innovative and competitive technologies. As examples, Margheritini & Nørgaard (2012) presented five different multi-purpose functions for three wave energy converter concepts (Wave Dragon wave energy converter, Sea wave Slot cone Generator, and Wave Star wave energy converter). The multi-purpose functions were listed as; 1) *protection against shoreline erosion*, 2) *harbour protection*, 3) *fish farm*, 4) *water recirculation for polluted areas or areas suffering of Eutrophication*, and 5) *platform for combination with other renewable energy sources for better area utilization*.

1.4 Focus of the Study

Before constructing or upgrading a specific coastal protection structure an in-depth analysis is needed on the structural response due to the design wave. Small projects where costs of model tests are significant compared to the construction costs are typically designed solely based on semi-empirical design-formulae for structural response. Larger or more unconventional projects are typically supported by physical laboratory tests. However, before initiating such model tests an initial design is needed. If the initial design gives responses, which are far from the expectations, several iterations are needed, which can significantly increase the expenses of these investigations. Thus, both small and large coastal protection projects require design tools, which provide reliable estimates.

Many state-of-the-art design tools are based solely on deep-water wave conditions such as the one by Franco et al. (1994) for estimation of single wave overtopping on vertical breakwaters, the one by Pedersen (1996) for estimation of wave loads on rubble mound breakwater crown walls, and the one by Van Gent (2002) for estimation of overtopping flow parameters on sea dikes. Using these formulae for construction of coastal defenses on shallow water may therefore lead to conservative and expensive designs. On the other hand, existing structures located in shallow water that are initially designed based on the conservative deep-water formulae may not be as vulnerable to climate changes as expected.

The present thesis performs an in-depth evaluation and extension of selected design formulae in order to include depth-limitation effects. Additionally, the performance of existing tools for description of waves in shallow waters is evaluated with special focus on low-exceedance wave heights, which will typically result in the largest wave loads and largest overtopping volumes. It is important to be able to determine the consequences of climate changes and the upgrade strategy.

Another focus in the thesis is evaluation of the potential for using innovative multi-purpose structures for coastal protection. More specifically, two of the multipurpose functions are investigated - suggested by Margheritini & Nørgaard (2012); *electricity producing multipurpose structures for coastal/harbour protection*, and *multipurpose storm surge barriers for improving water exchange*.

1.5 Thesis Outline

The remaining content of the thesis is divided into three main parts. Part 1 present the outline of the thesis and a description is given on the work done to upgrade selected tools to provide better estimates on the impact from climate changes on typical coastal protection structures.

Part 2 uses the upgraded tools in specific case studies to evaluate the impact from climate changes on typical coastal defenses and to evaluate the use of innovative multipurpose structures for coastal protection.

Part 3 summarizes the general findings and conclusions of the thesis and gives suggestions for future complementary work. The thesis outline is as follows:

Part 1: Evaluation and Modification of Existing Tools for Design of Coastal Structures in Shallow-Water Wave Conditions

Chapter 2: Distribution of Wave Heights and Wave Run-up Levels in Shallow-Water Wave Conditions
Chapter 3: Wave Loads on Crown Walls
Chapter 4: Single Wave Overtopping Volumes on Rubble Mound Breakwater Crown Walls
Chapter 5: Overtopping Flow Parameters on Sea Dikes

Part 2: Case Studies

Chapter 6: Dike Case Study
Chapter 7: Rubble Mound Case Study
Chapter 8: Dampening of Waves by Wave Energy Converters
Chapter 9: Dampening of Storm Surges by Barrier

Part 3: Conclusions

Chapter 10: Conclusions and Discussion

PART #1

Evaluation and Modification of Existing Tools for Design of Coastal Structures in Deep and Shallow-Water Wave Conditions

Storm Becky in Santander Bay, Spain 2010 (www.theseusproject.eu, 2013)

CHAPTER #2

DISTRIBUTION OF WAVE HEIGHTS AND WAVE RUN-UP LEVELS IN SHALLOW-WATER WAVE CONDITIONS

In this this chapter, the wave transformation processes in shallow water are described together with their influences on the wave height distribution. Additionally, a description is given of a method for modifying existing deep-water wave run-up formulae to include the effects of altered wave height distribution in shallow-water wave conditions.

2.1 Transformation of Waves in Shallow Water

A prerequisite for estimation of wave actions on coastal structures is a detailed insight in the transformation of waves as they propagate towards the shore.

Wind generated waves become swell when they propagate out of the windy area. Such swell waves are almost regular and of sinusoidal shapes if on deep water. However, when approaching shallow water and entering water depths of approximately one-half of their wavelength (Goda, 2010), they will change in length, height, directions, and shape, cf. Figure 3. Such waves are typically classified as *intermediate-depth water waves* and in depths of approximately one-twentieth the wavelength, the waves are named *long waves* (Goda, 2010).

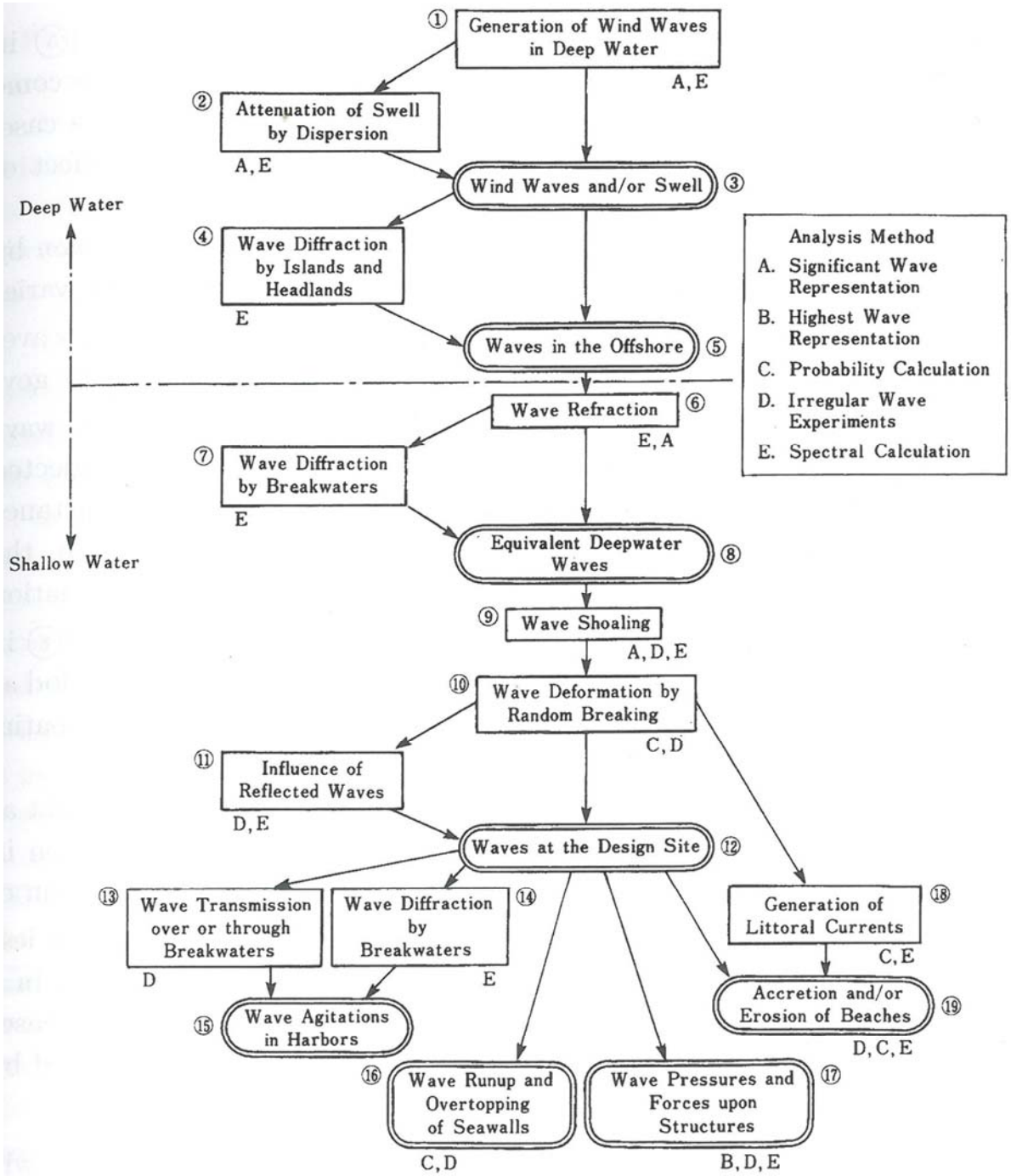

Figure 3. Wave transformations from deep to shallow water (Putz, 1952).

The decreasing water depth will decrease the wave celerity and thus decrease the wavelength. To maintain the same transport of energy in shallow water as in deep water the wave height changes when the wave group velocity changes (shoaling). This results in steeper waves and in the end it leads to instability (wave breaking). Additionally, the incident waves approaching the coast with and angle (oblique waves) will change direction and become more and more perpendicular to the bottom contours due to the decreasing celerity in shallow water (wave refraction).

Miche (1944) has theoretically shown that the particle velocity in a wave cannot exceed the phase velocity, which leads to the maximum steepness given in (1), where H is the wave height, L is the wavelength, h is the water depth, and k is the wavenumber.

$$H / L = 0.142 \cdot \tanh(kh) \tag{1}$$

The maximum wave steepness of regular waves in shallow water is found from (1) to be $H \leq 0.89 \cdot h$. However, the upper value of the regular wave height of $H \leq 0.78 \cdot h$ by Mcowan (1891) is more commonly used.

Observations from irregular waves shows that the maximum significant wave height in the time domain, $H_{1/3}$, is typically limited to $H_{1/3}/h \approx 0.5$ (Riedel & Byrne, 1986). In contrast, irregular waves in deep water, which are unaffected by depth induced wave breaking, are typically defined as $H_{1/3}/h \leq 0.2$ - named *deep-water waves* in the following. Waves affected by depth induced wave breaking ($H_{1/3}/h > 0.2$) are in the following classified as *shallow-water waves.*

2.2 Existing Wave Height Distributions in Deep and Shallow-Water Conditions

When designing coastal protection structures, information is especially needed on the low-exceedance probability wave heights. This is because these will typically lead to the highest wave loads or the highest single wave overtopping volumes. However, in many cases only wave measurements of significant wave heights in deep water are available and thus when designing structures in shallow-water wave conditions it is necessary translate the significant wave height from offshore to the site. Moreover, to estimate the low-exceedance wave heights a parametric probability distribution function is needed. Below is given a short review of existing wave height distributions.

2.2.1 Rayleigh-distribution

Wind generated irregular deep-water waves are generally known to follow the Rayleigh-distribution, given in (2), (Longuet-Higgins, 1952).

$$F(H) = 1 - \exp\left(-2 \left(\frac{H}{H_{1/3}} \right)^2 \right) \tag{2}$$

However, in depth-limited shallow-water conditions, the largest wave components are limited due to wave breaking and thus the Rayleigh-distribution is in many cases quite conservative.

2.2.2 Glukhovskii-distribution

Glukhovskii (1966) suggested a wave height distribution that includes the influence of depth-limitation effects by modifying the exponential Rayleigh-function to be dependent on the mean wave height to water depth ratio, H_m/h. The modified distribution function is given in (3).

$$F(H) = 1 - \exp\left(-\frac{\pi}{4} \left(\frac{\left(H / H_m \right)^{2/(1-\varsigma)}}{1 + \varsigma / \sqrt{2\pi}} \right) \right), \quad \varsigma = H_m / h \tag{3}$$

2.2.3 Battjes & Groenendijk-distribution

One of the most widely used wave height distribution functions is by Battjes & Groenendijk (2000), given in (4). This distribution function is recommended for use in shallow-water wave conditions in The Rock Manual (CIRIA et al., 2007), the EurOtop Manual (Pullen et al., 2007), and the DNV-OS-J101 standard on design of offshore wind turbine structures (DNV, 2010). The Battjes & Groenendijk (2000)-distribution is validated against model tests with shallow foreshores and bed slopes in the range 1:20 – 1:250. The model is a composite Weibull-distribution, which means that it is a Rayleigh-distribution with exponent k_1 equal to 2 for conditions with non-breaking waves in deep water below a certain transition wave height H_{tr}, given in (5). The wave height distribution changes to a Weibull-distribution with higher exponent k_2 for depth-limited waves in shallow water. The scale parameters H_1 and H_2 and the exponent for depth-limited waves k_2 in (4) were calibrated against model tests. H_1 and H_2 were set to vary for varying H_{tr}. k_2 was chosen to be constant, k_2=3.6. Input to the distribution is the foreshore bed slope α_f, water depth h, and the significant wave height in the frequency domain H_{m0}.

$$F(H) = \begin{cases} 1-\exp\left[-(H/H_1)^{k_1}\right] & \text{for} \quad H \le H_{tr} \\ 1-\exp\left[-(H/H_2)^{k_2}\right] & \text{for} \quad H \ge H_{tr} \end{cases} \tag{4}$$

$$H_{tr} = (0.35 + 5.8\tan(\alpha_f)) \cdot h \tag{5}$$

A number of recent studies have evaluated the performance of the Battjes & Groenendijk (2000)-distribution against model and prototype scale measurements, which has indicated a few important weak points, as discussed below.

Mai et al. (2010) evaluated the performance of the Battjes & Groenendijk (2000)-distribution against wave heights measured at three different locations at water depths from 8 *m* to 29 *m* in the North Sea. The study concluded that the shape parameter k_2 was not constant but was significantly varying depending on the location; i.e. $2.17<k_2\le2.46$ at water depth h=11 *m*, $k_2\approx2.30$ at water depth h=29 *m*, and $k_2\approx2.18$ at water depth h=18 *m*. In all cases the shape parameter was far from k_2=3.6 as given by the Battjes & Groenendijk (2000)-model.

Based on comparisons against laboratory wave data by Hamm & Pernard (1997), Goda (2012) noted that the k_2-parameter in the Battjes & Groenendijk (2000)-distribution varied across the surf zone. The comparisons showed that k_2 was varying in the range $2.2<k_2\le3.7$ for water depth to deep-water wave height ratios of $2.73<h/H_0\le0.66$. The suggested shape factor of k_2=3.6 by Battjes & Groenendijk (2000) was concluded to correspond approximately to the middle of the surf zone with h/H_0=0.66. Additionally, Goda (2012) observed a tendency of underestimating the biggest wave heights in intermediate water depths when comparing the Battjes & Groenendijk (2000)-distribution against measurements. Thus, Goda (2012) recommended using the breaker index method by Goda (2010), given in (6), instead of a parametric wave height distribution.

Caires & Gent (2012) evaluated the performance of the Battjes & Groenendijk (2000)-distribution on horizontal shallow foreshores, which is outside the range of validity. They compared low-exceedance probability wave heights obtained from the Battjes & Groenendijk (2000)-distribution, using the mildest validated slope of 1:250 in the distribution function, against measured data from two lakes with horizontal seabeds in the Netherlands, and against model test data from scaled model tests. From the analysis it was concluded that the highest measured wave heights on horizontal shallow beds were underestimated by up to 15%. Caires & Gent (2012) thus recommended using the conservative Rayleigh-distribution in such conditions instead of the non-conservative Battjes & Groenendijk (2000)-distribution.

2.2.4 Modified Battjes & Groenendijk-distribution

Caires & Gent (2012) recommended adjusting the Battjes & Groenendijk (2000)-distribution since the distribution was seen not to converge towards the Rayleigh-distribution in deep water, but instead provide

a slight overestimation. They suggested using the original formulation by Battjes & Groenendijk (2000) if the estimate was not exceeding those obtained by the Rayleigh-distribution and $H_{tr} < 2.75$, and otherwise using the Rayleigh estimate.

2.2.5 Goda Breaker Index Method

The breaker index by Goda (2010) denotes the wave height and water depth at location of wave breaking in the surf zone. The method is to propagate waves from Rayleigh-distributed deep-water wave conditions towards the breaker location. The influence from the sloping beach is accounted for using the shoaling factor K_s that can e.g. be approximated using linear wave theory. H_0' is the deep-water wave height corresponding to the significant wave, L_0 is the deep-water wavelength, and α_f is the foreshore bed slope.

$$H_{1/3} = \begin{cases} K_s H_0' & \text{for } h/L_0 \geq 0.2 \\ \min\left\{\left(\beta_0 H_0' + \beta_1 h\right), \beta_{\max} H_0', K_s H_0'\right\} & \text{for } h/L_0 < 0.2 \end{cases}$$
$$H_{1/250} = \begin{cases} 1.8 K_s H_0' & \text{for } h/L_0 \geq 0.2 \\ \min\left\{\left(\beta_0^* H_0' + \beta_1^* h\right), \beta_{\max}^* H_0', 1.8 K_s H_0'\right\} & \text{for } h/L_0 < 0.2 \end{cases} \quad (6)$$

Where

$$\beta_0 = 0.028\left(H_0'/L_0\right)^{-0.38}\exp\left(20\tan^{1.5}\alpha_f\right) \qquad \beta_0^* = 0.052\left(H_0'/L_0\right)^{-0.38}\exp\left(20\tan^{1.5}\alpha_f\right)$$
$$\beta_1 = 0.52\exp\left(4.2\tan\alpha_f\right) \qquad \beta_1^* = 0.63\exp\left(3.8\tan\alpha_f\right)$$
$$\beta_0 = \max\left\{0.92, 0.32\left(H_0'/L_0\right)^{-0.29}\exp\left(2.4\tan\alpha_f\right)\right\} \qquad \beta_{\max}^* = \max\left\{1.65, 0.53\left(H_0'/L_0\right)^{-0.29}\exp\left(2.4\tan\alpha_f\right)\right\}$$

2.3 Influence from Wave Height, Wave Period, and Bed Slope on Low Exceedance Wave Heights

As mentioned, the different state-of-art wave height distributions have different levels of details. The distribution by Glukhovskii (1966) is solely dependent on H_m, whereas the distributions by Battjes & Groenendijk (2000) and Goda (2010) have additional input parameters, i.e. α_f, H_{m0}, and α_f, $H_{1/3}$, L_0, respectively. To evaluate the influence from the missing input parameters in some of the distributions the wave height distributions are plotted in Figure 4 as function of $H_{1/3}/h$ for various T_p (top figure) and for various cot(α_f) (bottom figure).

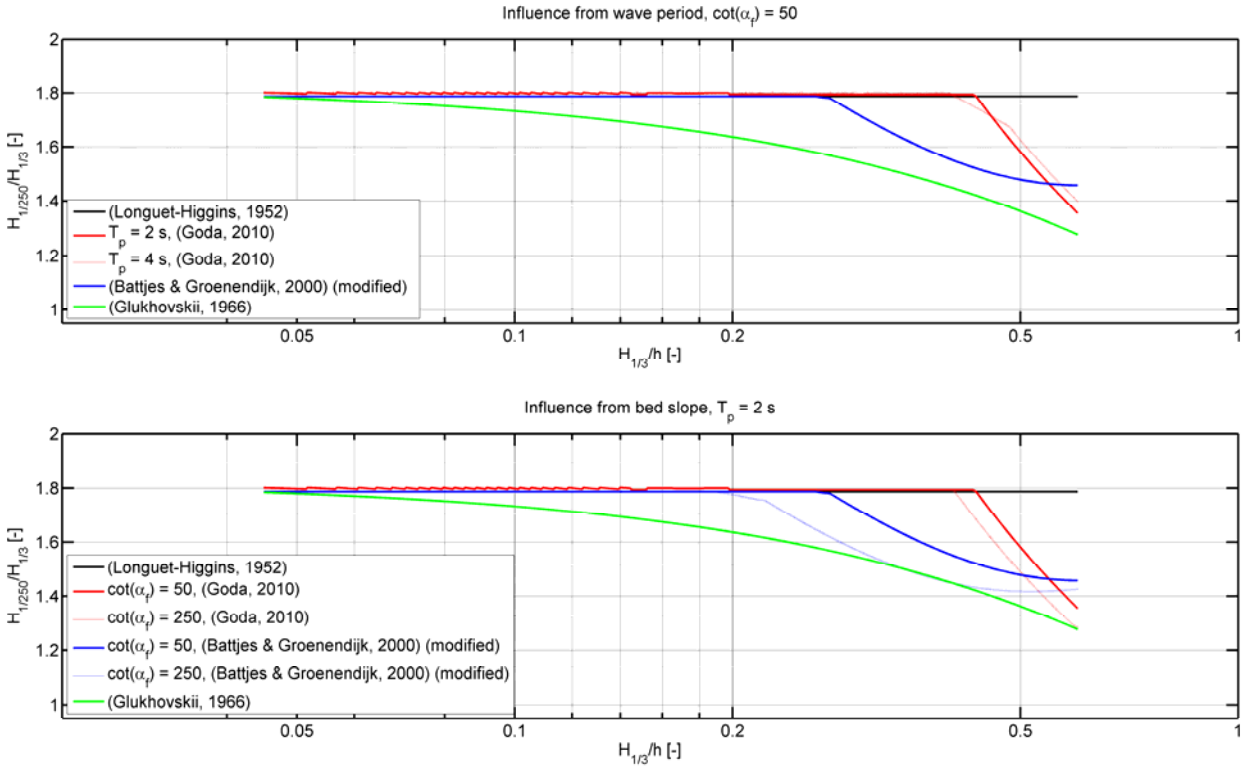

Figure 4. Comparison of state-of-art wave height distributions.

As can be seen, the wave height distributions especially differ in the interval from $0.2<H_{1/3}/h\leq 0.5$. The distribution by Glukhovskii (1966) generally provides the lowest extreme wave heights compared to the other evaluated formulations and only converges towards the deep-water estimates in very deep waters (low ratios of $H_{1/3}/h$). It is a problem that the state-of-art wave height distributions provides such big differences in the estimated low-exceedance wave heights, since small differences in the design wave height can be significantly amplified in the estimated wave actions on marine structures.

Both the wave period and bed slope seems to have relatively large influence on the low exceedance wave heights. Thus, when evaluating the impact from climate changes on the design wave conditions for coastal structures also the changes to the wave period and the foreshore morphology should be addressed and not only the impact on the SWL and the design wave height.

2.4 Evaluation of State-of-the-art Wave Height Distributions against New Model Tests

In Figure 5 and Figure 6, the previously described wave height distributions are compared against new model test data obtained from flume tests in deep and shallow-water wave conditions. The test setup for the experiments is described in Paper 7. The modified Battjes & Groenendijk (2000)-distribution based on the recommendations by Caires & Gent (2012) is included in the figures. The performances of the different formulations in Figure 6 are based on the standard error S_e given in (7) where n is the number of values, $meas_i$ are the measured values, and $calc_i$ are calculated estimates of $meas_i$.

$$S_e = \sqrt{\frac{1}{\nu}\sum_{i=1}^{n}\left(meas_i - calc_i\right)^2} \qquad (7)$$

$$\nu = n - 2$$

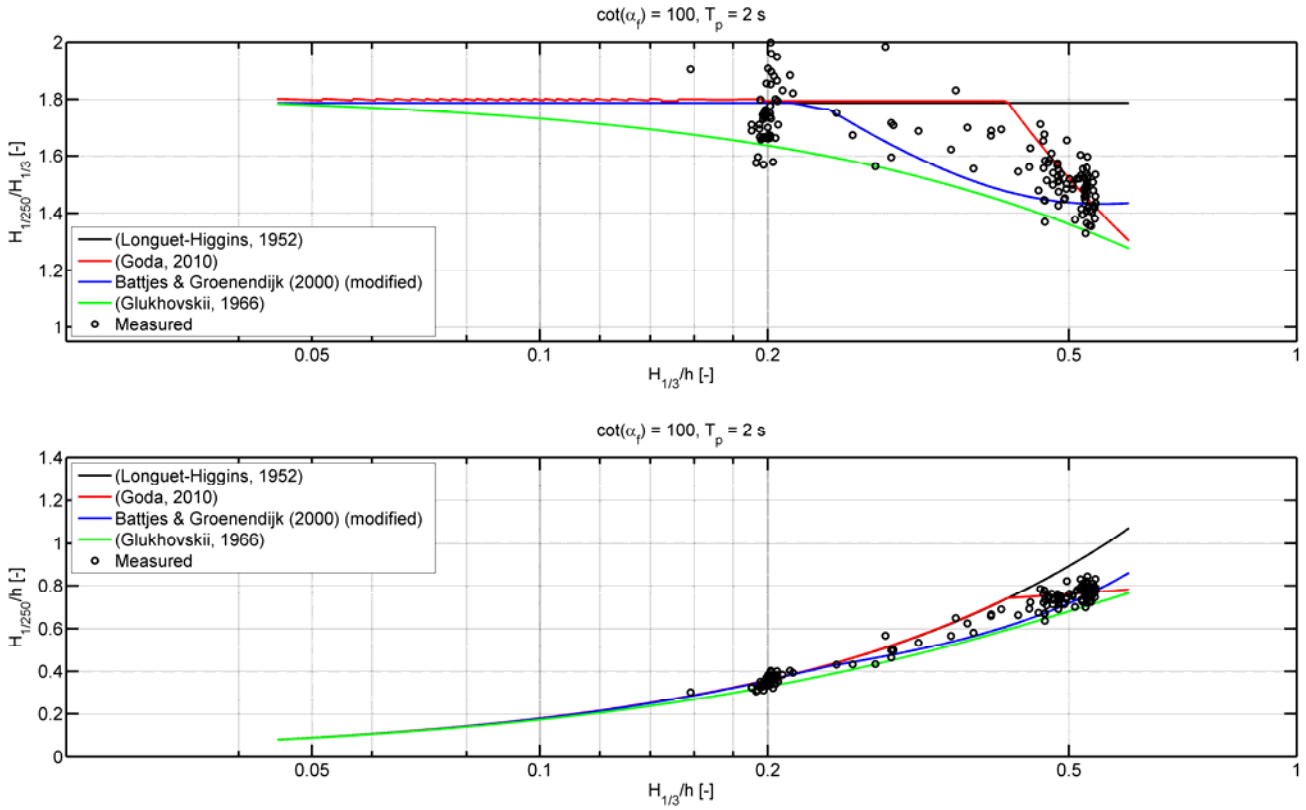

Figure 5. Comparison of wave height distributions against measured data from tests performed in deep to shallow-water wave conditions.

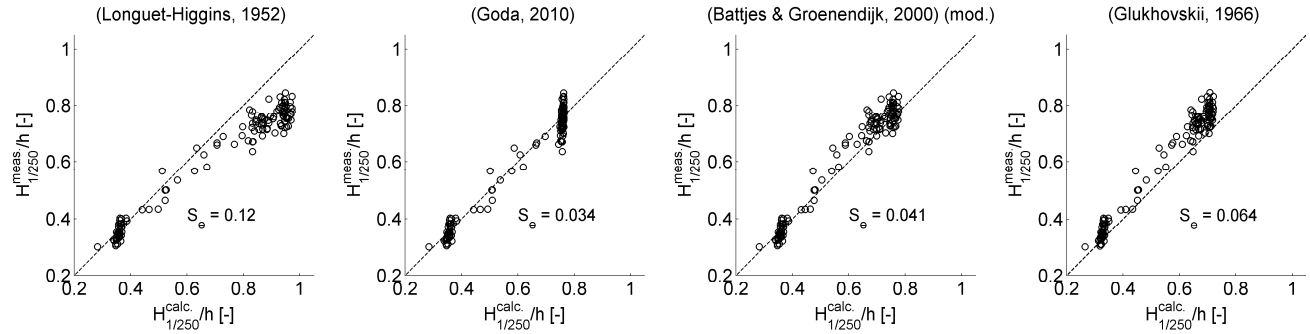

Figure 6. Direct comparison of measured and estimated $H_{1/250}$ in deep and shallow-water wave conditions.

As can be seen, all evaluated formulations provide relatively good estimations in deep-water conditions, $H_{m0}/h<\approx 0.2$. However, in shallow-water wave conditions the Rayleigh-distribution significantly overestimates the low-exceedance probability wave heights, whereas the distribution by Glukhovsky (1966) provides an underestimation. The modified Battjes & Groenendijk (2000)-distribution and the formulation by Goda (2010) both provide relatively reliable estimates in the considered wave conditions (cot(α_f)=100 and T_p=2 *s*).

The method by Goda (2010) gives slightly better estimates (S_e=0.034) than the distribution by Battjes & Groenendijk (2000) (S_e=0.041). However, in order to perform an in-depth comparison of the two methods an evaluation against additional bed slopes and wave periods is needed, cf. Figure 4.

In general, the method by Goda (2010) seems to be preferred over Battjes & Groenendijk (2000), since it includes the influence from the wave period, which is known to be a governing parameter for wave transformation in the surf zone. Moreover, the Goda (2010)-method is the more conservative of the two methods and additionally, the breaker index method can provide the shallow-water wave height at any position in the surf zone and directly propagate the deep-water wave height into shallow water. When

applying the Battjes & Groenendijk (2000)-distribution for estimation of e.g. $H_{0.1\%}$ the designer needs to first propagate the significant wave height from deep to shallow water.

A limitation in the breaker index method by Goda (2010) is, however, that only the shallow-water $H_{1/3}$ and $H_{1/250}$ can be obtained and not e.g. $H_{0.1\%}$, $H_{1\%}$, $H_{2\%}$, $H_{1/10\%}$ as with the distribution by Battjes & Groenendijk (2000).

In general, when applying a shallow-water wave height distribution, one should be aware of the range of validity of the chosen formulation since non-conservative estimations can be obtained in some cases, such as the case with the Battjes & Groenendijk (2000)-distribution at transitional water depths. If possible, one should compare against measured field data, or at least compare e.g. the low-exceedance probability wave heights obtained from various formulations, to check the variability and reliability of the estimates.

2.5 Existing Wave Run-Up Formulae

Pre-design formulae for design of coastal protection structures are typically developed empirically through physical model tests. As mentioned, the design formulae can provide the designer with initial estimates on the dimensions of the breakwater structure, which are often verified afterwards or slightly changed through physical model tests. Additionally, the design formulae can be used for evaluation of the influence from e.g. climate changes on an existing structure, which may not be included in the initial design.

The governing term in many design formulae is the fictional wave run-up level, such as in Pedersen (1996) for wave loads on rubble mound crown walls, and in Van Gent (2002) for overtopping flow parameters on sea-dikes. In this section, the wave run-up formulae used in these studies are extended to include the effects of depth limitation in shallow-water wave conditions.

Several authors have suggested wave run-up formulae for various types of structures. For example, Pedersen (1996) used the wave run-up height for deep-water wave conditions and non-overtopped straight slopes exceeded by 0.1% of the incident waves, $R_{u,0.1\%}$, (8) in Table 2, by Van der Meer & Stam (1992). Van Gent (2002) used the formula (9) in Table 2 by Van Gent (2001) for the wave run-up level exceeded by 2% of the incident waves, $R_{u,2\%}$, on impermeable smooth and rough slopes. T_m is the mean wave period in the time-domain, α is the seaward slope, γ_f is the friction factor, γ_β is a wave obliquity-factor accounting for influence from oblique and short-crested waves on overtopping flow parameters, which can be obtained from Paper 5.

Table 2. Selected wave run-up formulae, which are used in design formulae in the following chapters.

Author	Range of validity	Run-up formula	Surf parameter
Van der Meer & Stam (1992)	Rayleigh distributed wave heights in deep-water wave conditions with head-on wave attack on permeable rough straight slopes.	$\frac{R_{u,0.1\%}}{H_{1/3}} = \begin{cases} 1.12\xi_{m0} & \xi_{m0} \le 1.5 \\ 1.34\xi_{m0}^{\ 0.55} & \xi_{m0} > 1.5 \end{cases}$ (8) $\frac{R_{u,0.1\%}}{H_{1/3}} \le 2.58$	$\xi_{m0} = \frac{\tan\alpha}{\sqrt{\frac{2\pi}{g}\cdot\frac{H_{1/3}}{T_m^2}}}$
Van Gent (2001)	Relatively deep water to relatively shallow foreshores with head-on and oblique waves on impermeable smooth and rough slopes.	$\frac{R_{u,2\%}}{\gamma_f\cdot\gamma_\beta\cdot H_{1/3}} = 1.35\cdot\xi_{-1.0}$ for $\xi_{-1.0} \le 1.481$ (9) $\frac{R_{u,2\%}}{\gamma_f\cdot\gamma_\beta\cdot H_{1/3}} = 4.7 - \frac{2.963}{\xi_{-1.0}}$ for $\xi_{-1.0} \ge 1.481$	$\xi_{-1.0} = \frac{\tan\alpha}{\sqrt{\frac{2\pi}{g}\cdot\frac{H_{1/3}}{T_{-1.0}^2}}}$

Regarding studies on wave run-up on coastal structures, the following works should additionally be mentioned: Battjes (1974), Ahrens (1981), Allsop et al., (1985), de Waal, J.P. & van der Meer, J.W (1992), and Van der Meer & Janssen (1994). Moreover, an extensive summary of estimation of wave run-up levels is given in TAW (2002).

Many existing run-up formulae are based on Rayleigh-distributed deep-water wave conditions, which provide conservative estimates of wave actions on coastal structures in depth-limited shallow-water wave

conditions. Typically, wave parameters, such as the significant wave height in the time-domain, $H_{1/3}$, or frequency domain, H_{m0}, and the peak period, T_p, are used as input in such formulae.

However, the depth-limitation effects in shallow water have gained an increasing attention in recent time. The newest EurOtop Overtopping Manual (Pullen et al., 2007) used the first negative moment of the energy spectrum, $T_{-1.0}$, instead of the peak period T_p in almost all the design formulae since it is proportional to the wave energy flux (at least in deep water). Additionally, Van Gent (2001) found that $T_{-1.0}$ was a more appropriate parameter for run-up levels than e.g. T_p to account for the effects of changes in the wave energy spectra on shallow water, and additionally to account for the effects of double peaked spectra.

The Rock Manual (CIRIA et al., 2007) indicated that $H_{2\%}$, which is the wave height exceeded by 2% of incident waves, is a more appropriate parameter for estimation of the structural stability than e.g. $H_{1/3}$ or H_{m0}. The low-exceedance wave heights, such as $H_{2\%}$ or $H_{0.1\%}$, can be estimated using one of the previously mentioned wave height distributions, and $T_{-1.0}$ in shallow water can be estimated e.g. using the spectral SwanOne-model described in (Verhagen, 2008). However, although some design formulae depend on more appropriate wave parameters for shallow water, many design formulae are still too conservative in these conditions.

2.6 Extension of Deep-Water Wave Run-Up Formulae to Shallow-Water Wave Conditions

Van Gent (2001) based the calibration of his run-up formula on prototype tests and model tests on structures with foreshores on intermediate water depth and thus the depth limitation effects on the run-up level are to some extent already included in this formula. However, the formula by Van der Meer & Stam (1992) was calibrated against tests with Rayleigh-distributed deep-water waves, which resulted in conservative estimations in intermediate and shallow-water wave conditions.

Kobayashi et al. (2008) concluded that wave run-up levels are Rayleigh-distributed if also the incident irregular wave heights are Rayleigh-distributed (i.e. the distribution of run-up levels follows the incident wave height distribution). This assumption is further validated in Paper 5, where overtopping flow parameters on sea dikes (which are proportional to the run-up levels) are Rayleigh-distributed for Rayleigh-distributed incident waves, and in Paper 8 where wave loads on crown walls (which are proportional to the run-up levels) are seen to follow the incident wave height distribution. Thus, since according to the Rayleigh-distribution $H_{1/3}/H_{0.1\%}$ =0.538 the run-up formula by Van der Meer & Stam (1992) in (8) is adjusted to the run-up formula in (10).

$$\frac{R_{u,0.1\%}}{H_{0.1\%}} = \begin{cases} 0.603\xi_{m0} & \xi_{m0} \le 1.5 \\ 0.722\xi_{m0}^{\,0.55} & \xi_{m0} > 1.5 \end{cases} \qquad \frac{R_{u,0.1\%}}{H_{0.1}} \le 1.389 \tag{10}$$

The modified formula in (10) states that the run-up level remains unchanged compared to the original formulae when waves are Rayleigh-distributed, i.e. deep-water waves. However, when the incident wave height distribution is different from the Rayleigh-distribution, i.e. shallow-water conditions, the extreme run-up levels are reduced due to a reduced $H_{0.1\%}$ compared to the deep-water estimate. In principle, such extension to shallow-water wave conditions can also be performed for other run-up formulae, which are initially based on Rayleigh-distributed deep-water waves.

$R_{u,0.1\%}$ obtained from the modified formula in (10) is plotted in Figure 7 as function of ζ_{m0} and for various H_{m0}/h-ratios. A permeable rubble mound structure with a seaward slope of cot(α) = 2.5 and a foreshore seabed slope of cot(α) = 100 is evaluated in the example. $H_{0.1\%}$ is estimated using the Battjes & Groenendijk (2000)-distribution. As can be seen in Figure 7, the wave run-up level is significantly reduced in shallow-water wave conditions (H_{m0}/h=0.5) compared to deep water (H_{m0}/h=0.2).

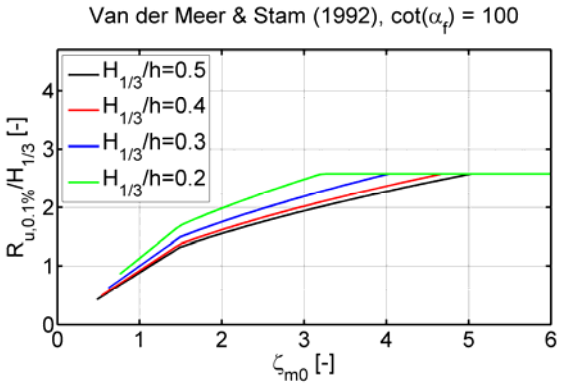

Figure 7. Modified formulae for $R_{u,0.1\%}$ (10) as function of ζ_{m0}.

2.7 Scale and Model Effects on Wave Run-Up Levels in Small Scale Model Tests

Since the wave run-up is one of the governing terms in many design formulae for wave actions on coastal protection structures, the reliability of the formulae is very sensitive to the accuracy of the estimated run-up level. One of the major uncertainties related to estimations of wave run-up levels from formulae based on small scale model tests are the effects of wind and scale effects on especially thin run-up flow layers and thus overtopping (Ward et al. 1994, 1996), (Medina, 1998), (De Rouck et al., 2001, 2007), (Burcharth & Lykke Andersen, 2007), (Lykke Andersen et al., 2011).

Based on scaled model tests with wind and waves Ward et al. (1994, 1996) found that the run-up level is significantly influenced at high wind speeds. Only little effect from wind was observed at low wind speeds. Also Medina (1998) evaluated wind effects on wave run-up levels measured on different breakwater geometries and contrary to the findings by (Ward et al. 1994, 1996) he found a significant effect from wind also at low wind speeds. De Rouck et al. (2001) did comparison of prototype measurements from the Zeebrugge breakwater in Belgium with scaled model tests in 2-D and found that the 2% wave run-up level in average was 7.8% higher in prototype scale compared to model scale. These observed differences were expected to be due to wind effects and effects from roughness of the slope. De Rouck et al. (2007) did further comparison of prototype measurements from the Zeebrugge breakwater with model tests in 2-D and 3-D and observed significant differences in measured run-up levels especially for low SWLs. They further stressed the needs for accurate modelling of porosity and permeability of armor units and core material in model scale compared to prototype scale, since these parameters were seen to have a high influence on the run-up level.

Deviations related to measurement techniques can also provide significant uncertainties in the estimations of wave run-up levels. Troch et al. (1996) noted, that the remaining distance between step gauges and the structure slope in small-scale model tests could cause underestimations by up to 20% compared to large scale. Van Gent (2001) noted the problem of measuring thin run-up layers in small-scale model tests. He concluded that ignoring the thin flow layers could cause underestimations by up to 10%. Typically, linear extrapolation of the thicker layers is used, which, however, also introduces some uncertainty.

2.8 Summary of Findings in Chapter

Deep-water waves are significantly modified when entering shallow water. This means that the wave height distribution in shallow water is different from the wave height distribution in deep water. Estimations of low-exceedance wave heights from existing state-of-art shallow-water wave height distributions are in the present chapter compared to measured low-exceedance wave heights from small-scale model tests. Especially the estimations obtained using distributions by Battjes & Groenendijk (2000) and Goda (2010) are seen to be in relatively good agreement with the measured wave heights. However, it is strictly advised to be careful when applying the distributions outside their ranges of validity, since recent research has shown that un-conservative estimates can be obtained otherwise.

When evaluating the influence from climate changes on the design wave conditions for a specific coastal protection structure in shallow water it is important also to address the possible changes to the foreshore morphology, since a steeper slope will lead to larger low-exceedance wave heights. Additionally, it is important to consider the possible changes to wave periods in the design sea state.

The wave run-up level is one of the governing terms in many design formulae for wave actions on coastal protection structures. A problem is, however, that many run-up formulae are based on deep-water wave conditions and they thus provide conservative estimates in depth-limited conditions. Therefore, it is suggested to modify the existing run-up formulae, which are initially based on Rayleigh-distributed wave heights, by incorporating the effects of changes to the wave height distributions in shallow-water wave conditions using e.g. the ratio $H_{1/3}/H_{0.1\%}$.

When using wave run-up formulae which are initially based on measurements from small-scale tests one should be aware that the wave run-up (and thus the wave actions) on structures in prototype scale may be higher due to scale and model effects.

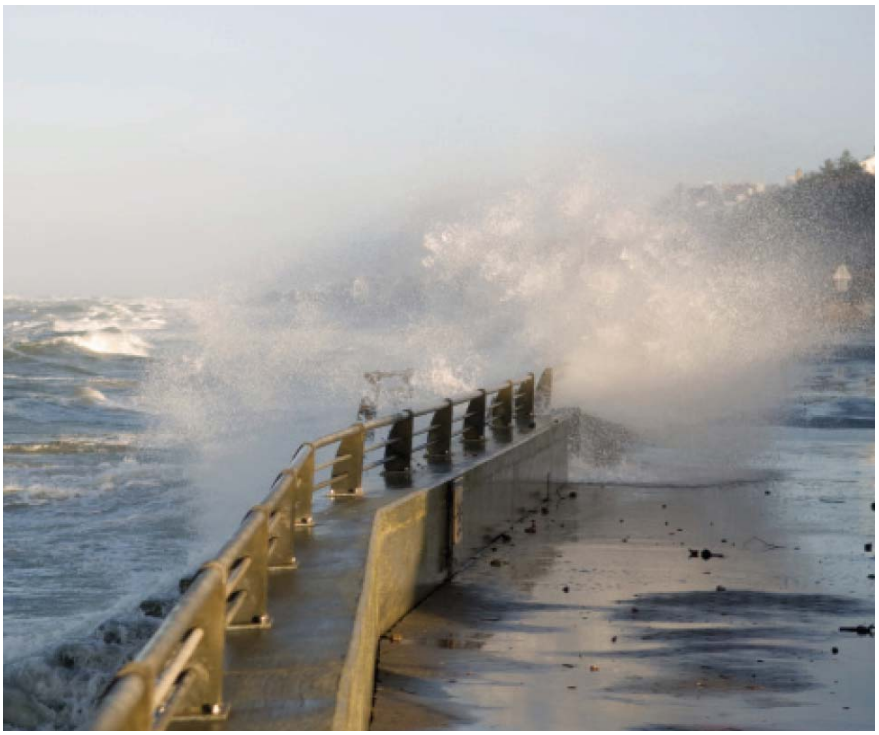

(www.hrwallingford.co.uk, 2013)

CHAPTER #3

WAVE LOADS ON CROWN WALLS

In this chapter, existing design formulae for estimation of wave loads on rubble mound breakwater crown walls are modified to provide more reliable estimates in shallow-water wave conditions.

3.1 Stability of Crown Walls

Concrete crown walls are typically used to limit the wave overtopping on breakwaters and to provide an access road on the crests. Additionally, for similar design conditions a breakwater with a crown wall is constructed from less material compared to a breakwater without a crown wall.

When designing a crown wall superstructure, several failure modes have to be considered, illustrated in Figure 8. Failure mode *a)* depends on the magnitude of the wave loads and the internal strength of the crown wall. Solely horizontal wave loads are needed to design for this failure mode. Failure modes *b)*, *c)*, and *d)* are more complex since these also involve the vertical uplift pressures and the soil properties of the foundation.

Horizontal wave loads are considered in detail in the present chapter and vertical uplift pressures are considered in less detail.

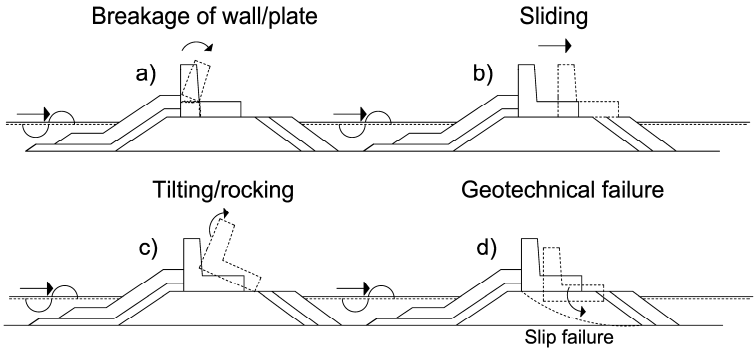

Figure 8. Typical failure modes of crown wall superstructures.

3.1.1 New Tests

In Paper 8 extensions are provided to the existing state-of-art formulae for horizontal wave loads on rubble mound breakwater crown walls to also cover shallow-water wave conditions.

The study is based on 2-D model tests using pressure transducers with very high eigen-frequencies to measure the impulsive wave loads on the crown wall. An illustration of the evaluated cross section is shown in Figure 9. Evaluated structure dimensions are given in Table 3 and target test ranges are given in Table 4.

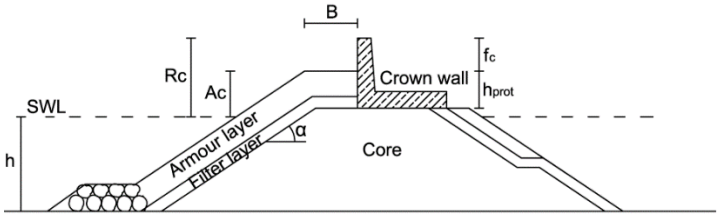

Figure 9. Evaluated cross section in model tests. (Paper 8)

Table 3. Ranges of structure dimensions for the breakwater model. (Paper 8)							
Test series	R_c [m]	A_c [m]	α [-]	B [m]	R_c/A_c [-]	A_c/B [-]	f_c/A_c [-]
Shallow water	0.20 – 0.29	0.20 - 0.24	1:1.5	0.24	1.00 – 1.33	0.83 – 1.00	0 – 0.35
Deep water	0.1 – 0.19	0.1 - 0.14	1:1.5	0.17	1.00 – 1.70	0.59 – 0.82	0 – 0.70

Table 4. Ranges of target conditions in deep water and shallow-water wave test series. (Paper 8)					
Test series	h [m]	H_{m0} [m]	$T_{m-1.0}$ [s]	H_{m0}/h [-]	A_c/H_{m0} [-]
Shallow water	0.300 – 0.360	0.150 – 0.180	1.826	0.500	1.00 - 1.600
Deep water	0.500 – 0.560	0.100	1.826	0.179 – 0.200	0.88 - 1.400

3.2 Evaluation of Existing Formulae for Horizontal Wave Loads

Günback & Ergin (1983) suggested linking the wave run-up level to wave loads on crown walls. Pedersen (1996) adopted the concept by Günback & Ergin (1983) and derived design formulae to estimate wave induced horizontal wave loads on stiff crown walls. The Pedersen formulae are included in the Coastal Engineering Manual (U.S. Army Corps of Engineers, 2002).

Martin et al. (1999) also adopted the concept by Günback & Ergin (1983) and derived a set of design formulae for estimation of horizontal wave loads on crown walls. The formulae were calibrated against physical model tests with monochromatic waves.

In Figure 10 the present measured horizontal wave loads $F_{H,0.1\%}$ exceeded by 0.1% of incident waves on the crown wall are compared with estimations from the formulae by Pedersen (1996) (*left*) and Martin et al. (1999) (*right*). The performances of the design formulae are evaluated using the standard error S_e defined by (7).

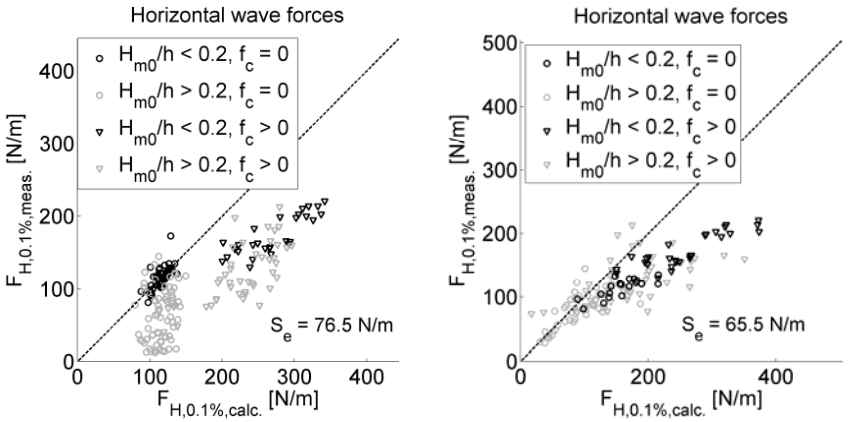

Figure 10. (*left*) Comparison of measured and estimated horizontal wave loads $F_{H0.1\%}$ using the formulae by Pedersen (1996). (*right*) Comparison of measured and estimated horizontal wave loads $F_{H0.1\%}$ using the formulae by Martin et al. (1999). Wave loads are in model scale (1:30). (Paper 8)

As can be seen in the figure, the best overall performance is obtained from the formulae by Martin et al. (1999), which provide reasonable estimates in both deep ($H_{m0}/h \leq 0.2$) and shallow-water ($H_{m0}/h > 0.2$) wave conditions and for both protected ($f_c=0$) and un-protected ($f_c>0$) wall faces, cf. Figure 9. However, if focus is only on the performance in deep-water wave conditions and protected walls, the formulae by Pedersen (1996) provide the best load model. It is thus decided to solely consider the formulae by Pedersen (1996) and upgrade the formulae to provide reliable estimates in shallow-water wave conditions as well and on un-protected crown wall faces. (Paper 8)

3.3 New Formulae for Wave Loads on Crown Walls in Shallow-Water Wave Conditions

In Paper 8 it is shown that the over-prediction for shallow-water waves is caused by too high predicted run-up levels in the Pedersen formulae. Therefore the modified fictional run-up height $R_{u,0.1\%}$ in (10) is used to include the depth-limitation effects in the formulae by Pedersen (1996). Additionally, in Paper 8 it was observed that the pressure transducers used in the tests by Pedersen (1996) suffered from dynamic amplification, which resulted in overestimated wave loads on the unprotected crown wall face. Thus, the empirical calibration factor used in (Pedersen, 1996) for loads on the unprotected wall face was re-calibrated in Paper 8 against new model tests using high eigen-frequency transducers. Finally, in Paper 8 adjustments to the formula for estimation of horizontal overturning moments were performed to provide better estimates for fully protected and partly protected crown wall faces.

The modified design formulae are given in (11) for estimation of horizontal wave loads $F_{H,0.1\%}$ and in (12) for estimation of wave induced horizontal overturning moments $M_{H,0.1\%}$ and base front corner

pressures $P_{b,0.1\%}$. $F_{Hl,0.1\%}$ is the 0.1%-exceedance wave load on the lower wall face protected by armor units $w_f<(z+w_f)\leq A_c$, cf. Figure 11, and $F_{Hu,0.1\%}$ is the 0.1%-exceedance wave load on the upper un-protected wall face $A_c<(z+A_c)\leq f_c$. The run-up wedge volumes *V1* and *V2* in (12) are illustrated in Figure 11 (*right*).

$$F_{Hu,0.1\%} = a \cdot \sqrt{\frac{L_{m0}}{B}} \cdot p_m \cdot y_{eff} \cdot b \qquad , \qquad a = 0.21,\ b = 1.0$$

$$F_{Hl,0.1\%} = \frac{1}{2} \cdot a \cdot \sqrt{\frac{L_{m0}}{B}} \cdot p_m \cdot V \cdot h_{prot}$$

$$F_{H,0.1\%} = F_{Hu,0.1\%} + F_{Hl,0.1\%} = a \cdot \sqrt{\frac{L_{m0}}{B}} \cdot \left(p_m \cdot y_{eff} \cdot b + \frac{p_m}{2} \cdot V \cdot h_{prot} \right) \qquad (11)$$

$$p_m = g \cdot \rho_w \cdot (R_{u,0.1\%} - A_c)$$

$$V = \begin{cases} \dfrac{V_2}{V_1} & \text{for} \quad V_2 < V_1 \\ 1 & \text{for} \quad V_2 \geq V_1 \end{cases}$$

$$M_{H,0.1\%,\text{mod.}} = \left(h_{prot} + \frac{1}{2} \cdot y_{eff} \cdot e_2 \right) \cdot F_{Hu,0.1\%} + \frac{1}{2} \cdot h_{prot} \cdot F_{Hl,0.1\%} \cdot e_1 \qquad , \qquad e_1 = 0.95,\ e_2 = 0.40 \qquad (12)$$

$$P_{b,0.1\%} = d \cdot V \cdot g \cdot \rho_w \cdot (R_{u,0.1\%} - A_c) \qquad , \qquad d = 1.0$$

The standard deviations of the coefficients *a*, *b*, *d*, e_1, and e_2 are given in Paper 8.

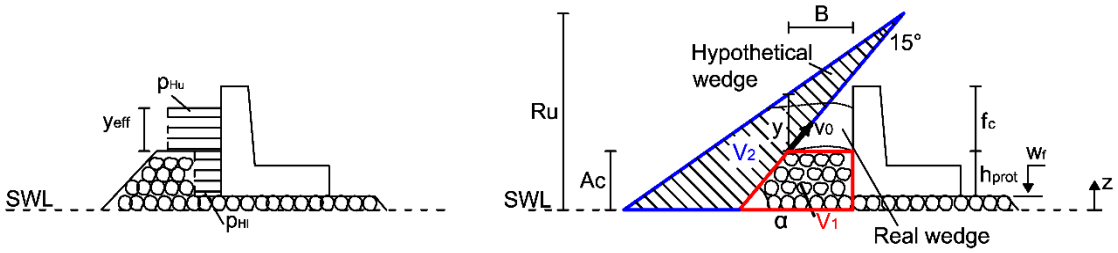

Figure 11. *(left)* Assumed pressure distribution on crown wall. *(right)* Assumed run-up wedge in (11) and (12). (Paper 8)

In Figure 12, the modified formulae are plotted against test data from new model tests and data from model tests by Pedersen (1996) with f_c=0. As can be seen, the formulae provide good estimates in both deep and shallow-water wave conditions and on both the protected and unprotected parts of the crown wall faces.

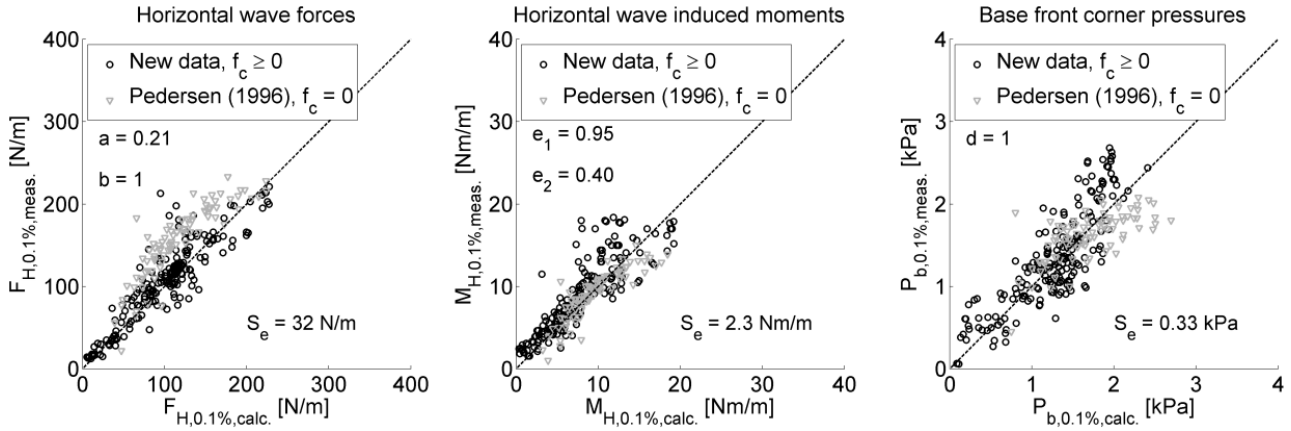

Figure 12. Comparison of estimations from new modified design formulae against new model tests with $f_c \geq 0$ and model tests by Pedersen (1996) with f_c=0. Wave loads are in model scale (1:30). (Paper 8)

Evaluated ranges of wave conditions in Figure 12 are summarized in Table 5 and it is recommendable to only apply the modified design formulae within these ranges.

Table 5. Investigated parameter ranges in modified design-formulae for $F_{H,0.1\%}$, $M_{H,0.1\%}$, and $P_{b,0.1\%}$. (Paper 8)

Parameters	Ranges $f_c = 0$	Ranges $f_c > 0$
ξ_m	2.30 - 4.90	3.31 - 4.64
H_s/A_c	0.50 - 1.63	0.52 - 1.14
R_c/A_c	0.78 – 1.00	1.00 - 1.70
A_c/B	0.58 - 1.21	0.58 - 1.21
H_{m0}/h	0.19 – 0.55	0.19 – 0.55
H_{m0}/L_{m0}	0.018 – 0.073	0.02 – 0.041

3.4 Correlation between Horizontal and Vertical Loads

As previously mentioned, the vertical wave loads on the crown wall are needed to ensure sufficient stability against the failure modes *b)*, *c)*, and *d)* in Figure 8. However, vertical measured wave loads in small-scale model tests are influenced by scale effects due to the non-turbulent flow through the model core material while in the prototype being fully turbulent in the main part. A compensation can be done by increasing the stone sizes in the core in the model as suggested by Burcharth et al. (1999) but typically a triangular pressure distribution is assumed below the base slap of crown walls arising from the base front corner pressure P_b, as illustrated in Figure 13. Hydrostatic pressure is added to the triangular pressure assumption in case of SWL higher than the location of the base plate.

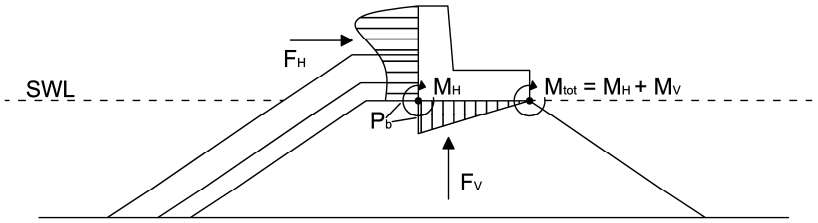

Figure 13. Assumed triangular vertical pressure distribution based on p_b.

In Figure 14 the measured vertical wave load $F_{V,0.1\%,meas.}$, obtained from the model tests described in Paper 9, is compared to the assumed vertical wave load based on the triangular pressure distribution, $F_{V,0.1\%,triang.}$. As can be seen, the estimated vertical wave loads are highly overestimated in most cases compared to the measured wave loads. Additionally, when assuming a triangular pressure distribution arising from P_b the time-lag between the horizontal and vertical wave loads is ignored.

An extra safety is thus included in the design of crown walls on existing breakwaters when the design is based on the assumption of triangular vertical pressure distribution at the instance of maximum horizontal wave load.

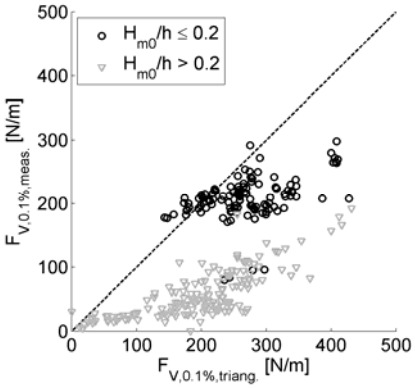

Figure 14. Comparison between measured $F_{v,0.1\%,meas.}$ and estimated $F_{v,0.1\%,triang.}$ based on assumed triangular pressure distribution below the base slap. Wave loads are in model scale (1:30).

Based on model tests with both regular and irregular waves on a caisson breakwater positioned on porous material Pérez et al. (2010) and Clavero et al. (2012) noted that vertical loads on the caisson were increasing with the increment of the foundation depth due to the flow through the core. The same is observed for the crown wall in Figure 15 where the measured vertical wave loads, $F^*_{V,0.1\%,meas.}$, given in (13), are plotted as function of the relative foundation depth, $w_f/H_{0.1\%}$, cf. Figure 11. Increasing SWL can thus be very critical when resulting in a water level just beneath the base plate.

$$F^*_{V,0.1\%,meas.} = \frac{F_{V,0.1\%,meas.}}{\rho_w \cdot g \cdot H_{0.1\%} \cdot L_{-1.0}} \tag{13}$$

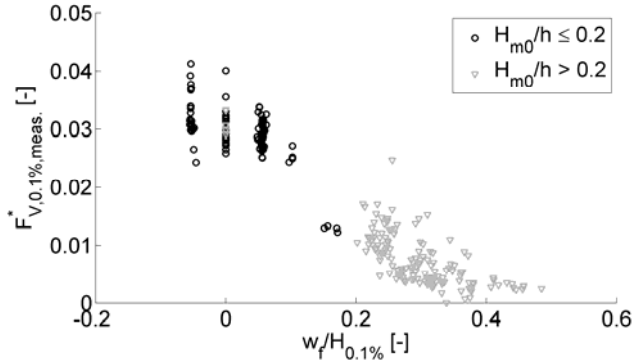

Figure 15. Relative influence from foundation depth on vertical wave loads under the base slap.

3.5 Structural Response of Crown Walls Subjected to Impulsive Wave Loading

Crown walls are typically designed to remain stable at all times. However, since wave loads may increase due to future climate changes small displacements could be accepted, instead of increasing the mass of the structure.

The horizontal wave loads described in the previous section are measured on a model structure in a fixed position. However, due to the dynamic behavior of the wave loads, the crown wall failure-modes also need to be treated dynamically. When measuring wave loads on a static structure the load reduction due to sliding, tilting, and rocking of the structure (failure modes *b)*, *c)*, and *d)* in Figure 8) are not included.

Paper 9 evaluates the wave load reduction on a moveable structure relative to a fixed structure. Moreover, the validity of a simple one-dimensional model is evaluated based on integration of the equation of motion to determine the displacement of a rubble-mound breakwater crown-wall during extreme conditions. The study is performed using the same test setup as described in Paper 8 where wave loads are measured on a fixed part of the crown wall using pressure transducers. However, in this case a part of the structure is allowed to move.

Figure 16. Picture of moveable section in the test setup (the effect of horizontal loading from armor units on the crown wall is not included in the study). (Paper 9)

Measured time series from the pressure transducers mounted on the fixed crown wall part are used to estimate the horizontal displacement of the structure by using the equation of motion as proposed by Burcharth et al. (2008). Figure 17 (*left*) illustrates the calculated accumulated sliding distance together with the measured accumulated sliding distance. As can be seen, the calculated estimated sliding distance is significantly overestimated compared to the measured. This is due to the ignored increasing crest width in front of the crown wall and, thereby, also the ignored dampening effect on the loads on the front faces, after some sliding. Paper 9, therefore suggests including the load reduction factor, $\lambda_{sliding}$, (14) in the estimation of the displacement, to incorporate the dampening effect of the crest width to the total resulting wave load, $F_{res}=(F_H^2+F_V^2)^{0.5}$, cf. (15).

$$\lambda_{sliding}=\frac{\sqrt{L_{m-1.0}/\left(B_{initial}+\Delta B\right)}}{\sqrt{L_{m-1.0}/B_{initial}}} \quad , \quad \Delta B=B_{actual}-B_{initial}$$
$$\lambda_{sliding}\left(i\right)=\sqrt{\frac{B_{initial}}{B_{initial}+x\left(i\right)}} \tag{14}$$

B_{actual} is the accumulated crest width during sliding of the superstructure, $B_{initial}$ is the initial crest width, and $x(i)$ is the accumulated horizontal sliding distance at time instance *i*.

$$F_{red}=\lambda_{sliding}\cdot F_{res} \tag{15}$$

F_{red} is the reduced total wave load on the structure.

The influence from $\lambda_{sliding}$ is illustrated in Figure 17 (*right*) where it is seen, that the calculated and measured sliding time-series stabilizes at the approximately same level. This indicates that when the wall is not moving the suggested load correction provides a good estimation. However, the displacements for each event are larger in the physical model than in the numerical model, indicating that the load is also reduced due to the instantaneous movements (velocities) of the structure.

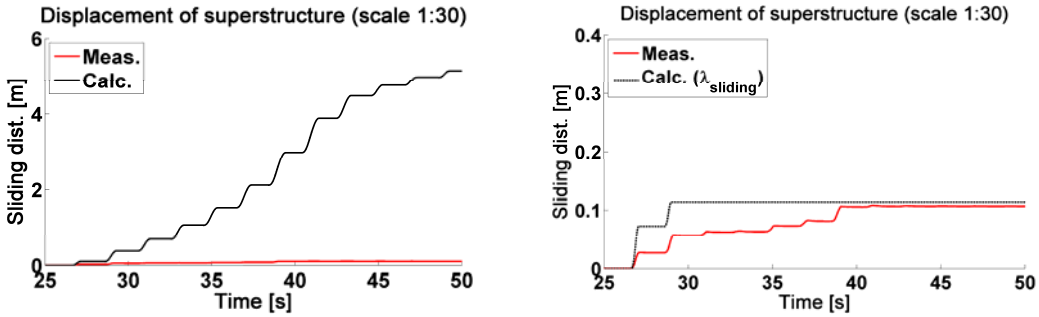

Figure 17. (*left*) Measured and calculated sliding distances of crown wall. (*right*) Measured and calculated sliding distances with load reduction factor due the effect of increasing crest width. Sliding distances and time are in model scale (1:30). (Paper 9)

Paper 9 incorporates a rough estimate on the effect of the reduced relative velocity of the wave and the moveable section compared to the static fixed structure, by using (16). The estimate is based on the maximum particle velocity in the incident wave, $v_{particle,max}$, and the maximum sliding velocity of the crown-wall, $v_{wall,max}$.

$$v_{particle,\max} \approx 0.6\ m/s,\ v_{wall,\max} \approx 0.1\ m/s \qquad F_{H,reduction\ factor} \approx \frac{(0.6m/s - 0.1m/s)^2}{(0.6m/s)^2} = 0.694 \qquad (16)$$

Realistically, the load reduction is slightly lower than in (16) since the average relative velocity is smaller during displacement of the crown wall. In Figure 18 a reduction factor of 0.75 is used together with the reduction factor due to increasing crest width, which results in relatively good agreement between measured and calculated sliding distances.

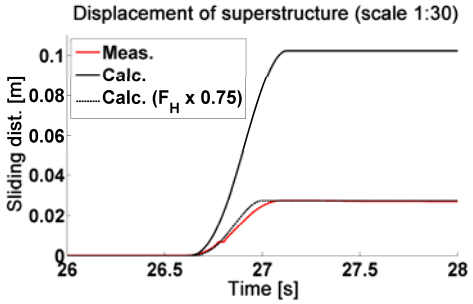

Figure 18. Sliding distance of crown-wall with and without load reduction factor due to decreased relative velocity and reduction factor due to increased crest width. Sliding distances and time are in model scale (1:30). (Paper 9)

Paper 9 additionally uses a sophisticated two-dimensional Finite-Element model to determine the influence from other failure modes than sliding of the superstructure, such as geotechnical slip failure or rocking of the crown wall (failure modes *c)*, and *d)* in Figure 8). The Finite-Element model includes the effects of both plasticity and elasticity of the rubble structure and foundation material. The conclusion from the comparison is that within realistic variations of elasticity modules, the elasticity of the breakwater core material is of minor importance, and only insignificant plastic failure is observed in the core material. Horizontal sliding and overturning is thus concluded to be the most important failure mode for crown walls, meaning that the simple one-dimensional model, which assumes a stiff underlying material, should be sufficient to estimate the sliding displacement of a stiff crown wall superstructure on a typical rubble mound breakwater.

3.6 Summary of Findings in Chapter

The formulae by Pedersen (1996) are seen to significantly overestimate the wave loads on rubble mound breakwater crown walls in shallow-water wave conditions due to the ignored influences from wave

breaking. The formulae are thus modified in the present chapter using the suggested modified run-up formula in Chapter 2. Additionally, the formulae by Pedersen (1996) are seen to overestimate the wave loads on un-protected crown wall faces due to over-predictions in the measurements caused by dynamic amplifications in the pressure transducers. The formulae are thus modified in this thesis based on measured wave loads from new pressure transducers with higher eigen-frequencies.

Typically, a triangular vertical load distribution is assumed on the base slap of a crown wall arising from the front corner pressures on the vertical front face. However, such assumed vertical pressures are seen to be highly conservative compared to measured vertical loads. Additionally, when ensuring sufficient stability of the crown wall in the design conditions an extra safety is included if using the assumed vertical pressures due to the ignored time lag between horizontal and vertical wave loads on the superstructure. An SWL-rise resulting in SWL just beneath the crown wall base plate can be critical, since this is seen to significantly increase the vertical loads on the monolithic structure.

The design formulae by Pedersen (1996) are based on the wave loads on a static structure. However, if allowing for small displacements of the crown wall in the design conditions the loads are significantly reduced, which indicates an extra safety in many existing structures. By using a Finite Element model it is concluded that the most important failure mode of a crown wall is sliding on the core material.

(www.findlays.com, 2013)

CHAPTER #4

SINGLE WAVE OVERTOPPING VOLUMES ON RUBBLE MOUND BREAKWATER CROWN WALLS

In this chapter existing design formulae for estimation of individual wave overtopping volumes on rubble mound breakwaters are modified to provide better estimates in shallow-water wave conditions.

4.1 Wave Overtopping on Rubble Mound Breakwaters in Deep and Shallow-Water Wave Conditions

Recently, Pullen et al. (2007) suggested using the maximum overtopping volume V_{max} during a storm instead of the average overtopping discharge q since V_{max} provides more direct estimates of hazards from wave overtopping on coastal protection structures. Such, low-exceedance overtopping volumes require knowledge on the distribution of individual overtopping volumes, which is evaluated for a number of different coastal structures by Franco et al (1994), Van der Meer & Jansen (1994) and Victor et al. (2012). However, the studies are based on conditions with relatively deep-water Rayleigh-distributed waves.

Paper 7 describes a physical study with 162 model tests conducted to determine the influence from finite water depth on the distribution of individual overtopping wave volumes. The study is performed in a wave flume and covers tests with both deep and shallow-water wave conditions. Target test ranges are given in Table 4. The procedure in Paper 7 was to evaluate the performance of selected state-of-art tools for estimation of average overtopping discharges in deep and shallow-water wave conditions. These overtopping discharges were hereafter used for estimation of the number of overtopping waves in deep and shallow-water wave conditions, which again were used for estimation of individual wave overtopping volumes. The study in Paper 7 concluded that existing tools for estimation of number of overtopping waves and estimation of distribution of overtopping wave volumes were not covering the effects of shallow-water wave conditions. The tools were thus extended in Paper 7 to include the effects of depth-limited waves.

The procedure of including the depth-limitation effects is briefly described in the following. However, initially the performance of existing state-of-art tools is evaluated for estimation of average overtopping discharges.

4.2Average Overtopping Discharge in Deep and Shallow-Water Wave Conditions

The crest freeboard on rubble mound breakwaters is typically designed based on the average overtopping discharge q with a specific return period. One of the most recent state-of-art tools for estimation of q is the *CLASH Overtopping Neural Network* (Van Gent et al., 2007) which is developed based on 10532 wave overtopping tests on various coastal structures, see (Verhaege et al., 2003) and (Van der Meer et al., 2009).

In Figure 19, measured average overtopping volumes from tests on a rubble mound breakwater in deep and shallow-water wave conditions, described in Paper 7, are compared to the estimated volumes from the Overtopping Neural Network. As can be seen, good agreement is obtained between measured and estimated q for both the evaluated deep-water and shallow-water wave conditions, except for the smallest discharges which are slightly overestimated by the neural network. Evaluated ranges for q are summarized in Table 6.

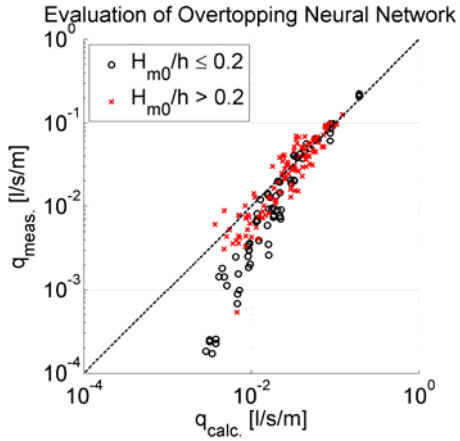

Figure 19. Evaluation of Overtopping Neural Network for estimation of average overtopping discharges in deep and shallow-water wave conditions. Discharges are in model scale (1:30). (Paper 7)

4.3 Number of Overtopping Waves on Rubble Mound Breakwaters in Deep and Shallow-Water Wave Conditions

Besley (1999) derived the formulae in (17) for estimation of the number of overtopping waves N_{ow}. N_w is the number of waves during the storm.

$$\begin{aligned}
&\frac{N_{ow}^{Besley}}{N_w} = 55.4 \cdot Q_*^{0.634} && \text{for } Q_* < 8 \cdot 10^{-4} \\
&\frac{N_{ow}^{Besley}}{N_w} = 2.50 \cdot Q_*^{0.199} && \text{for } Q_* < 8 \cdot 10^{-4} \le 1 \cdot 10^{-2}, \quad Q_* = q / \left(T_m \cdot g \cdot H_{1/3} \right) \\
&\frac{N_{ow}^{Besley}}{N_w} = 1 && \text{for } Q_* > 1 \cdot 10^{-2}
\end{aligned} \tag{17}$$

Measured ratios of N_{ow}/N_w are compared to the estimates by Besley (1999) in Figure 20. As can be seen, N_{ow} is underestimated for intermediate to shallow-water waves, H_{m0}/h>0.2, because the overtopping volumes are more evenly distributed in shallow-water conditions compared to deep-water conditions.

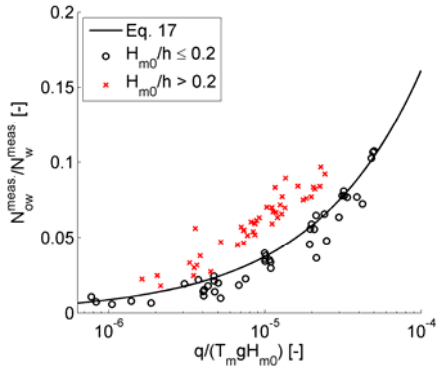

Figure 20. Comparison of measured number of overtopping waves N_{ow} against the estimated values by Besley (1999). (Paper 7)

4.3.1 New Correction Factor

To incorporate the effects of depth limitation in the formula by Besley (1999), Paper 7 suggests including a correction factor *C1* based on the incident wave height distribution by using the ratio $H_{m0}/H_{1/10}$. The factor is given in (18) (valid for $Q_* \le 10^{-4}$) and the performance of the factor is illustrated in Figure 21 where relatively good agreement is obtained between measured and estimated values of N_{ow} (using the modification factor). Evaluated ranges for N_{ow} are summarized in Table 6.

$$N_{ow}^{\text{mod}} = N_{ow}^{Besley} \cdot C1$$

$$C1 = \begin{cases} 1 & \text{for} \quad H_{m0} / H_{1/10} \le 0.848 \quad \text{or} \quad H_{m0} / h \le 0.2 \\ -6.65 + \dfrac{H_{m0}}{H_{1/10}} \cdot 9.02 & \text{for} \quad H_{m0} / H_{1/10} > 0.848 \quad \text{and} \quad H_{m0} / h > 0.2 \end{cases} \tag{18}$$

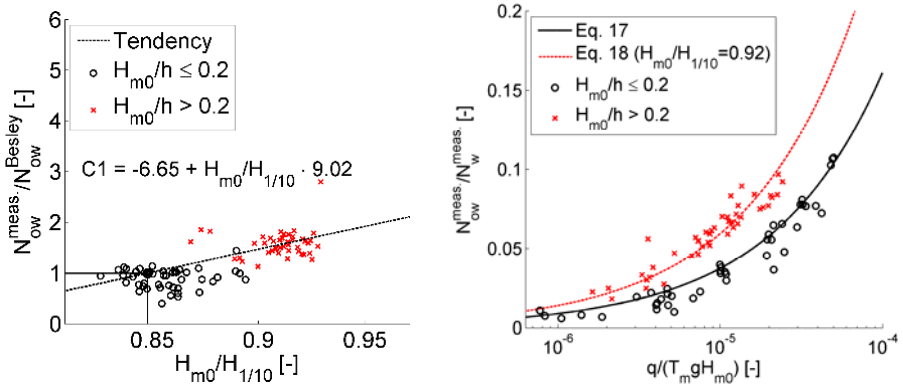

Figure 21. ***(left)*** **Influence from the ratio $H_{m0}/H_{1/10}$ on the number of overtopping waves N_{ow}.** ***(right)*** **Evaluation of modification factor for including the effect shallow water wave conditions on the incident waves in estimation of N_{ow}. (Paper 7)**

4.4 Individual Wave Overtopping Volumes on Rubble Mound Breakwaters in Deep and Shallow-Water Wave Conditions

For caisson breakwaters in deep-water wave conditions Franco et al. (1994) found that the distribution of individual overtopping wave volumes follows a Weibull-distribution, which can be re-written to obtain the maximum overtopping volume V_{max}, given in (19). A is a scale factor, and b is a shape factor, and they are related using (20).

$$V_{\max} = \frac{A}{N_{ow}} \cdot \left[Ln\left(N_{ow} + 1\right) \right]^{1/b} \cdot V_{total} \tag{19}$$

$$A = \frac{1}{\Gamma\left(1 + \frac{1}{b}\right)} \tag{20}$$

Van der Meer & Jansen (1994) and Franco et al. (1994) obtained a shape-factor of approximately 0.75 for both dikes and caisson breakwaters in relatively deep-water wave conditions. Victor et al. (2012) suggested the prediction formula in (21) for low-crested smooth structures including the effects of the structure front-slope cotα (range $0.36<\cot\alpha\le 2.75$) and the relative crest ratio R_c/H_{m0} (range $0.1\le R_c/H_{m0}\le 1.69$).

$$b\left(\frac{R_c}{H_{m0}}, \alpha\right) = \exp\left(-2.0\frac{R_c}{H_{m0}}\right) + \left(0.56 + 0.15\cot\alpha\right) \tag{21}$$

In Figure 22, the performances of the shape factors by Van der Meer & Jansen (1994), Franco et al. (1994), and Victor et al. (2012) are evaluated in deep and shallow-water wave conditions. As can be seen, good estimates are obtained on V_{max} in deep water but the estimates are significantly overestimated in shallow-water conditions.

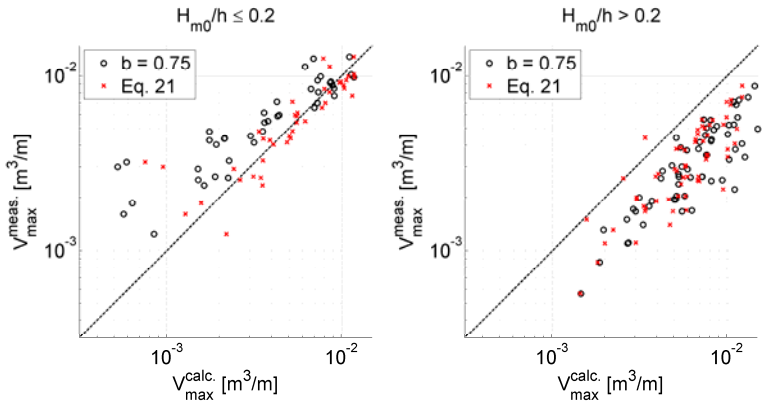

Figure 22. (*left*) Comparison between measured and estimated V_{max} in deep water wave conditions ($H_{m0}/h \leq 0.2$). (*right*) Comparison between measured and estimated V_{max} in shallow-water wave conditions ($H_{m0}/h > 0.2$). Volumes are in model scale (1:30). (Paper 7)

4.4.1 New Shape Factor

The variation of b is plotted as function of $H_{m0}/H_{1/10}$ in Paper 7. b is based on a least square fit against the 30% highest measured individual overtopping volumes from the tests. A formula for direct estimation of b is suggested and given in (22). Alternatively, a correction factor $C2$ for modification of the shape factor by Victor et al. (2012) is given in (23).

$$b\left(\frac{H_{m0}}{H_{1/10}}\right)=\begin{cases}0.75 & \text{for} \quad H_{m0}/H_{1/10}\leq 0.848 \quad \text{or} \quad H_{m0}/h\leq 0.2\\ -6.1+\dfrac{H_{m0}}{H_{1/10}}\cdot 8.08 & \text{for} \quad H_{m0}/H_{1/10}>0.848 \quad \text{and} \quad H_{m0}/h>0.2\end{cases} \tag{22}$$

$$b\left(\frac{R_c}{H_{m0}},\alpha,\frac{H_{m0}}{H_{1/10}}\right)=\left[\exp\left(-2.0\frac{R_c}{H_{m0}}\right)+\left(0.56+0.15\cot\alpha\right)\right]\cdot C2\left(\frac{H_{m0}}{H_{1/10}}\right)$$

where

$$C2\left(\frac{H_{m0}}{H_{1/10}}\right)=\begin{cases}1 & \text{for} \quad H_{m0}/H_{1/10}\leq 0.848 \quad \text{or} \quad H_{m0}/h\leq 0.2\\ -10.8+\dfrac{H_{m0}}{H_{1/10}}\cdot 13.9 & \text{for} \quad H_{m0}/H_{1/10}>0.848 \quad \text{and} \quad H_{m0}/h>0.2\end{cases} \tag{23}$$

The modified shape factors are plotted against measured V_{max} in Figure 23. As seen, relatively good agreement is obtained in both deep and shallow-water wave conditions using both formulations of the shape factor. However, it is expected that the shape factor by Victor et al. (2012) modified for shallow-water wave conditions will provide better estimates in situations with low R_c/H_{m0} ratios and for situations with front slopes that are very different from the evaluated in the present case.

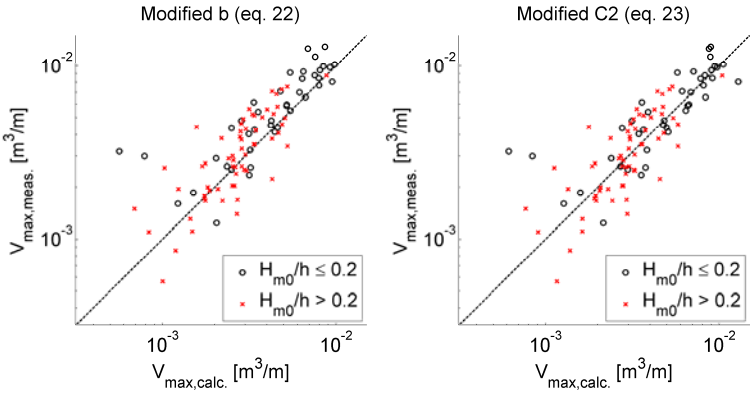

Figure 23. ***(left)*** **Evaluation of calculated maximum overtopping single volume with modified *b* in accordance with (22).** ***(right)*** **Evaluation of calculated maximum overtopping single volume with modified *C2* in accordance with (23). Volumes are in model scale (1:30). (Paper 7)**

Table 6. Investigated parameter ranges in modified design formulae for V_{max}. (Paper 7)

Parameters	Ranges
H_{m0}/h	0.19 – 0.55
R_c/H_{m0}	0.9 – 2.0
ξ_m	3.3 – 4.6
N_{ow}/N_w	0.006 – 0.12
$q/(T_m g H_{m0})$	$7.729 \cdot 10^{-7}$ – $6.19 \cdot 10^{-5}$

4.5 Summary of Findings in Chapter

Besides wave loads on coastal protection structures also the wave overtopping is an important design parameter. In this chapter, the performance of existing state-of-art tools for estimation of average and single overtopping wave volumes on rubble mound breakwaters is evaluated in deep and shallow-water wave conditions.

It is concluded, that the *CLASH Overtopping Neural Network* (Van Gent et al., 2007) is providing predictions which are in relatively good agreement with small scale measurements from model tests in deep and shallow-water wave conditions.

However, problems are observed from a comparison between measured and estimated single overtopping wave volumes on structures in shallow water. Initially, the formulae by Besley (1999) are seen to underestimate the number of overtopping waves on rubble mound breakwaters in shallow-water wave conditions. Secondly, existing studies on the Weibull-distribution shape factors (which are used to describe the distribution of individual overtopping volumes) seems to ignore the influence from shallow-water wave conditions. The depth-limitation effects in the formulae by Besley (1999) and in the Weibull-distribution shape factor are thus included in the present chapter by introducing the effects of altered wave height distributions in shallow-water wave conditions.

Juvre Dike breached after the storm surge in 1999 (www.kyst.dk, 2013)

CHAPTER #5

OVERTOPPING FLOW PARAMETERS ON SEA DIKES

In this chapter existing design formulae for estimation of overtopping flow parameters on sea-dikes are extended to provide better estimates in oblique and short-crested waves.

5.1 Overtopping Flow Parameters on Sea Dikes

In low-lying areas, dikes and levees are used as coastal defense structures for protection against flooding. Experiences from the Netherlands have shown that breaches of dikes are often caused by wave overtopping, and that the failure mostly starts on the crest and landward slope of the structures (Van der Meer et al., 2006). Thus, wave overtopping is an important parameter for the design crest level of such structures and an increased wave overtopping due to SWL-rise, can have fatal consequences.

Extensive analysis is required on the loading on dike slopes from wave overtopping. In recent time, the hydraulic load from wave overtopping on sea dikes has been directly related to the overtopping flow parameters, such as the overtopping flow velocity, *u*, and the overtopping flow depth, *h.* The overtopping flow parameters are coupled to the erosion of the dike in Van der Meer et al. (2006, 2010).

However, until now the estimation of wave overtopping flow parameters and the investigation of dike erosion have been limited to long-crested head-on waves, although wave overtopping in many sites was caused by short-crested oblique waves.

The objective in Paper 5 was to cover this white spot by extending formulae for estimation of overtopping flow parameters on sea dikes to cover also the influence from short-crested and oblique waves. Additionally, the objective was to analyze the probability distribution of flow parameters.

5.2 Existing Knowledge on Influence from Oblique and Short Crested Waves on Sea Dikes in 3-D

De Waal & van der Meer (1992) evaluated the influence of berms, roughness of the slope, and oblique short-crested waves on wave overtopping and wave run-up levels on sea dikes. The effects were incorporated using so-called reduction factors γ.

For wave overtopping De Waal & van der Meer (1992) suggested to include the influence from oblique waves using the reduction factor, γ_β, defined in (24), based on tests with smooth impermeable 1:2 and 1:4 slopes. β is the angle between the mean wave direction of wave propagation and the axis perpendicular to the structure (for head on wave attack $\beta = 0°$).

$$\text{Long-crested waves: } \gamma_\beta = \begin{cases} 1.0 & \text{for,} \quad 0^\circ \le \beta \le 10^\circ \\ \cos^2(\beta - 10^\circ) & \text{for,} \quad 10^\circ \le \beta \le 50^\circ \\ 0.6 & \text{for,} \quad \beta \ge 50^\circ \end{cases} \tag{24}$$

$$\text{Short-crested waves: } \gamma_\beta = 1 - 0.0033 \cdot \beta$$

For wave run-up, De Waal & van der Meer (1992) suggested including the effect of oblique and short-crested waves by using the reduction factor, γ_β, defined in (25).

$$\text{Long-crested waves: } \gamma_\beta = \begin{cases} 1.0 & \text{for,} \quad 0^\circ \le \beta \le 10^\circ \\ \cos(\beta - 10^\circ) & \text{for,} \quad 10^\circ \le \beta \le 50^\circ \\ 0.6 & \text{for,} \quad \beta \ge 50^\circ \end{cases} \tag{25}$$

$$\text{Short-crested waves: } \gamma_\beta = 1 - 0.0022 \cdot \beta$$

5.3 Existing Knowledge on Overtopping Flow Parameters in 2-D

Schüttrumpf (2001), Van Gent (2002), and Schüttrumpf & Van Gent (2003) developed semi-empirical formulae for estimation of overtopping flow parameters in case of long-crested and head-on waves. The formulae were calibrated against small and large-scale model tests in wave flumes. Bosman (2008) carried out further analysis on the test data by Schüttrumpf (2001) and Van Gent (2002), where the formulae were extended to include a better description of the influence from the seaward slope.

Formulae on the flow velocity exceeded by 2% of the incoming waves on the seaward slope $u_{2\%,sea}$, on the dike crest $u_{2\%,crest}$, and on the landward slope, $u_{2\%,land}$, are presented in Table 7. Formulae on the overtopping flow depths exceeded by 2% of the incoming waves are presented in Table 8 with the definitions in Figure 24. $R_{u,2\%}$ in Table 8 is given in (9) in Table 2.

Table 7. ***Flow velocity prediction formulae.*** **(Van Gent, 2002)**

Structure part	Flow velocity formulae
Seaward slope	$\frac{u_{2\%,sea}(Z_A)}{\sqrt{gH_{m0}}} = c^*_{A,u}\sqrt{\frac{R_{u,2\%}-Z_A}{H_{m0}}}$
Dike crest	$\frac{u_{2\%,crest}(x_c)}{u_{2\%,sea}(R_C)} = \exp\left(-c^*_{C,u}\frac{x_c \cdot f}{h_{2\%,crest}}\right)$
Landward slope	$u_{2\%,land}(s_B) = \frac{k_2}{k_3} + k_4 \exp(-3 \cdot k_2 \cdot k_3^2 \cdot s_B)$ *with* $k_2 = \sqrt[3]{g \cdot \sin\alpha_l}$; $k_3 = \sqrt[3]{\frac{1}{2} \cdot \frac{f}{h_{0,2\%} \cdot u_{0,2\%}}}$ $k_4 = u_{0,2\%} - \frac{k_2}{k_3}$

$c^*_{A,u}$ and $c^*_{C,u}$ are empirical coefficients calibrated to be 1.30 and 0.5, respectively.

Table 8. ***Flow thickness prediction formulae.*** **(Van Gent 2002)**

Structure part	Flow depth formulae
Seaward slope	$\frac{h_{2\%,sea}(Z_A)}{H_{m0}} = c^*_{A,h}\frac{R_{u,2\%}-Z_A}{H_{m0}}$
Dike crest	$\frac{h_{2\%,crest}(x_c)}{h_{2\%,sea}(R_C)} = \exp\left(-c^*_{C,h}\frac{x_c}{B}\right)$
Landward slope	$h_{2\%,land} = \frac{h_0 \cdot u_0}{u_{2\%,land}(s_b)}$

$c^*_{A,h}$ and $c^*_{C,h}$ are empirical coefficients calibrated to be 0.15 and 0.40, respectively. B is the crest width cf. Figure 24, h_0 and u_0 are the flow depth and the flow velocity, respectively, in the beginning of the landward slope.

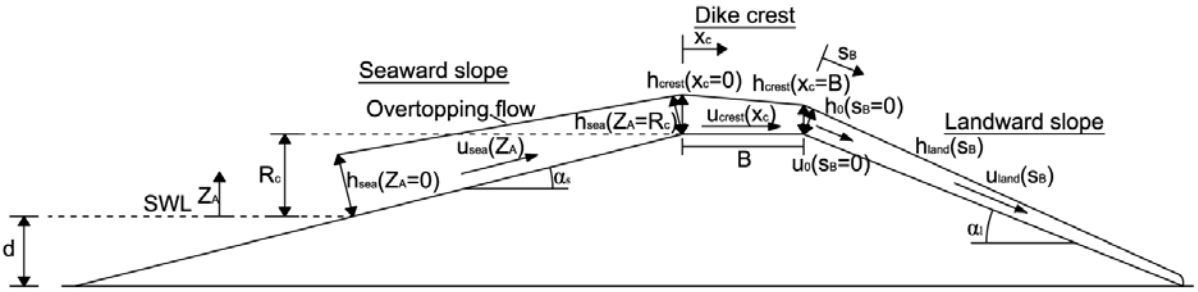

Figure 24. Definitions used in study on overtopping flow parameters on sea dikes. (Paper 5)

5.4 New Investigations on Overtopping Flow on Sea Dikes in Oblique and Short-Crested Waves

3-D tests were performed in a wave basin at Aalborg University – described in Paper 5. Two different models were evaluated in the study with two different orientations to the wave paddles. In Figure 25 the model with 37.5° orientation is illustrated. A typical Dutch dike geometry in scale 1:30 was evaluated in the study. Dimensions of the evaluated dike geometries are given in Paper 5.

Figure 25. Illustration of Dike Model Setup with and orientation of 37.5° relative to the wave paddles. (Paper 5)

5.4.1 New Measurement Procedure for Flow Velocities on Sea Dike Crests in Oblique and Short Crested Waves

Flow depths and flow velocities along the seaward slope, crest, and landward slope of the dike model were measured using resistance type depth gauges mounted on the dike surface. The flow depths were determined directly from the depth gauges, whereas the flow velocities were determined based on the detected time-lag between each pair of wave gauges when the overtopping wave volume passed the dike. The method (described in details in Paper 6) gave both the flow depth and flow velocity for each overtopping event. The flow velocities were for long-crested head-on waves validated against micro-propeller measurements.

5.4.2 New Investigations on Overtopping Flow Directions on Dike Crest in Oblique and Short Crested Waves

Examples of detected intensity of overtopping flow velocities and their flow directions on the dike crest are illustrated in Figure 26 and 27 in case of long and short-crested perpendicular and oblique waves, respectively. The conclusion in Paper 5 is that the flow directions for the highest measured velocities, which are of greatest importance in terms of erosion on the dike slopes, are very similar to the directions of the incident waves. This is valid both for long-crested and short-crested waves.

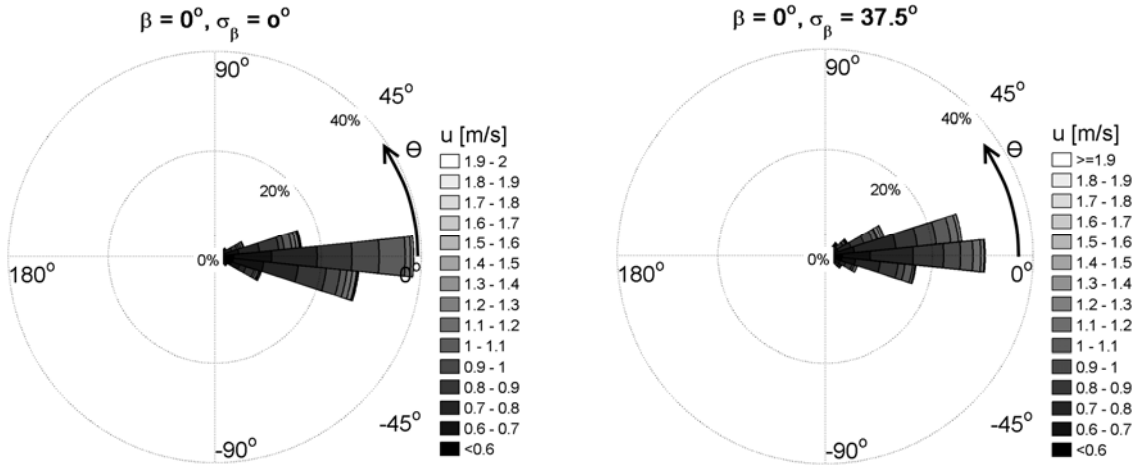

Figure 26. ***(Left)*** **Intensities of flow velocities and their directions on dike crest for long-crested waves with mean wave direction β = 0°.** ***(Right)*** **Intensities of flow velocities and their directions on dike crest for short-crested waves with mean wave direction β = 0°. (Paper 5)**

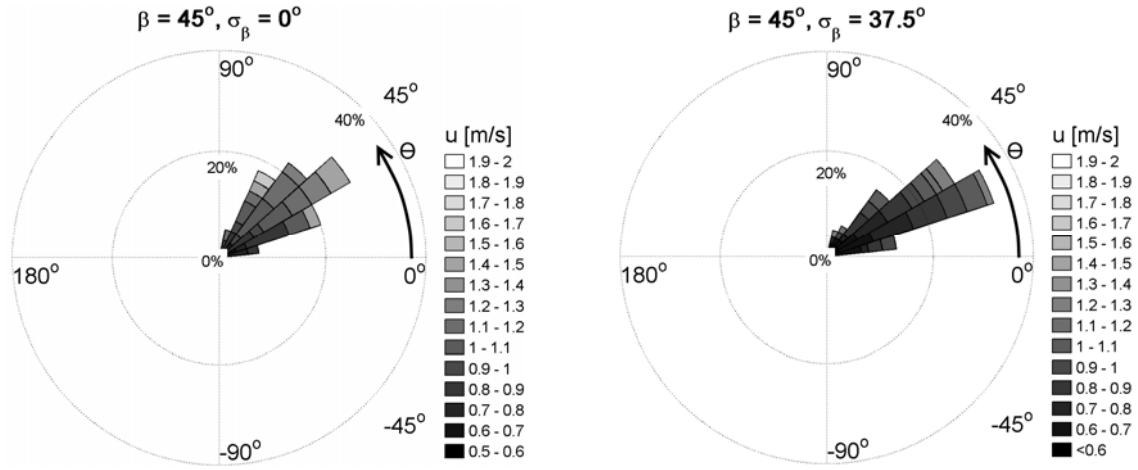

Figure 27. ***(Left)*** **Intensities of flow velocities and their directions on dike crest for long-crested waves with mean wave direction β = 45°.** ***(Right)*** **Intensities of flow velocities and their directions on dike crest for short-crested waves with mean wave direction β = 45°. (Paper 5)**

5.4.3 New Suggested Reduction Factor for Flow Parameters in Oblique and Short-Crested Waves

In paper 5, the influence from wave spreading and wave obliqueness on flow depths and velocities is incorporated in the formulae by Van Gent (2002) in Table 7 and 8 using the factor γ_β in (26) on the run-up levels. The factor is based on a least square fit to the data in Figure 28, which is obtained by adjusting the wave obliquity factor γ_β to fit to the measured flow depths and flow velocities from the tests. The proposed reduction factors for long and short-crested waves are similar to the formulae (25) of De Waal & Van der Meer (1992).

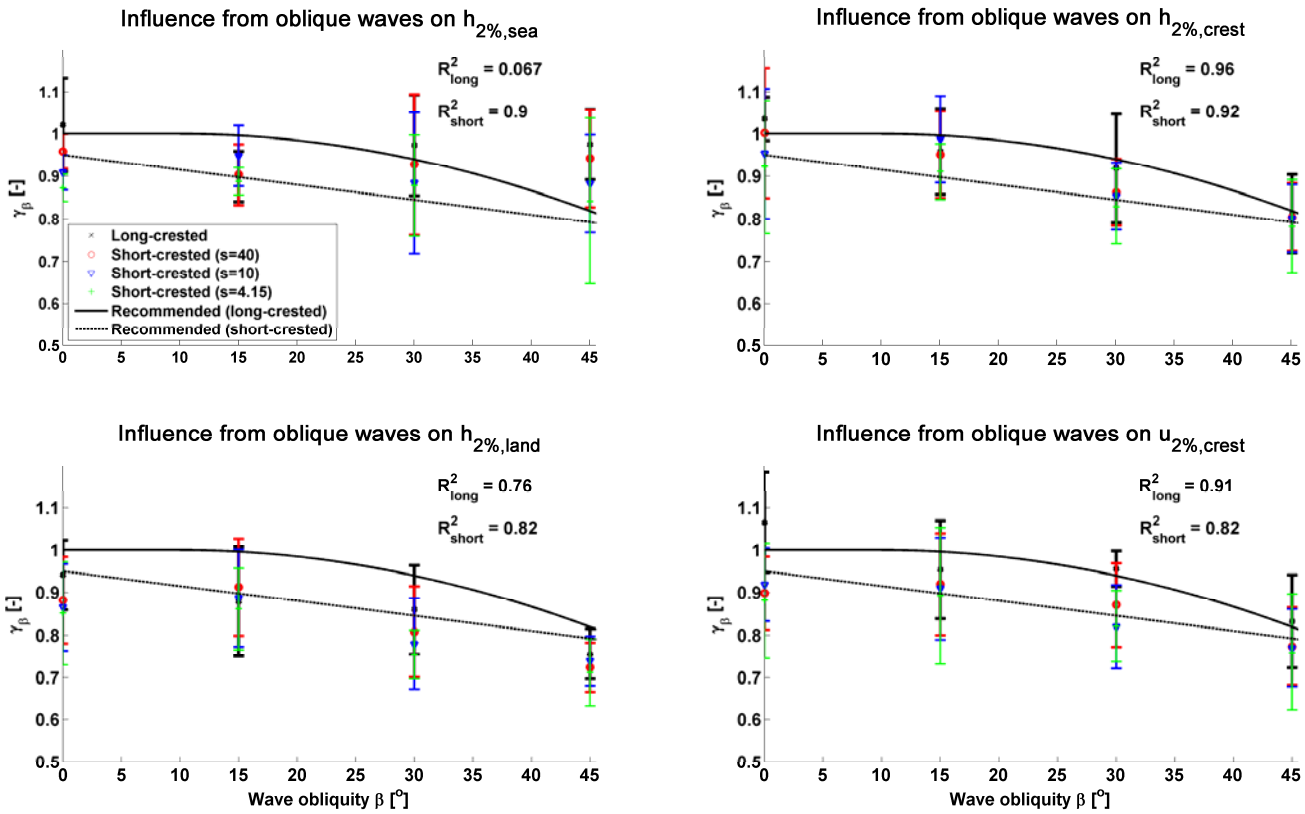

Figure 28. Suggested factors for the formulae by Van Gent (2002) to include the effects of oblique and short-crested waves. (Paper 5)

$$\text{Long-crested waves: } \gamma_\beta = \begin{cases} 1.0 & \text{for,} \quad 0^\circ \le \beta \le 10^\circ \\ \cos(\beta - 10^\circ) & \text{for,} \quad 10^\circ \le \beta \le 45^\circ \end{cases} \tag{26}$$

$$\text{Short-crested waves: } \gamma_\beta = 0.95 - 0.0035 \cdot \beta$$

5.4.4 New Investigations on Distribution of Individual Flow Parameters in Oblique and Short Crested Waves

The statistical distributions of *h* and *u* for individual overtopping events are determined in Paper 5. This gives the possibility of determining the cumulative erosion on the dike slopes and to estimate *u* and *h* with other exceedance probabilities than 2%.

If incident waves are Rayleigh-distributed, *h* and u^2 are found also to be Rayleigh-distributed, cf. Figure 29 and 30.

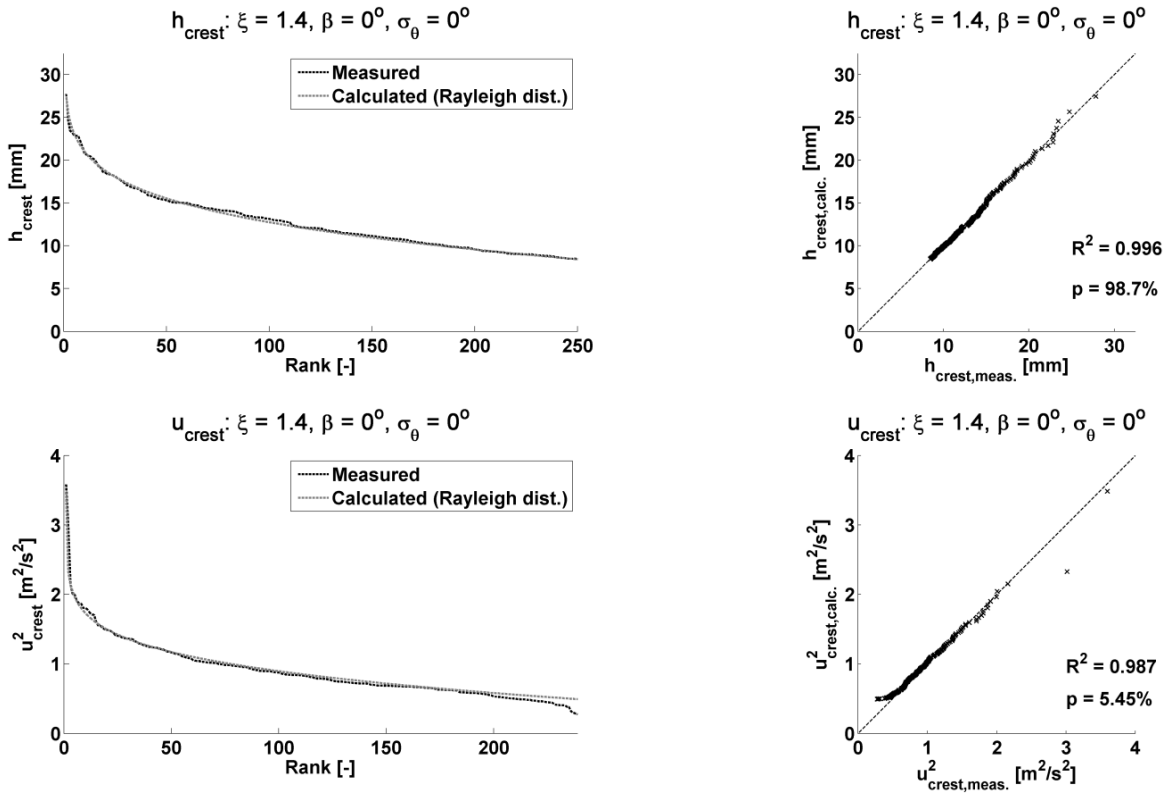

Figure 29. Statistical distributions of measured and calculated individual flow velocities and flow depths on dike crest in case of long-crested head-on waves. Flow depths and flow velocities are in model scale (1:30). (Paper 5)

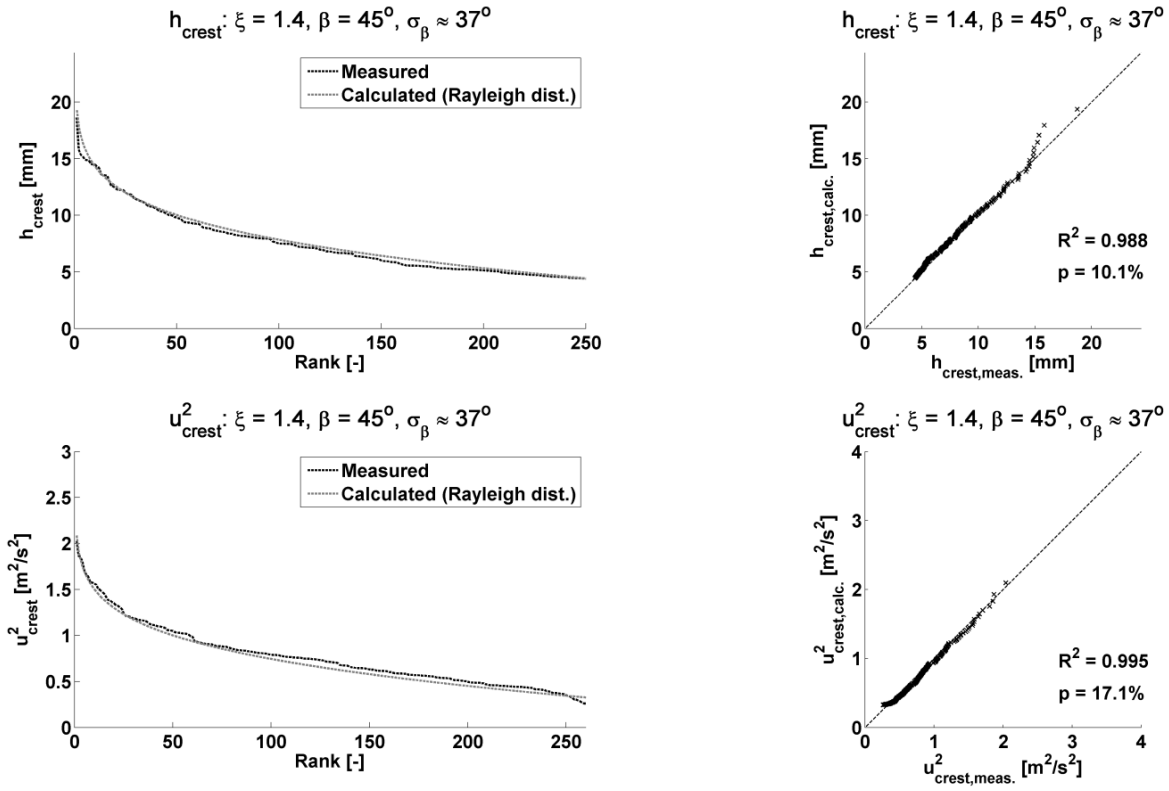

Figure 30. Statistical distributions of measured and calculated individual flow velocities and flow depths on dike crest in case of short-crested waves with β = 45 °. Flow depths and flow velocities are in model scale (1:30). (Paper 5)

The wave spreading and wave obliquity are seen not to affect the distribution of the overtopping flow parameters. It could have been expected that long and short-crested waves would not follow the same distribution because oblique overtopping events give more reduced flow velocities and flow depths. However, this does not seem to be the case.

5.5 Summary of Findings in Chapter

Overtopping flow velocities and flow depths are important parameters in relation to design of sea dikes to resist wave overtopping and to avoid dike breaches due to eroded crests and landward slopes. So far, the simulated overtopping volumes are based on assumed head-on long-crested waves, and thus the effects from possible short-crested oblique waves are ignored.

Extensions to existing formulae for estimation of overtopping flow depths and flow velocities on sea-dikes are suggested in this chapter to include the effects of wave obliquity and wave spreading. Additionally, the overtopping flow directions on the dike crest from oblique waves are investigated together with the distribution of individual overtopping flow parameters. The overtopping wave volumes with the highest flow velocities are seen to have the same direction as the incident wave obliquity, and individual overtopping flow parameters are seen to follow the incident wave height distribution.

PART #2

Case Studies

Damage after flood in the Netherlands, 1953 (Art Klein, Nederlands Fotoarcheif)

CHAPTER #6

DIKE CASE STUDY

In this chapter a case study is performed to evaluate the influence from climate changes and oblique short-crested waves on the overtopping flow parameters on sea-dikes.

6.1 Resilience of Sea Dikes against Wave Overtopping and Experience from In-Situ Tests

In general, two different failure mechanisms arise from wave overtopping on sea dikes (Steendam et al., 2010). The first failure mechanism arises from violent overtopping wave volumes, which erode the cover layer and after some time lead to the initial breaches. The second failure mechanism is the slip failure of steep landward slopes, which can lead to direct breach of the dike. Most sea-dikes in the past 50 years have been constructed with relatively mild sloping landward slopes (1:2.5 - 1:3) where it is more unlikely that slip failure will occur due to wave overtopping (Steendam et al., 2010).

The resilience of cover layers against wave overtopping is still not well documented, since small scale tests cannot be performed due to problems of scaling soil properties. Only a few large-scale tests have been performed in the Delta flume in the Netherlands by Oumeraci et al. (2000). However, such tests are very costly, so in recent time the erosion of cover layers on crests and landward slopes of sea dikes have been performed using in-situ tests with the so-called Wave Overtopping Simulator (Van der Meer et al., 2006, 2010), and (Steendam et al., 2010). The main approach in the studies with the Overtopping Simulator is to release water volumes from a reservoir on e.g. the dike crest corresponding to a certain sea condition. The flow parameters are then measured from each released volume, and the correlation with the slope erosion is determined. The principle of the Overtopping Simulator is illustrated in Figure 31

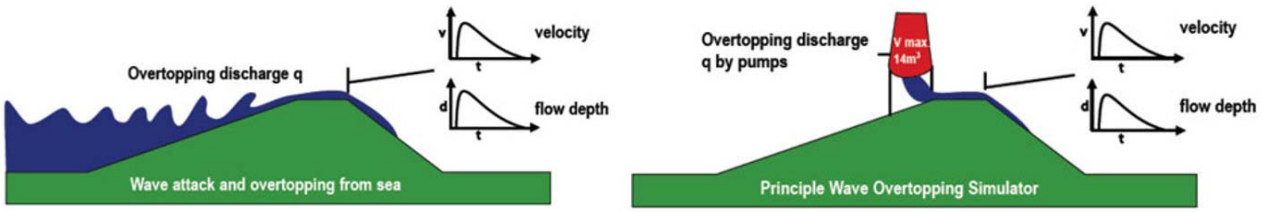

Figure 31. Principle of the Overtopping Simulator (vandermeerconsulting, 2013).

Typically, a few large volumes and many small volumes characterize the distribution of overtopping wave volumes (cf. Chapter 4). The individual wave volumes have different flow depths and flow velocities, which can then be related to the observed erosion on the cover layers.

As an example, using the overtopping simulator, Van der Meer et al. (2010) observed initial damage for flow velocities above 4 *m/s* on the Dutch "Vechtdijk". Moreover, Tung et al. (2012) observed initial damages for flow velocities between 2.1 *m/s* and 4 *m/s* - depending on the quality of the grass slope - on a sea dike in Vietnam. Steendam et al. (2011) observed initial damage on sea dikes in Belgium at flow velocities of 3.1 *m/s*. Photographs taken from the obtained failure modes in the prototype tests are shown in Figure 32.

Figure 32. Failures of landward slopes. (*left*) (Steendam et al., 2011), (*middle*) (Van der Meer, 2010), (*right*) (Tung et al., 2012).

The formulae by Van Gent (2002) (e.g. including the modification factor for oblique and short-crested waves) are used for calibration of the Overtopping Simulator. Additionally, the knowledge on the flow directions on the dike crest (which are discussed in the previous chapter) should be used in the future to correctly simulate the effects of oblique waves in the in-situ tests.

The influence from continuous overtopping wave volumes is in Van der Meer et al. (2010) incorporated using the so-called cumulative hydraulic load, D, (27) where u_c is the critical flow velocity (indicating the threshold for initial damage) and u_i are the individual measured flow velocities for each wave overtopping event i.

$$D = \sum_{i=1} \left(u_i^2 - u_c^2 \right) \quad \text{for} \quad u_i > u_c \tag{27}$$

As an example Van der Meer et al. (2010) made the following conclusions for the Vechtdijk using a critical flow velocity of u_c = 4 m/s:

- Start of damage: D = 500 m^2/s^2
- Various damaged locations: D = 1000 m^2/s^2
- Failure (by mole holed): D = 3500 m^2/s^2
- Non-failure for normal slope: D = 6000 m^2/s^2

The knowledge on the distribution of individual flow velocities presented in the previous chapter can be used to estimate the cumulative hydraulic load.

The resilience against wave overtopping on sea dikes is very individual due to the various types of cover layers and soil properties. Additionally, recent tests have shown that especially the transitions from slope to horizontal and slopes with obstacles such as stairs, are typically the most critical locations for erosion due to wave overtopping (Steendam et al., 2010). Thus, more in-situ tests are needed to provide well-documented guidelines for practical design.

6.2 Case Example on Influence from Oblique and Short-Crested Waves and SWL-rise on Flow Parameters

A case example is performed to illustrate the influence from oblique and short-crested waves on the overtopping flow velocities on the dike crest and landward slope. The case example is performed on the geometry illustrated in Figure 33, using intermediate water depth wave conditions; T_p=8 s, H_{m0}=2.56 m, H_{m0}/h=0.35, cot(α_s)=4, and B=9 m.

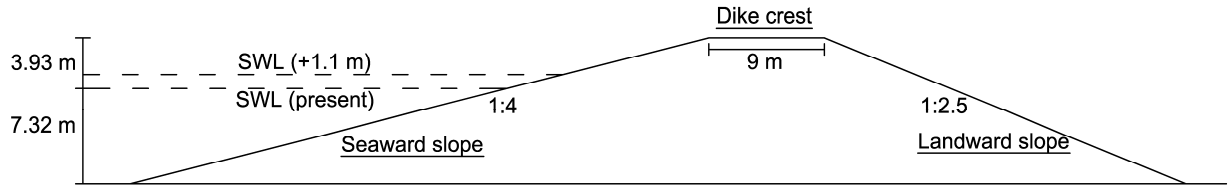

Figure 33. Dike structure evaluated in case example on influence from oblique and short-crested waves on overtopping flow parameters.

6.2.1 Influence from Oblique and Short-Crested Waves on Flow Parameters

The influence from wave obliquity for long- and short-crested waves on $u_{2\%}$ on the dike crest in case of varying R_c/H_{m0}-ratios is illustrated in Figure 34. Different values of the critical velocity, u_c, are included in the plot. Note that when u_c is higher than u the cover layer is eroded. As can be seen, the wave obliquity significantly influences $u_{2\%}/gH_{m0}^{0.5}$ on the dike crest where a higher influence from the wave obliquity is obtained for increasing R_c/H_{m0}-ratios.

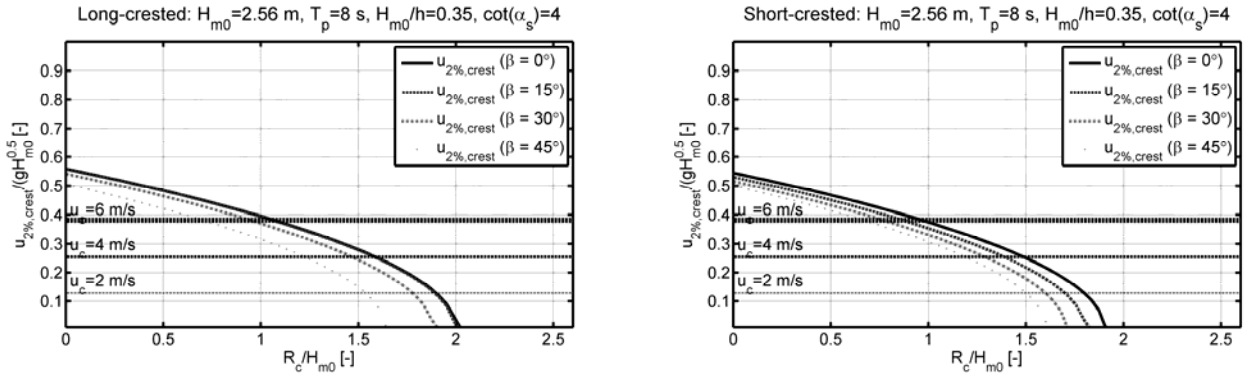

Figure 34. Comparison between flow velocities in oblique and head-on long- and short-crested waves.

6.2.2 Influence from SWL-rise on Flow Parameters

An SWL-rise of 1.1 *m* (illustrated in Figure 33) is assumed by year 2100 compared to present. The influence from the SWL-rise on the flow velocity is shown in Figure 35 in case of long and short-crested head-on and oblique waves (β=30°). As seen in Figure 35 (*left*) the flow velocity is especially increased on the dike crest in case of oblique and short-crested waves (163.8% by year 2100). For comparison, the flow velocity is increased by 58.26% in year 2100 in case of head-on long-crested waves.

In Figure 35 (*right*) it is seen, that if the cover layer on the crest of a sea dike in oblique (β=30°) and short-crested waves is initially designed for a critical velocity of 4 *m/s* (based on the formulae by Van Gent (2002) - without accounting for oblique and short-crested waves) the SWL can increase by up to 0.59 *m* to maintain the initial performance criteria.

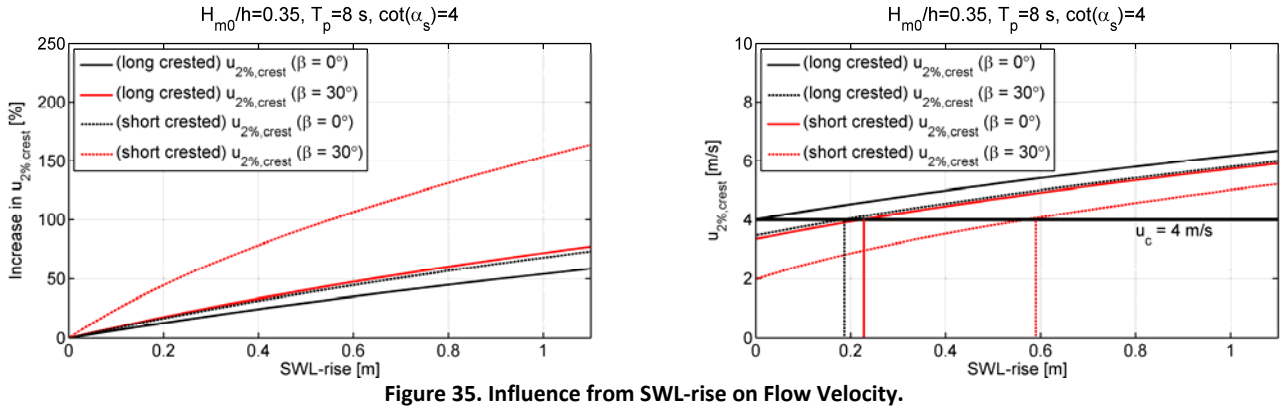

Figure 35. Influence from SWL-rise on Flow Velocity.

6.3 Summary of Findings in Chapter

Three-dimensional effects from oblique and short-crested waves have a significant influence on the overtopping flow parameters on sea dikes. It is thus important to include these effects when e.g. performing in-situ tests on the resistance against erosion of cover layers. Conservative and perhaps expensive structures can be obtained if applying the original formulae by Van Gent (2002) without accounting for the possible effects of 3-D-waves present at the site.

A structure which is initially designed based on head on long-crested waves but is attacked by oblique short-crested waves can withstand an SWL-rise of up to 0.59 *m* to keep the initial performance criteria.

Broken crown wall sections on the Tripoli Harbor NW breakwater after a storm in 1981 (Pedersen, 1996)

CHAPTER #7

RUBBLE MOUND BREAKWATER CASE STUDY

In this chapter a case study is performed to study the influence from SWL-rise on typical rubble mound breakwaters positioned in deep and shallow-water wave conditions. The study is performed using existing and modified design-formulae described in Part 1 of the thesis.

7.1 Design of Rubble Mound Breakwaters

External loads on rubble mound structures, due to wave attack, are typically defined by the environmental, hydraulic, geotechnical, and structural parameters (Van der Meer, 1995). Internal loads on the structure are the penetration of waves through the armor layers and core, leading to variations in pore pressures.

The structure response is defined by the loads and strength and can be described by parameters such as the damage to armor units, damage to superstructures, and the amount of wave overtopping. Thus, modifications should be performed to the structural parameters if obtaining undesired responses of the structure due to e.g. climate changes. The upgrades can be to modify the structure height, the armor configuration, or the superstructure.

In the following, the influence from SWL-rise on the structural response of rubble mound breakwaters in deep and shallow-water wave conditions is evaluated, using existing and present design formulae. The three most important design parameters for the design of rubble mound breakwaters are considered: damage to armor layer, wave overtopping, and stability of superstructures.

7.2 Deep and Shallow Water Examples

A case study is performed on the shallow and deep-water structures in Figure 36. The foreshore slope is $\cot(\alpha_f)$=100 and the armor units in both cases are designed for a so-called damage parameter of S = 3. Additionally, both structures are designed for average overtopping discharges of approximately 3 *l/s/m* in the design conditions.

Projections on future SWL-rise vary significantly and are highly dependent on the evaluated SRES-scenario, cf. Table 1. In the following an SWL-rise of 1.1 *m* by year 2100 compared to present is assumed. The SWL-rise is illustrated in Figure 36. $T_{-1.0}$ = 10 *s* is used in the examples. Both the water depth h and wave height H_{m0} are increased in the shallow-water case to maintain a constant ratio of H_{m0}/h=0.5 when increasing the SWL.

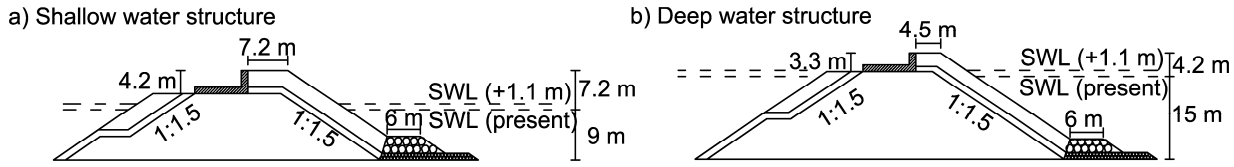

Figure 36. (*left*) Considered breakwater designed for shallow-water wave conditions. (*right*) Considered breakwater designed for deep-water wave conditions.

7.3 Stability of Armor Layer in Deep and Shallow Water-Wave Conditions

The formulae by Van der Meer (1988) for stability of rock slopes in deep and shallow-water wave conditions are applied to evaluate the influence from SWL-rise on the damage parameter S. The Battjes & Groenendijk (2000)-distribution is applied to the Van der Meer (1988) formula based on $H_{2\%}$ in the shallow-water case due to non-Rayleigh distributed waves. The increase in S is plotted in Figure 37.

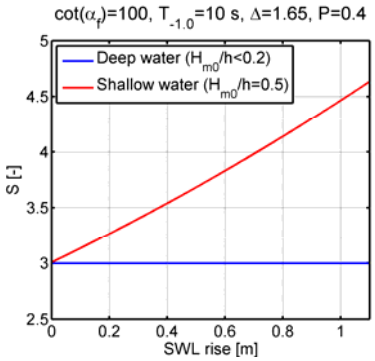

Figure 37. Influence from SWL-rise on the average overtopping discharge in deep and shallow-water wave conditions.

As can be seen in Figure 37 the SWL-rise will not lead to increase in damage on the armor for the deep-water structure. Contrary, the stability of the armor units in the shallow-water case is influenced due to increases in wave height. However, according to Van der Meer (1988) a damage of S = 3 – 5 denotes intermediate damage and S = 8 denotes total failure of the two diameter thick rock armor layer slopes. Thus, the influence of climate changes on armor stability can be seen to be rather small, but more frequent repairs are expected in shallow water. It should be mentioned, that stability of the toe and stability of armor units on the crest and at the rear side can also be critical design parameters. However, these are not evaluated in the present case.

7.4 Wave Overtopping on Rubble Mound Breakwaters in Deep and Shallow-Water Wave Conditions

The structures in Figure 36 are considered again and the CLASH Neural Network (Van Gent et al., 2007) is used to evaluate the influence from the SWL-rise on the average overtopping discharge in Figure 38. As can be seen, the wave overtopping is increased by more than a factor 5 in the shallow-water case and by a factor 3 in the deep-water case for a 1.1 *m* SWL-rise.

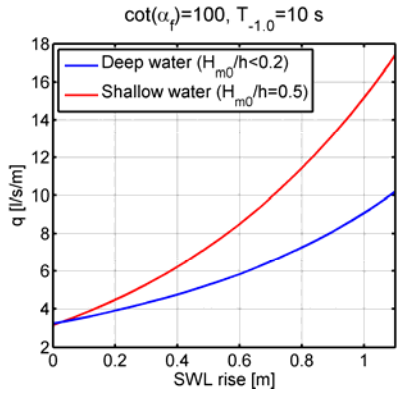

Figure 38. Influence from SWL-rise on the average overtopping discharge in deep and shallow-water wave conditions.

The modified formulae in (18) and (22) are used in (19) to estimate the influence from SWL-rise on V_{max} on the structures in Figure 36. The estimated influence on V_{max} from a 1.1 *m* SWL-rise is shown in Figure 39 (*left*). From the comparison, it is seen that V_{max} is increased by 129% in the shallow-water case, and by 79% in the deep-water case by year 2100. In Figure 39 (*right*) a comparison is made between the estimated V_{max} in the shallow-water case using the original and modified design formulae. From the comparison it is seen that when applying the modified formulae the SWL can rise by up to 0.9 *m* to maintain the same V_{max} as obtained using original conservative formulae. The Battjes & Groenendijk (2000)-distribution is used to estimate $H_{1/10}$. Again, both the water depth h and the wave height H_{m0} are increased in the shallow-water case.

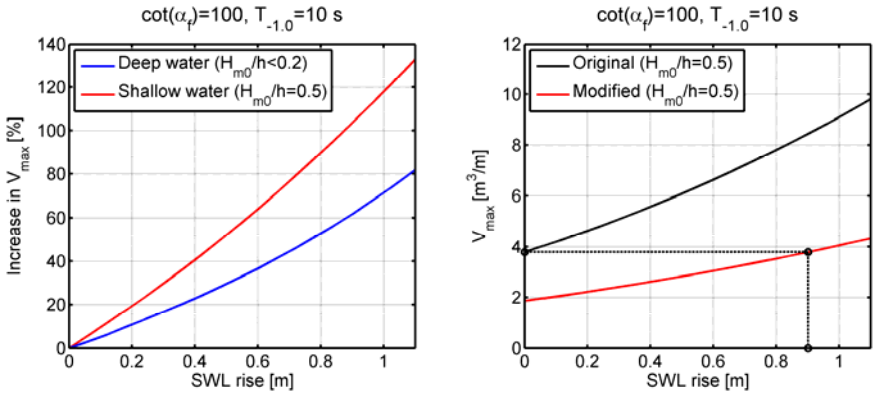

Figure 39. Influence from SWL-rise on V_{max} estimated using original and modified design formulae.

7.5 Wave Loads on Crown Walls in Deep and Shallow Water Wave Conditions

The modified run-up formula in (10) and the modified design formulae in (11) are used in Figure 40 to estimate the influence from SWL-rise on $F_{H,0.1\%}$ on the structures in Figure 36. As can be seen, the loads on the crown wall increase by up to 105% in the shallow-water case, whereas the loads increase only by approximately 30% in the deep-water case.

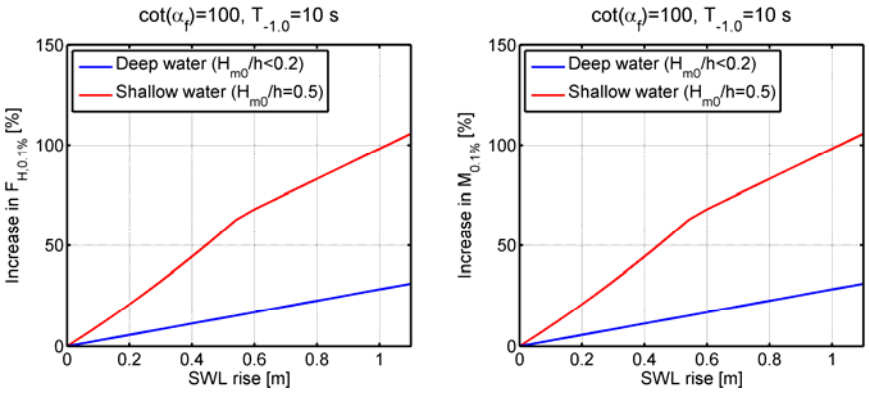

Figure 40. Influence from SWL rise on wave loads on crown walls in deep and shallow-water wave conditions.

To evaluate the actual effect from SWL-rise on the stability of the considered superstructures in Figure 36 the stability functions $g_{sliding}$ and $g_{overturning}$ are considered for sliding (28) and overturning (29), respectively. F_g and M_g in (28) and (29) are the stabilizing vertical load and stabilizing overturning moment of the crown wall, respectively. Hydrostatic pressure is added to the triangular pressure if the SWL is above the base slap. μ is the friction coefficient between the base slap and the core material of the breakwater (μ = 0.6 in the given example). The crown walls on both the deep water and shallow-water structures are initially designed to have a *g*-factor of 1.2. If *g*<1 the crown wall becomes unstable (sliding or overturning).

$$g_{sliding} = \frac{\left(F_g - F_{V,0.1\%}\right)\mu}{F_{H,0.1\%}} \left(<1 \quad \Rightarrow \quad \text{sliding}\right) \tag{28}$$

$$g_{overturning} = \frac{M_{g,0.1\%}}{M_{tot,0.1\%}} \left(<1 \quad \Rightarrow \quad \text{overturning}\right) \tag{29}$$

The stability factors in (28) and (29) are plotted as function of the SWL-rise in Figure 41. As can be seen, the stability of the crown walls against sliding and overturning is very vulnerable to SWL-rise. Especially in the shallow-water case the SWL-rise proves to have a significant effect on the crown wall stability where the structure becomes unstable already at an SWL-rise of ≈0.08 *m*.

$g_{sliding}$ seems to decrease faster than $g_{overturning}$, which confirms the conclusions presented in Paper 9 that sliding is in many cases the most important failure mode. The sudden decrease in $g_{sliding}$ and $g_{overturning}$ at SWL-rise above 0.9 *m* in the deep-water case is due to an added hydrostatic pressure from SWL on the access road. It should be mentioned, that the vertical loads will increase dramatically when the SWL is just beneath the base slap, cf. Figure 15. This effect is, however, not included in the present example. Additionally, it should be mentioned that the assumed triangular vertical wave pressure based on the base front corner pressure $P_{b,0.1\%}$ provides very conservative estimates, cf. Figure 14.

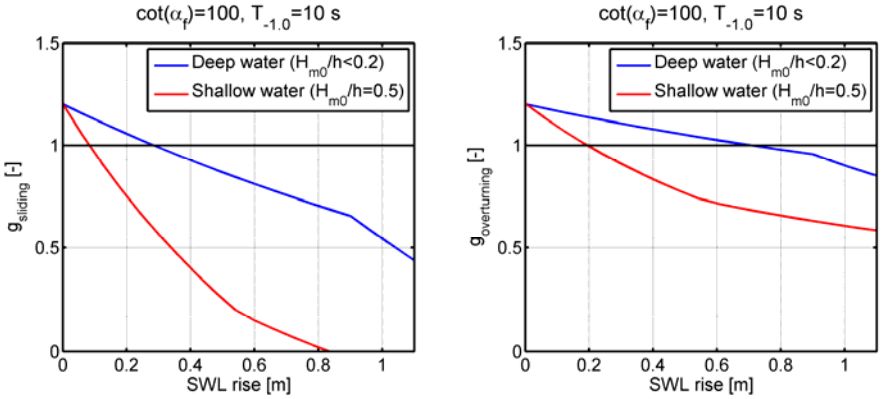

Figure 41. Influence from SWL rise on stability of crown walls in deep and shallow-water wave conditions.

Figure 42 shows the evaluation of the effect of the incorporated depth-limitation in the updated formulae (10) and (11), which are compared to the original design formulae. Only the shallow-water case is considered, and as can be seen, an SWL-rise of up to 0.83*m* can be accepted in the evaluated example in order to reach the same initial conditions as obtained by the Pedersen-formulae. This demonstrates that shallow-water structures designed after the original Pedersen (1996) formula are quite conservative and can withstand even a large SWL-rise.

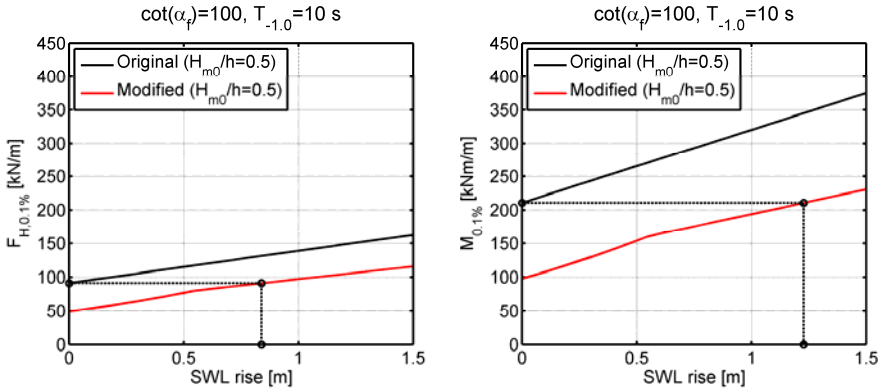

Figure 42. Influence from SWL rise on wave loads estimated using original and modified design formulae.

7.6 Summary of Findings in Chapter

Based on the considered structures in Figure 36 and an assumed SWL-rise of 1.1 *m* by year 2100 the conclusion is, that an SWL-rise will only have minor effect on the armor unit stability in the structure lifetime, since only intermediate damage is obtained in year 2100. In fact, since most structures are designed for a lifetime of approximately 50 years, i.e. SWL rise of <0.55 *m* (compared to year 2100 with SWL rise of 1.1 *m*), the influence from an SWL-rise on the stability of armor units is almost negligible.

The average overtopping discharge is increased by more than a factor 5 in the shallow-water case in year 2100. However, if considering only the next 50 years, the influence from an SWL rise on *q* is relatively small. Additionally, it should be kept in mind that if the structures are designed based on model scale tests (which is the typical procedure in many projects) the design overtopping discharge is already significantly influenced by scale and model uncertainties, cf. Chapter 2.

The influence from an SWL-rise on the maximum overtopping wave volumes is somewhat smaller than the influence on overtopping discharges. If the structures are initially designed based on the original formulae for estimation of V_{max} an SWL-rise by up to 0.9 *m* can be accepted to maintain the same V_{max} as in the initial design conditions.

Wave loads on the crown wall superstructure are dramatically increased in shallow-water wave conditions. If considering the stability against sliding and overturning an increase in SWL-rise of only ≈0.08 *m* will result in sliding of the crown wall. Additionally, it should be kept in mind, that extra safety is included

in the crown wall design if allowing for small displacements, since this will dampen the wave loads on the structure, cf. Chapter 3.

To summarize, rubble mound breakwaters in shallow waters are significantly influenced by SWL-rise compared to structures in deep water due the increase in the maximums wave heights in depth-limited conditions. However, some designs may already include an extra safety against the effects of climate changes since originally based on deep-water design formulae.

Wave Dragon wave energy converter (www.wavedragon.dk)

CHAPTER #8

DAMPENING OF WAVES BY WAVE ENERGY CONVERTERS

This chapter evaluates the potential of using wave energy converters for coastal protection. Among others, the evaluation is based on a case study in Santander bay, Spain.

8.1 Wave Energy Converters for Coastal Protection

Academic research groups and companies worldwide have investigated and developed a significant amount of Wave Energy Converters (WECs). Although many designs have been evaluated through small scale testing in the laboratory, only a limited number of concepts have progressed to sea testing (WAVEPLAM, 2009). Typical barriers for the development are the funding of the projects, the survivability of the devices, and the costs of produced electricity (compared to other renewable energy sources such as solar and wind energy). However, as the technology is continuously improving, it is expected that with time more and more concepts will reach the final phases of development in large scale, such as the Pelamis-device (Pelamis, 2013), the WaveStar-device (WaveStar, 2013), and the Oyster-device (Oyster, 2013).

WECs can both be floating structures positioned offshore in relatively deep water to avoid influences from wave dissipation processes, such as WaveDragon (2013) and DEXA (2013), or they can be structures installed onshore e.g. in breakwaters such as the SSG-device (Margheritini et al., 2009) or the OBREC-device (Vicinanza, 2012*a*, 2012*b*, 2013).

The use of electricity producing multipurpose structures for coastal and harbor protection is evaluated in this thesis. Solely the wave transmission and thereby the reduction of wave energy in the wake of the WECs is evaluated. Aspects such as survivability and costs are not included in the analysis. Moreover, solely floating offshore WECs are considered.

8.2 Existing Studies on Wave Height Reduction behind WECs

Floating WECs partly absorb, partly reflect, and partly transmit the incident wave energy. The amount of absorbed, reflected, and transmitted energy is highly dependent on the geometry of the devices and their orientation to the incident waves. One of the main goals for developers is to optimize the amount of absorbed energy in order to obtain the highest possible electricity production. However, a number of recent studies have also focused on the transmitted energy in the wake behind offshore floating WECs. This is to evaluate the either positive or negative effect on the environment from the wake of a single or multiple devices, and to evaluate the potential for using the devices for coastal protection or e.g. protection of other types of offshore installations such as wind turbine parks. Moreover, focus has been on the wave scattering of individual devices in a farm to ensure an optimum overall electricity production of the devices.

Venegupal & Smith (2007) used the depth-integrated MIKE21 Boussinesq model to analyze the wake effects behind an array of offshore WECs situated offshore of the Orkney Islands. Various hypothetical transmission coefficients and different wave conditions were evaluated in the study. Palha et al. (2010) used the depth-integrated mild-slope REFDIF model to analyze the wake of a farm of offshore Pelamis WECs situated on the west coast of Portugal. They used the wave transmission coefficient as specified by the developer and studied different farm configurations and various sinusoidal wave conditions. Beels et al. (2010) and Stratigaki et al. (2011) used the depth-integrated mild-slope MILDwave model to study the wake behind a single and multiple Wave Dragon WECs. The wave transmission coefficients of the devices were estimated based on integration of wave energy passing under the floating structure. Both long-crested and short-crested waves were considered in the study. Roul et al. (2011) used the simplified CERC formula to evaluate the long-shore sediment transport in presence and absence of offshore DEXA WECs located at the Italian site; Marina di Ravenna beach. Wave transmission coefficients of the device were based on the model tests by Zanuttigh et al. (2010). Monk et al. (2012) developed an approximate analytical model to analyze the transmitted and diffracted wake about a single row of hypothetical overtopping WECs. The goal was to perform faster computations in large temporal and spatial domains. Zanuttigh & Angelelli (2012) made 3-D laboratory tests in model scale 1:30 to evaluate the wave transmission and reflection from a single and multiple DEXA devices under a variety of wave conditions.

Venegupal & Smith (2007), Palha et al. (2010), Beels et al. (2010), and Stratigaki et al. (2011) all used depth-integrated numerical wave propagation models to simulate the wake effects from floating three-dimensional devices. This leaves the question of whether or not depth-integrated models can be used to simulate three-dimensional problems, where the heave, surge, and pitch movements of the floating

devices are neglected. The study by Roul et al. (2011) evaluated the influence on the sediment transport from multiple devices based on the wave transmission characteristics obtained from a single device. It was therefore assumed, that the wave transmission from a single device was unaffected by the presence of neighboring devices.

8.3 Present Study on Use of WECs for Coastal Protection

Lykke Andersen et al. (2010) discuss different wave energy concepts for coastal protection in present and future sea conditions. One of the devices, which is believed to be well suited for the purpose, is the floating so-called Wave Dragon (WD) due to its large energy absorption/reflection capacities and its low sensitivity to rise in SWL. The wave transmission characteristics of the WD are evaluated in Paper 1, 2, and 3 in the present thesis.

8.3.1 Wave Dragon Device

The considered WD-device is the 24 *kW/m* model illustrated in Figure 43. The WD is classified as a *terminator* and *overtopping*-type and has two wave reflectors, which focus the incident wave energy towards an overtopping ramp on the so-called main body where waves overtop into a reservoir. Electricity is produced when the overtopped water drains through the turbines in the reservoir. To optimize the energy capture the crest level of the device automatically adjusts in relation to the incident wave conditions. The device uses a single main mooring line, which allows the floating structure to turn and face the incident wave direction. Additionally, tension cables are used to support the reflectors of the WD, cf. Figure 43.

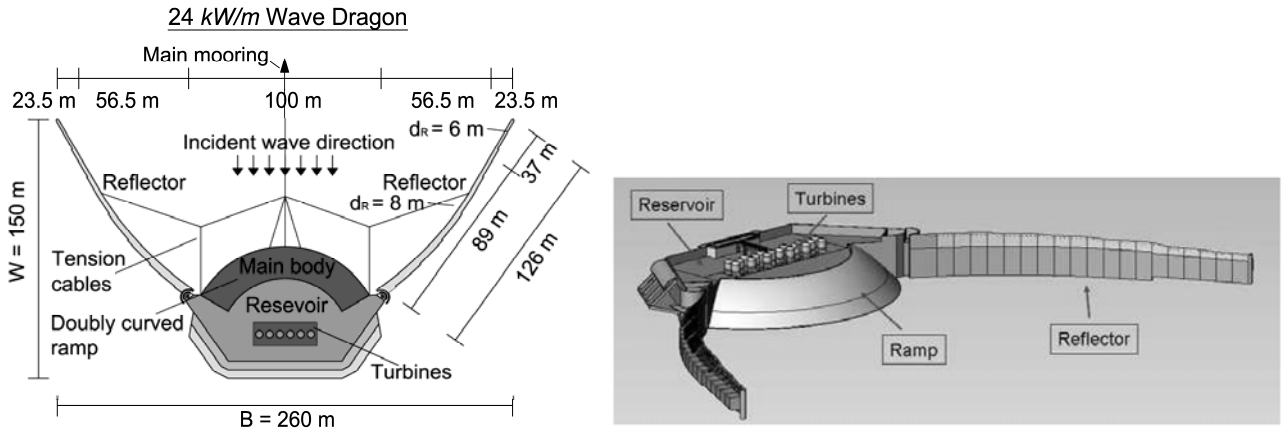

Figure 43. ***(left)*** **Illustration the considered 24** ***kW/m*** **Wave Dragon-device.** ***(right)*** **Three-dimensional illustration of the floating Wave Dragon-device (Tedd, 2007).**

The drafts of the wave reflectors vary from 8 *m* at the shoulders to 6 *m* and the reflector tips. The draft along the main body is constant but will, as mentioned, change during operation to optimize the wave energy capture.

8.3.2 Physical Investigation of Wave Transmission from Wave Dragon Devices

In Paper 1 the wave transmission/reflection characteristics are evaluated from a physical model test study in scale 1:51.8. Due to reflections from the basin boundaries, the actual transmission and reflection-coefficients of the model are not determined directly from the physical model test study. Instead, the wave disturbance coefficients, $K_d=H_{m0,measured}/H_{m0,generated}$, are determined in the near field of the device where $H_{m0,generated}$ is the incident significant wave height in the frequency domain, and $H_{m0,measured}$ is the measured significant wave height in the near field of the model.

Long-crested irregular waves are considered in the study where six different wave steepness (H_{m0}/L_p) are evaluated together with two different floating ratios (R_c/H_{m0}). L_p is the peak period wave-length and R_c is the crest freeboard of the ramp. Additionally, the so-called *"normal"* and *"fixed"* mooring setups are

considered in the study. In the *"normal"* setup the stiffness in the main mooring line and tension cables are scaled according to suggestions by Hald & Frigaard (2001). In the *"fixed"* mooring setup the model (main body and reflectors) is fixed to the floor using adjustable supports, which leave the device fixed in all its degrees of freedom. The two mooring setups are used to determine the influence from the realistic heave, surge, and pitch movements of the device on the wave transmission. An illustration of the test setup is given in Figure 44.

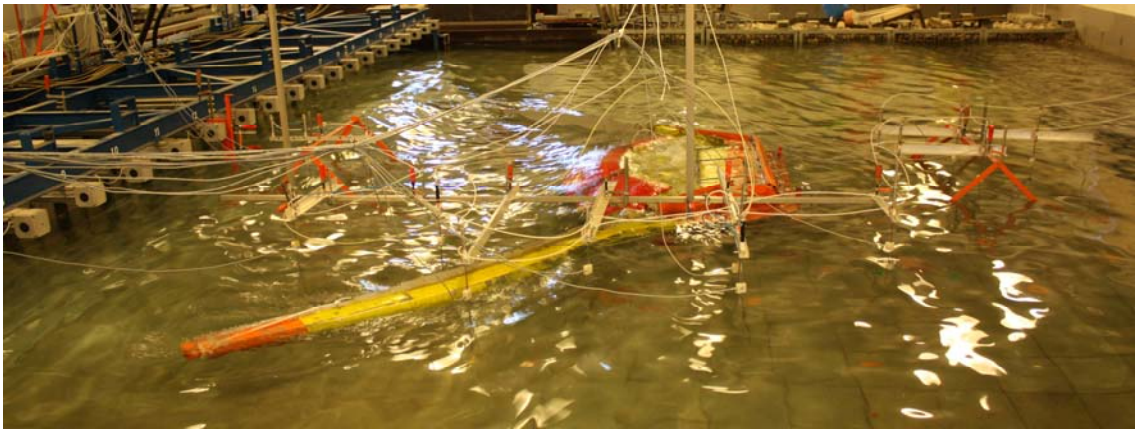

Figure 44. Photo of laboratory setup in scale 1:51.8.

Paper 1 concluded that the wave disturbance behind the floating device is affected more by the peak period wavelength in the frequency domain, L_p, than by the floating ratio R_c/H_{m0}. Moreover, it is concluded that the wave transmission is reduced if the device is fixed in its position

8.3.3 Calibration of Numerical Wave Propagation Model

In Paper 2 the data from the model tests presented in Paper 1 is used for calibration and validation of the depth-integrated numerical Boussinesq wave propagation model MIKE21 BW.

Initially, the empty laboratory basin is implemented with correct reflection characteristics obtained from the model tests. Hereafter, the WD geometry is implemented using frequency dependent so-called porosity layers which are calibrated against the surface elevations measured at the positions; A – O, in Figure 45. Layers with varying porosity are used across the WD-structure in the numerical model to obtain the desired transmission characteristics.

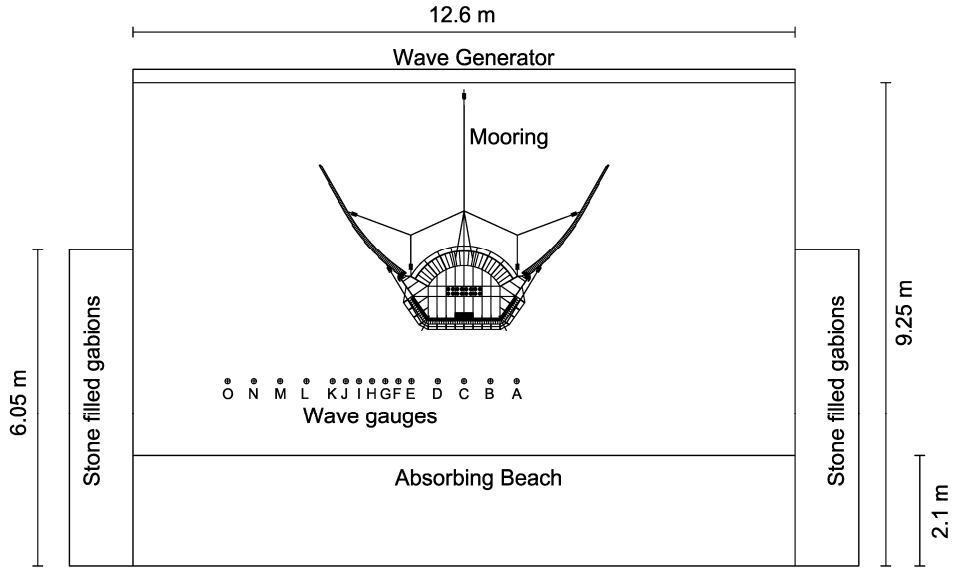

Figure 45. Illustration of wave gauges located behind the floating device. (Paper 2)

The MIKE21 BW model is calibrated against the smallest L_p and validated against the longest L_p in the model tests. Generally, very good agreement is obtained between modelled and measured K_d, cf. Figure 46. The conclusion is, that the depth-integrated MIKE21 BW model using calibrated frequency dependent porosity layers is well suited for modelling wave disturbance behind a floating structure.

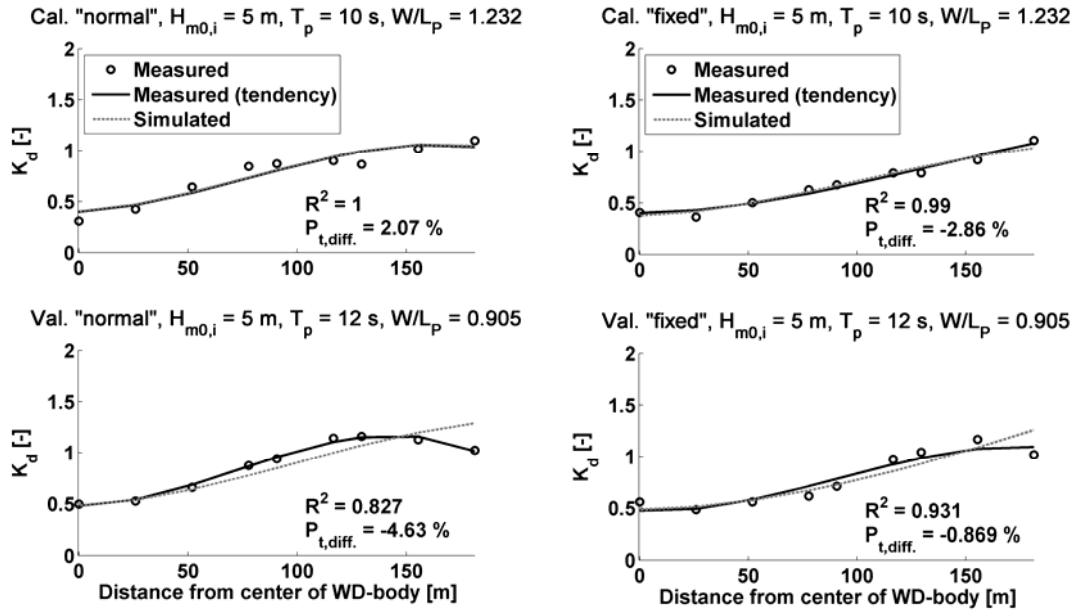

Figure 46. (*left*) Comparison of measured and simulated K_d for *"normal"* WD-setup (Paper 2). (*right*) Comparison of measured and simulated K_d for *"fixed"* WD-setup. (Paper 2)

8.3.4 Single and Multiple Device Transmission

Another objective in Paper 2 is to determine the actual wave transmission coefficients, $K_t = (P_t/P_i)^{0.5}$, of a single WD-device in varying wave conditions and with different mooring stiffness. P_i is the incident wave power and P_t is the transmitted power, which is determined in a big model bathymetry with uniform depth to avoid disturbance from reflecting boundaries.

K_t from a single WD-device is illustrated in Figure 47, which also includes the wave transmission from a simpler model based on integration of wave energy flux below the floating device, described in Paper 2. When comparing the two models, it is seen that the simple model provides estimations of K_t which are in the range of the *"normal"* and *"fixed"* mooring setups.

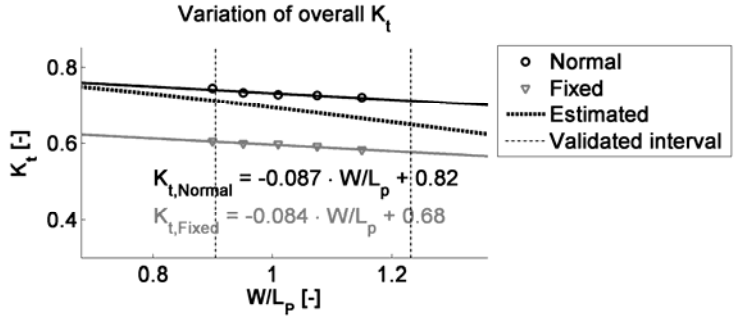

Figure 47. K_t from a single WD-device in case of varying L_p using both *"normal"* and *"fixed"* mooring setups and long-crested waves at uniform depth, h = 25 *m*. (Paper 2)

In Paper 3 the overall wave transmission is determined from multiple devices positioned in a staggered grid, as illustrated in Figure 48. Additionally, both long and short-crested waves are included in the study. The comparison is illustrated in Figure 49 where a good approximation to K_t is also obtained by the simplified approach.

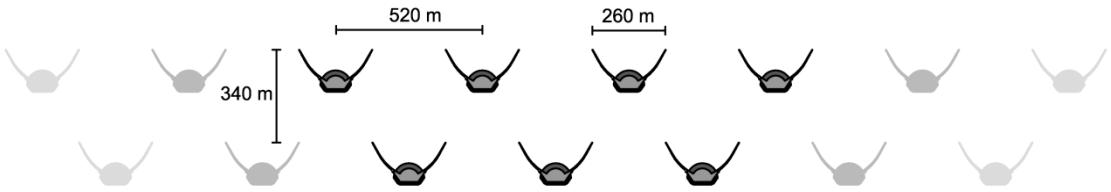

Figure 48. Continuous line of WDs in a farm for comparison of overall K_t against K_t from a single device. (Paper 3)

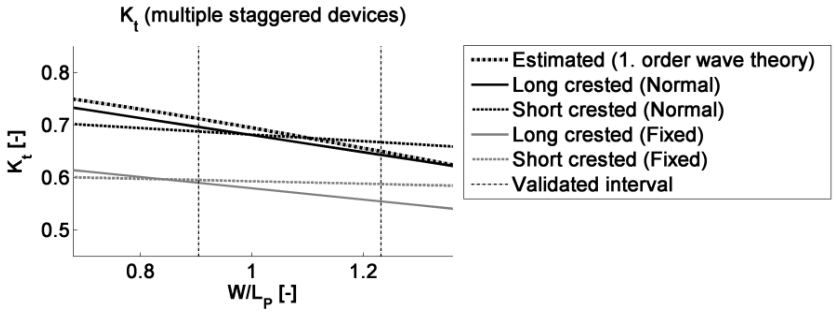

Figure 49. Overall wave transmission coefficient from a farm of staggered WDs. (Paper 3)

The simple approach based on integration of flux below the draft of the WD is thus concluded in Paper 2 and Paper 3 to be well suited for first estimates of the wave transmission from a single and multiple floating WDs.

8.3.5 Case Application using Calibrated Numerical Model

In Paper 3 a case study is performed where the calibrated MIKE21BW model is used to simulate the influence from a farm of offshore WDs on the wave climate in Santander bay, Spain. Typical storm conditions are evaluated in the study with peak wave periods in the range; T_p = 10 – 14 *s* and H_{m0} = 5 *m*. The effects from the offshore WDs are compared along two output lines located at the sand spit and Magdalena beach in Santander bay, Spain, illustrated in Figure 50. The output lines are located outside the wave-breaking zone in the model. The wave propagation model for Santander bay is not calibrated against actual wave measurements from the site. Instead, the influence from the offshore WDs is based on relative changes in wave power along the output lines in the presence or absence of the WD-farms.

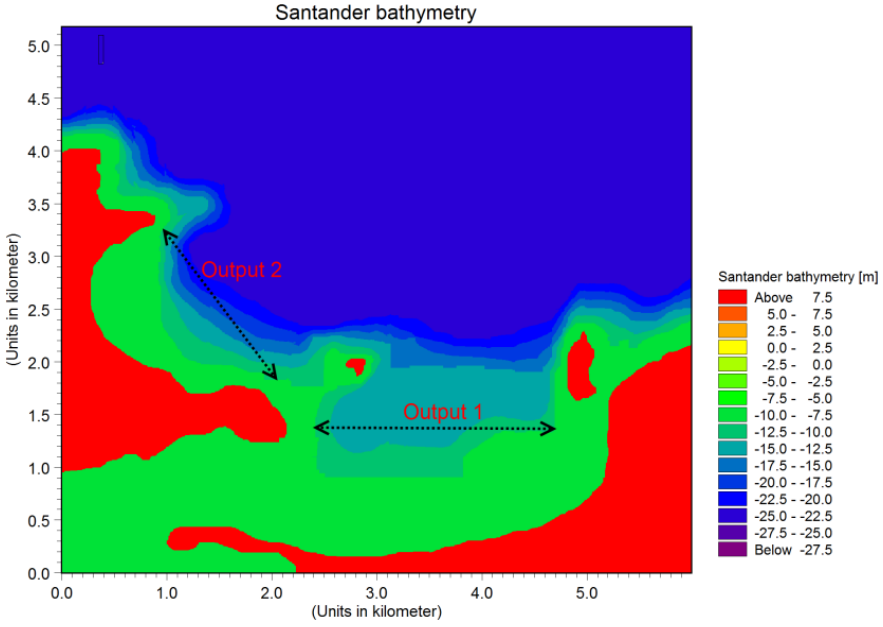

Figure 50. Illustration of "*Layout 2*". (Paper 3)

H_{m0}-contours are illustrated in Figure 51 for the empty bay with long and short crested waves. As can be seen, diffraction is present at the sponge layers in the western and eastern boundaries. However, the diffracted waves are not entering the area of interest.

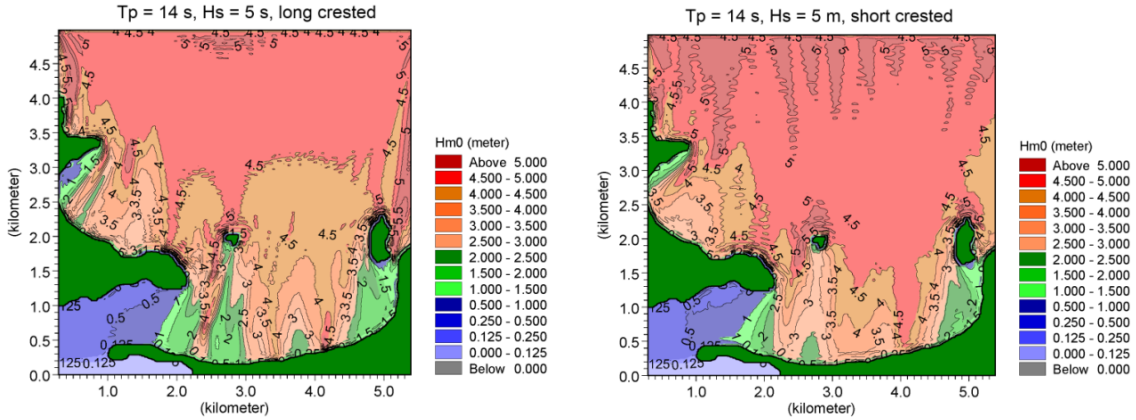

Figure 51. (*left*) H_{m0}-contours in the empty bay in case of long-crested waves from north. (*right*) H_{m0}-contours in the empty bay in case of short-crested waves from north. (Paper 3)

Two different farm layouts (illustrated in Figure 52) are considered in the study; *"Layout 1"*, which is believed to best suited for coastal protection, and *"Layout 2"* which is believed to be best suited for electricity production. Both farms are located at 25 *m* water depths. The *"normal"* mooring stiffness is considered to obtain realistic estimates of the wave transmissions.

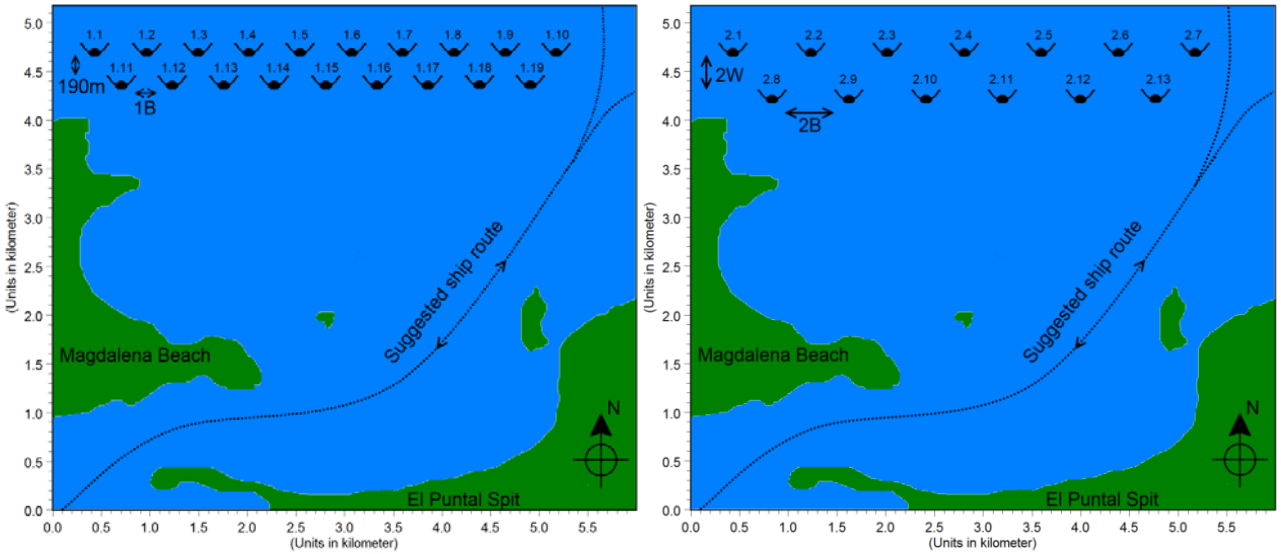

Figure 52. (*left*) Illustration of "*Layout 1*". (*right*) Illustration of "*Layout 2*". (Paper 3)

H_{m0}-contours for *"Layout* 1*"* and *"Layout* 2", using the *"normal"* setup, are illustrated in Figure 53 and 54, respectively, with long-crested waves in the left figures and short-crested waves in the right figures. The conclusion is that "*Layout 1*" is the best overall farm layout since the difference in electricity production compared to "*Layout 2*" is small, whereas the transmitted wave power from "*Layout 1*" is significantly smaller. A realistic estimate on the wave power reduction behind "*Layout 1*" is around 55% using the evaluated T_p.

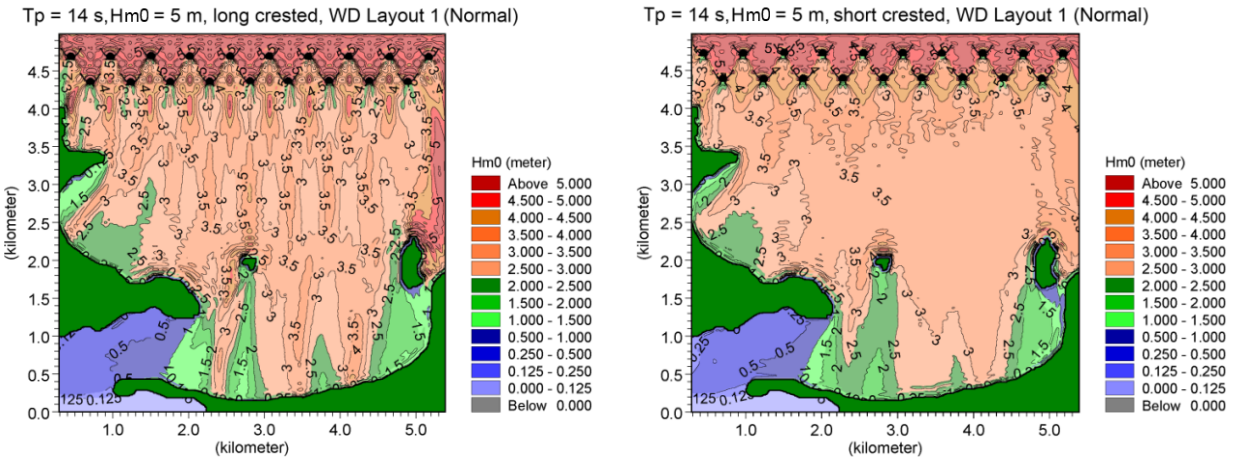

Figure 53. (*left*) H_{m0}-contours for "*Layout 1*" in long-crested waves using the *"normal"* WD-setup. (*right*) H_{m0}-contours for "*Layout 1*" in short-crested waves using the *"normal"* WD-setup. (Paper 3)

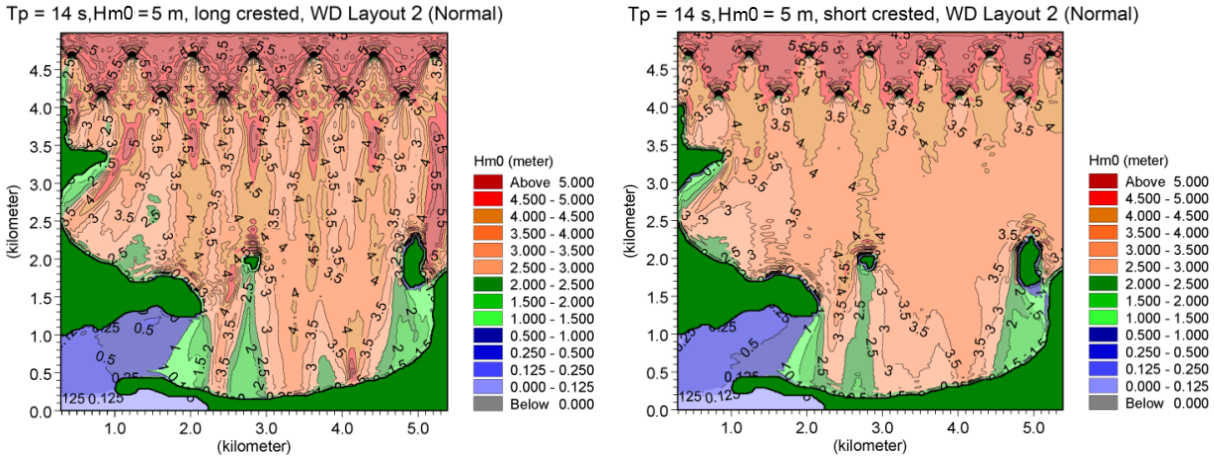

Figure 54. (*left*) H_{m0}-contours for "*Layout 2*" in long-crested waves using the *"normal"* WD-setup. (*right*) H_{m0}-contours for "*Layout 2*" in short-crested waves using the *"normal"* WD-setup. (Paper 3)

Paper 3 evaluates the possibility of modelling a farm of WDs using a simplified homogeneous geometry instead of the exact geometry of each device with identical K_t as obtained using the approach by described in Paper 2. In Figure 55, the implementation of the simplified geometry is illustrated.

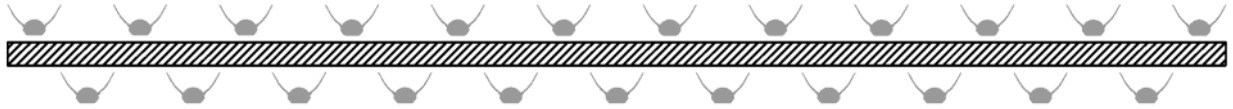

Figure 55. Illustration of simplified modelling of wave transmission from a farm of staggered WDs based on overall wave transmission coefficients (Paper 3).

In Figure 56 an example-case is illustrated where H_{m0} is plotted along the output lines in Santander bay in long-crested and short-crested waves. As can be seen, very similar wave height reductions are obtained when comparing the two geometries, especially in case of short-crested waves.

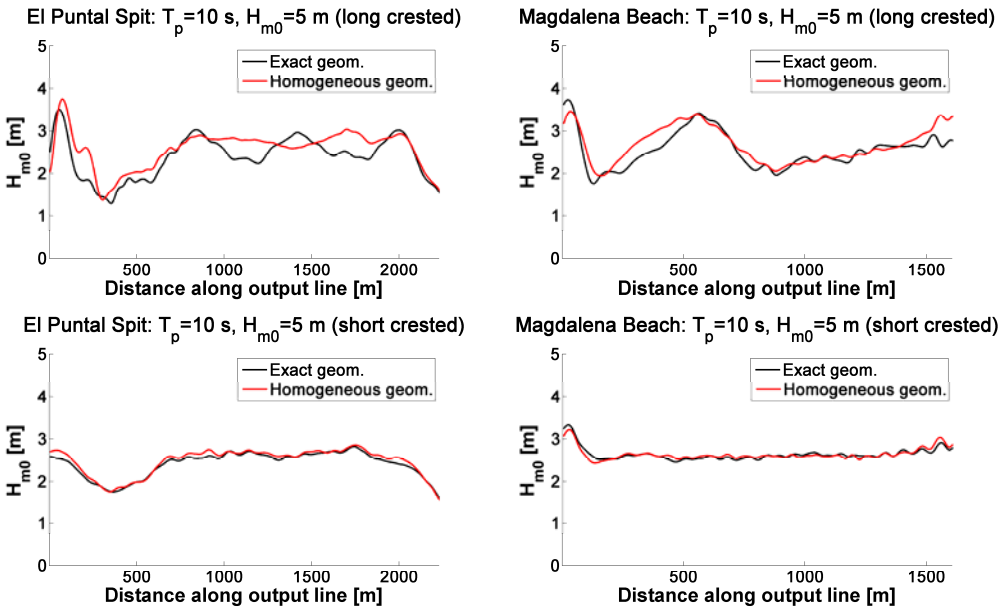

Figure 56. Wave height reduction behind from exact WD geometry and homogeneous simplified WD geometry. (Paper 3)

8.4 Summary of Findings in Chapter

The potential of using a farm of WDs for coastal protection is evaluated in the present chapter. The aim is to reduce the costs of produced energy by sharing the costs between electricity production and coastal protection.

Physical tests in model scale are performed to measure the wave height reduction behind a single floating device. Different setups of the mooring system are evaluated in the tests to investigate the sensitivity of the mooring stiffness on the wave transmission and to investigate the possibilities for optimizing the wave height reduction behind the device. It is generally concluded, that a very stiff mooring system will significantly reduce the wave transmission from the floating device.

The measurements from the physical model are used for implementation of the WD in a numerical wave propagation model in order to determine the overall wave transmission from a single and multiple devices in a big domain without influences from e.g. reflecting boundaries. In general, the wave transmission is seen to increase for increasing wavelength, since long waves are simply passing under the floating structure. Additionally, it is concluded that the wave transmission characteristics of a floating device can be modelled with good accuracy in a depth-integrated wave propagation model if implemented using frequency dependent porosity layers.

The calibrated and validated numerical wave propagation model are used to investigate the wave height reduction from multiple WD-devices in Santander bay, Spain, where a farm of staggered WDs is seen to reduce the wave power along the shoreline by up approximately 55%. Instead of implementing the geometry of each specific WD-devices when simulating the wave height reduction behind a farm, it is concluded to be sufficient to use a homogeneous box with correct overall wave transmission coefficient.

Harbour of Løgstør during January storm in 2005 (www.tv2.dk, 2013)

CHAPTER #9

DAMPENING OF STORM SURGES AND IMPROVEMENT OF WATER EXCHANGE BY BARRIER

In this chapter, the potential of using a multi-purpose barrier is evaluated for protection of an estuary against storm surges and for improving the water exchange.

9.1 Multipurpose Storm Surge Barriers

In recent time, there has been an increasing demand for defenses, which have minimal environmental and visual effects to the surroundings. Worldwide this has resulted in the construction of dynamic barriers such as e.g. the Oosterschelde storm surge barrier in the Netherlands and the Thames Barrier in London, England. Moreover, at present time a dynamic storm surge barrier is being constructed at the entrance of the lagoon to Venice, Italy.

Typically, a storm surge barrier permits the normal tides to flow in and out of e.g. a river or an estuary, whereas it closes when a storm surge is forecasted in order to protect the hinterland. When planning a new storm surge barrier a cost-benefit analysis is made on the costs related to the construction and maintenance of the structure, and the costs related to the case where no action is taken (i.e. costs of flooded areas behind the defense). The costs of building a defense can thus be reduced by either reducing the construction costs or e.g. by sharing costs with other functions of the structure, such as electricity producing turbines or control of the water flow passing through the barrier gates for improving the water quality.

In this thesis the potential of combining a barrier for reduction of peak storm surge water levels and for regulation of water flow is evaluated in order to improve the salinity and water exchange, and thereby the water quality, in an estuary. The research, which is documented in Paper 4, is based on a case study performed on the largest Danish estuary "the Limfjord" and is performed using a numerical three-dimensional hydrodynamic model, which is calibrated against measured time-series.

9.2 Case Application of Storm Surge Barrier for Flood Protection and Improvement of Water Exchange in the Limfjord

The Limfjord, illustrated in Figure 57, has a length of 180 *km*, a volume of 7.4 km^3 and an average water depth of 4.9 *m*. The water exchange, salinity, and water level in the Limfjord are mainly controlled by the two connections to the North Sea and the Kattegat in Thyborøn and Hals, respectively, together with wind setup inside the fjord. Additionally, the Limfjord receives approximately 2.7 km^3 fresh-water from run-off of the 1730 km^2 surrounding agricultural areas.

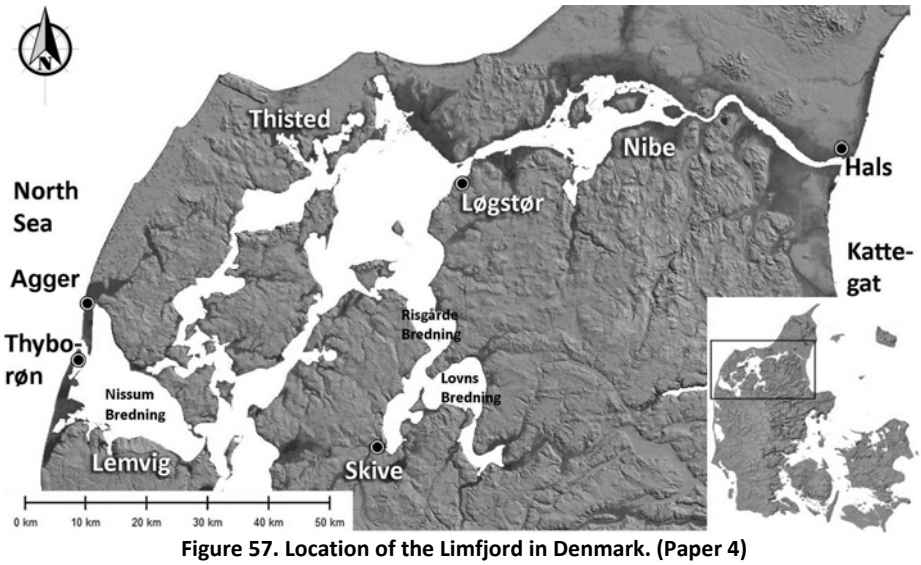

Figure 57. Location of the Limfjord in Denmark. (Paper 4)

The salinity in the Limfjord decreases from west to east with approximately 33 *PSU* in the North Sea and around 25 *PSU* in the Kattegat. The surrounding run-off areas have relatively high concentrations of nutrients in terms of nitrogen and phosphorus and in recent time, especially during summer periods, the Limfjord has suffered from severe eutrophication with a high production of algae and oxygen depletion

near the seabed. It is generally believed, that an improved water exchange and an improved salinity in the fjord can improve the water quality in the Limfjord.

Looking back in history, the Limfjord has been significantly influenced by storm surges, which are expected to become more intense and more frequent in the future due to climate changes, cf. (Haugen & Iversen, 2008) and (Debernard & Røed, 2008).

Larsen (2007) evaluated the 20 largest storm surge water levels in the period 1931 to 2005, measured at Thyborøn harbor. It was concluded, that the 18 out of 20 highest storm surge water levels appeared in the period 1969 – 2005. The highest storm surge water level in Thyborøn was measured on 8 January 2005 with 2.97 *m* above Mean Sea Water Level (MSL) and the highest measured water level inside the fjord was measured to 2.35 *m* above MSL on the same day before the data station broke down.

Larsen (1985, 2007, 2009) recommended constructing a storm surge barrier in the Thyborøn channel as illustrated in Figure 58. A ship sluice was suggested in the middle of the barrier along with the gate openings to regulate the flow. The flow area in the Thyborøn channel is approximately 7500 m^2.

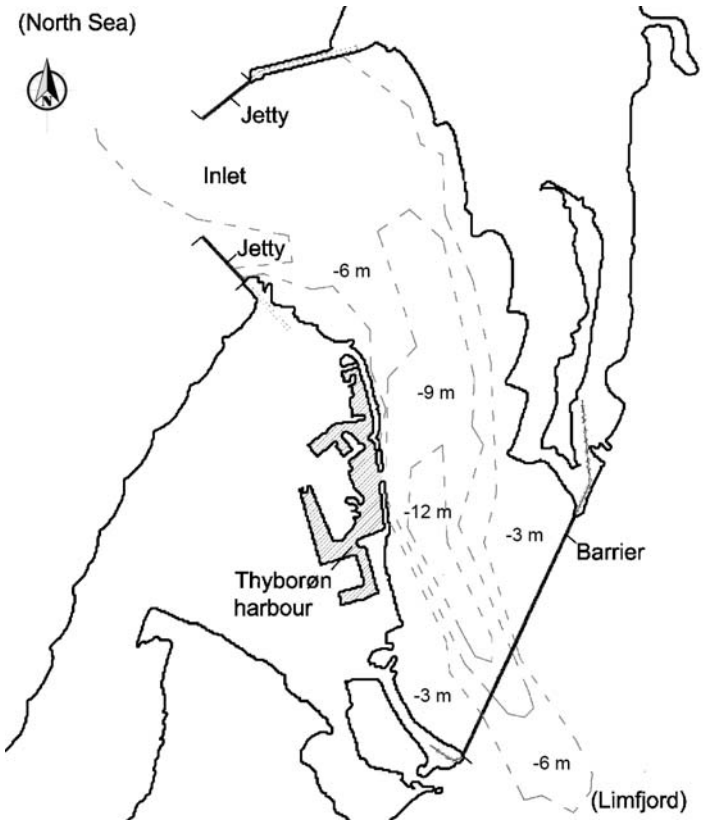

Figure 58. Placement of the storm surge barrier. (Paper 4)

Paper 4 calibrates and validates the commercial three-dimensional hydrodynamic model MIKE3 by DHI, Denmark, against a comprehensive set of data gathered from 44 stations in the Limfjord area. The data contains measurements of salinity, wind speed/direction, water level, and fresh water discharges from the period January 2005 to December 2005. The bathymetry in MIKE3 is discretised into 23,776 elements in the horizontal domain and 10 equidistant layers in the vertical domain. Time steps are set to vary between 0.001 *s* to 600 *s*. The computational mesh used in the numerical model is illustrated in Figure 59.

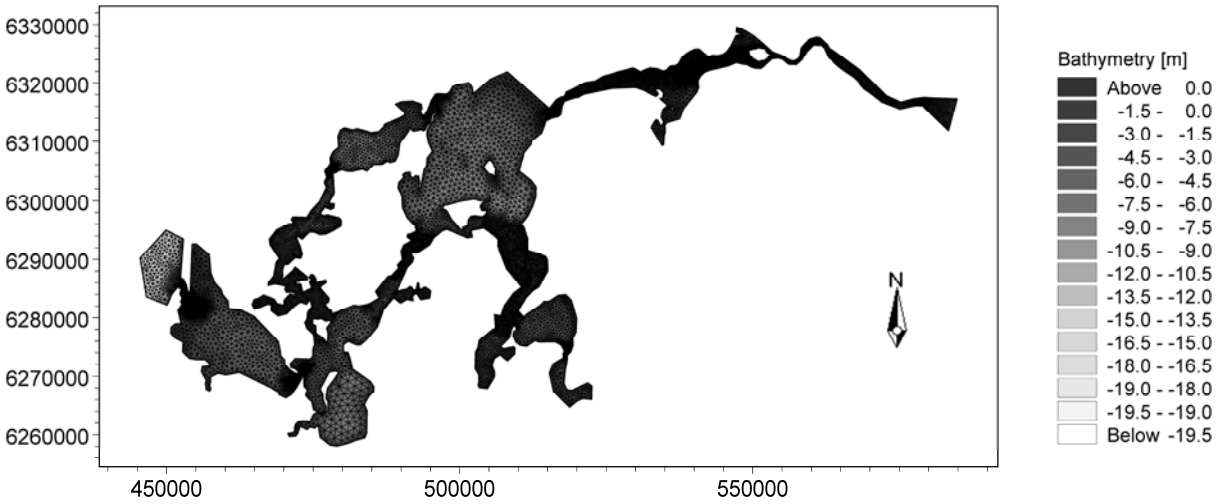

Figure 59. Computational mesh in the MIKE 3 flow model. (Paper 4)

The numerical model is calibrated against the storm surge in January 2005 (06/01-2005 – 11/01-2005) and validated against the water levels and salinity in the period 01/01-2005 – 31/12-2005. During the calibration, the bed roughness and wind friction are adjusted. For the calibration of the water level the two locations, Skive and Løgstør, are evaluated. Measured and simulated water levels are illustrated in Figure 60 where good agreement is generally obtained.

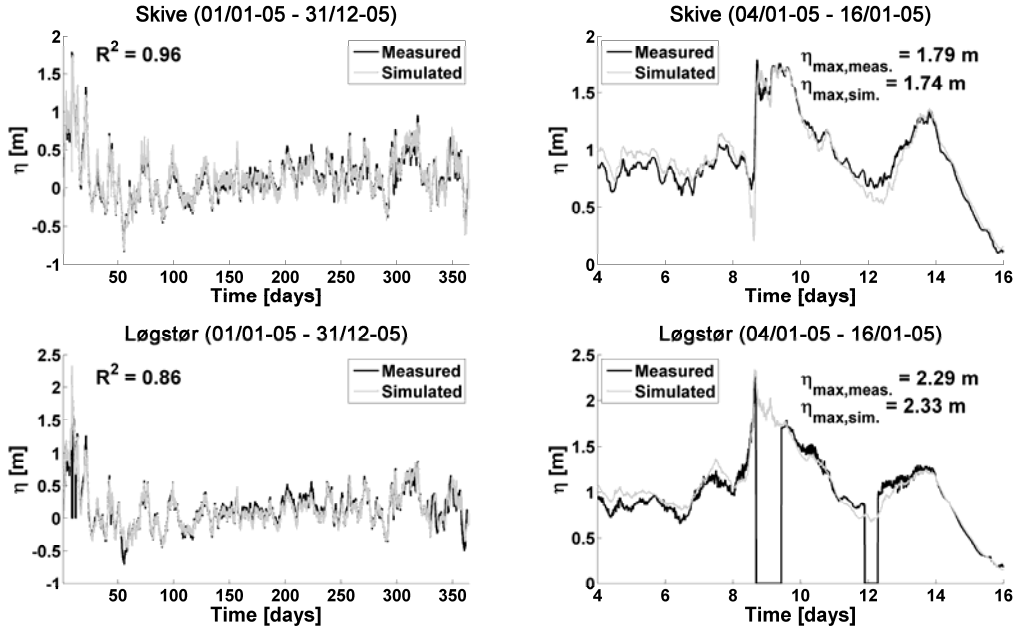

Figure 60. Measured and simulated water surface elevation in Skive and Løgstør in 2005. (Paper 4)

For the validation of the salinity in the Limfjord six locations are evaluated; Nissum, Risgaarde, Løgstør, Lovns, Skive, and Nibe, illustrated in Figure 57. As an example, the measured and simulated salinities for the Skive location are illustrated in Figure 61, where good agreement is obtained.

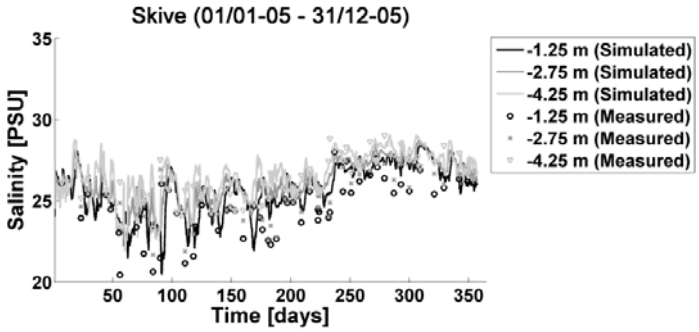

Figure 61. Measured and simulated salinities at three different water depths in Skive. (Paper 4)

Three different gate opening areas in the storm surge barrier are also evaluated: 500 m^2, 1000 m^2, and 1500 m^2. Moreover, different strategies for closing the channel are evaluated, where the channel is closed up to five days before the storm surge peak. The reductions in peak storm surge water levels are illustrated in Figure 62. As can be seen, the water levels are significantly reduced by the presence of the barrier and especially if the barrier is closed in sufficient time before the storm surge is fully developed.

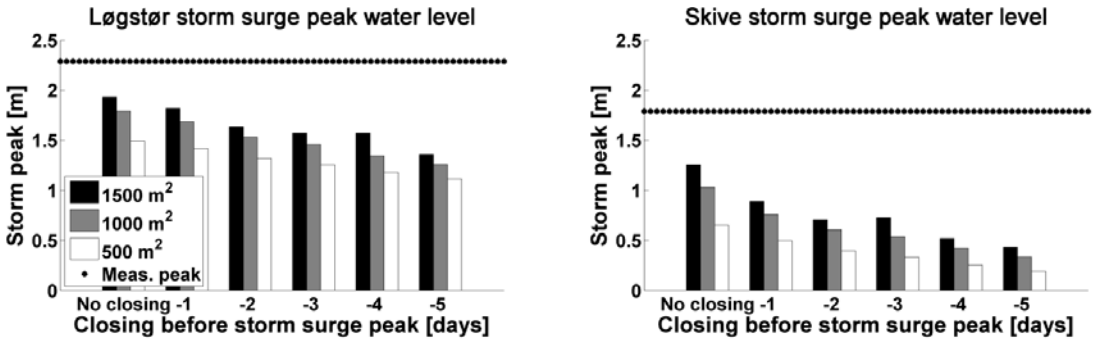

Figure 62. Relative change of peak water level for situation of closed channel compared with open channel. (Paper 4)

To account for the influence from climate changes in year 2100, the water levels in Hals and Thyborøn and the wind speed in the Limfjord area have increased by up to 0.6 *m* and up to 10 *%*, respectively (regional increases obtained from STOWASUS (1998)). Figure 63 illustrates the influence from the additions to the storm surge peak and the influence from closing the storm surge barrier 5 days before the storm surge peak. The time axes in Figure 63 (*left*) and (*right*) are normalized with respect to the storm surge peak at day 0. As can be seen, a significant increase in the storm surge water levels can be expected in year 2100, but the presence of the storm surge barrier provides a notable reduction.

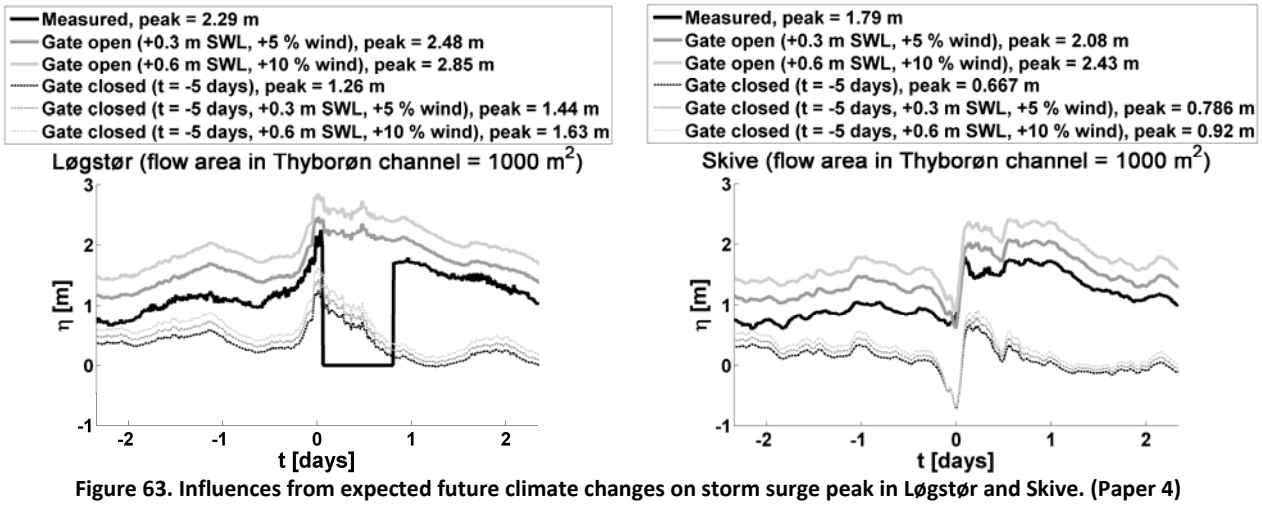

Figure 63. Influences from expected future climate changes on storm surge peak in Løgstør and Skive. (Paper 4)

It has previously been suggested in a report from the "Thyborøn commission" of 1942 (Ministeriet for Offentlige Arbejder, 1942), that the water exchange, and thereby the salinity and water quality in the Limfjord, could be improved by using a storm surge barrier, which only allows in-going currents. Paper 4 applies such control strategy to the storm surge barrier, and Figure 64 illustrates the influence on the salinity for the six evaluated locations using three different sluice areas in the barrier. As can be seen in the figure, the salinity is generally increased where a higher salinity is obtained for a bigger sluice area in the barrier. An improved salinity also means improved water exchange since, as mentioned, the salinity is higher in the North Sea than in the estuary.

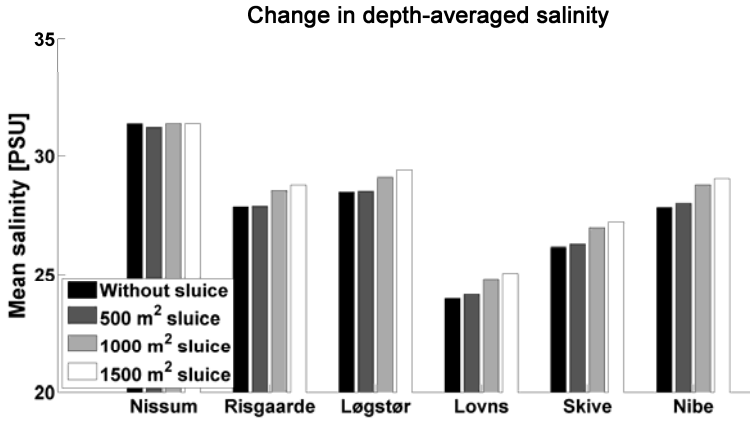

Figure 64. Simulated salinities with and without a one-way sluice in the Thyborøn channel. (Paper 4)

9.3 Summary of Findings in Chapter

The protection of the Limfjord estuary using a storm surge barrier has been discussed for almost a century now. However, so far the storm surge barrier has not been realized, due to costs of constructing the barrier and due to local political opposition.

In this chapter a case study is performed on the Limfjord estuary to evaluate the cost-sharing between storm surge protection and improvement of water exchange using a multipurpose barrier. A calibrated three-dimensional hydrodynamic model is used for the study and simulations indicate that the water level in the Limfjord is significantly reduced if closing the barrier in sufficient time before the storm surge. Additionally, it is observed from the case study that the salinity and thus the water exchange in the Limfjord can be improved by controlling the storm surge barrier to allow only for ingoing flow from the North Sea.

PART #3

Conclusions

The author of the thesis enjoying the increasing storminess, Klitmøller, Denmark, 2011

CHAPTER #10

CONCLUSIONS AND DISCUSSION

This chapter draws the general conclusions on key findings in the thesis and discusses the results. Additionally, recommendations for future supplementary studies are given.

10.1 General Findings in Thesis

This thesis has evaluated a number of selected areas within the field of coastal protection in a changing climate. Special focus has been on the performance of existing structures especially in shallow water to withstand the influence from climate changes. Additionally, since climate changes demands for innovative ideas for protection of coastal areas in the future, the potential of using innovative multipurpose structures for coastal protection is evaluated (wave energy converters and controlled storm surge barriers).

10.1.1 Wave Actions on Rubble Mound Breakwaters with Crown Walls in Deep and Shallow-Water Wave Conditions

The research presented in this thesis has identified a number of uncovered areas in relation to design of coastal protection structures in especially shallow-water wave conditions. Many existing design formulae are based on deep-water wave conditions with Rayleigh-distributed wave heights, which provide conservative estimates on the wave actions in shallow-water wave conditions.

In this thesis selected design formulae for estimation of wave run-up levels and wave loads on rubble mound breakwater crown walls and for estimation of single overtopping wave volumes are modified to include the effects of shallow-water wave conditions. Additionally, the performances of existing shallow-water wave height distributions are evaluated for estimation of low-exceedance wave heights, since these are used in the design formulae to estimate the low-exceedance wave actions on the structures.

Existing state-of-art shallow-water wave height distributions are compared to measured low-exceedance wave heights from scaled model tests with shallow to deep-water wave conditions. The distributions by Battjes & Groenendijk (2000) and Goda (2010) are seen to provide relatively good estimates. However, it is strictly advised to only apply the wave height distributions within the validated ranges of bed-slopes etc., since recent research has shown that un-conservative estimates can be obtained otherwise.

The formula for estimation of wave run-up levels by Van der Meer & Stam (1992) is modified to include the effects of depth-limited waves by introducing the effects of changes in the incident wave height distribution in such conditions. The modified run-up formula is hereafter used to include the effects of shallow-water wave conditions in the formulae by Pedersen (1996). This procedure is validated against a comprehensive set of scaled model tests in deep and shallow-water wave conditions.

Additionally, the original formulae by Pedersen (1996) are seen to overestimate the wave loads on un-protected crown walls due to dynamic amplification in the pressure transducers used in the calibration. Recalibration of the formulae is thus performed in the present thesis based on new model tests using pressure transducers with high eigen-frequencies.

The formulae by Besley (1999) are seen to underestimate the number of overtopping waves on rubble mound breakwaters in shallow-water wave conditions and are thus modified to include the depth limitation effects in such conditions. Overtopping single wave volumes are more evenly distributed in shallow-water wave conditions compared to deep water, which results in a higher number of overtopping volumes. The included depth-limitation effects are based on the changes in the incident wave height distribution in shallow water compared to deep water using the ratio $H_{m0}/H_{1/10}$. The extended formulae are calibrated against a comprehensive set of new model tests performed in deep and shallow-water wave conditions.

The Weibull-distribution shape factors by Van der Meer & Jansen (1994), Franco et al. (1994), and Victor et al. (2012) for distribution of single overtopping wave volumes on dikes, caisson breakwaters, and low-crested smooth structures, respectively, are modified to include the effects of shallow-water wave conditions in the distribution of single overtopping waves on rubble mound breakwaters. The original shape factors are seen to provide conservative estimates on the maximum overtopping single wave volumes in depth-limited wave conditions. Thus, similarly to the modification performed to the formula by Besley (1999), it is suggested in this thesis to include the depth-limitation effects in the shape factors using the ratio $H_{m0}/H_{1/10}$. The modified shape factors are calibrated against a comprehensive set of new model

tests performed in deep and shallow-water wave conditions and are seen to increase for increasing $H_{m0}/H_{1/10}$-ratios.

A case study is performed on two typical rubble mound breakwater geometries on deep and shallow water to identify the most vulnerable parts of the structures (stability of armor units, wave overtopping, and wave loads on crown walls) to an SWL-rise of 1.1 *m* by year 2100. The case study is performed using the extended and modified design formulae, which includes the effects of shallow-water wave conditions. From the case study it is observed that especially the structure on shallow water is affected by SWL-rise due to the increase in low-exceedance wave heights in such conditions.

The rising SWL has no influence on the stability of the front slope armor units on the deep-water structure, and only a minor effect is obtained on the shallow-water structure. A larger effect is observed in relation to the influence from climate changes on the average overtopping discharge and maximum overtopping single wave volumes on the structure. However, the largest effect of SWL-rise is observed on the stability of the crown walls against sliding and overturning, which in the evaluated examples are seen to become unstable already at an SWL-rise of 0.08 *m* on the shallow-water structure and 0.3 *m* on the deep-water structure compared to the present design conditions. The estimates are, however, very conservative due to an assumed triangular vertical pressure distribution where the time-lag between horizontal and vertical loads is ignored. Additionally, it should be noted that an extra safety is included in the crown wall design if allowing for small displacements in the design conditions.

10.1.2 Influence from Realistic Three-Dimensional Waves on Overtopping Flow Parameters on Sea Dikes

Wave overtopping on sea-dikes can lead to complete failures due to erosion on the landward slopes. An in-depth assessment of the overtopping flow parameters is therefore of significant importance when investigating the influence from climate changes on the dikes, and when deciding whether the dikes can be left as they presently are or whether they should be reinforced/upgraded. In this thesis, extensions to existing formulae for estimation of overtopping flow depths and flow velocities on sea-dikes are introduced to include the effects of wave obliquity and wave spreading, and to evaluate the effects of including more realistic three-dimensional waves in the design of the structures instead of perfectly long-crested head-on waves. The extensions are based on a comprehensive set of 3-D model tests with various wave obliquities and wave spreading's.

The effects from wave obliquity and directional wave spreading are seen to significantly reduce the overtopping flow velocities on a sea dike, and thus ignoring these effects will lead to conservative estimates and perhaps un-necessary or expensive upgrades of the structures. Additionally, the flow directions and distribution of individual overtopping flow parameters are evaluated, which can be used for calibration of e.g. a wave overtopping simulator when performing in-situ tests on dike resilience against wave overtopping. It is concluded, that the overtopping volumes with the highest flow velocities on the dike crest have the same direction as the incident waves. Additionally, it is concluded that the individual overtopping flow parameters on the dike crest are Rayleigh-distributed if the incident waves are Rayleigh-distributed.

10.1.3 Innovative Multipurpose Structures for Coastal Protection

A simple approach is introduced in the thesis for estimating the wave transmission coefficients of a single floating wave energy device and a farm of multiple devices, together with an approach for simple implementation of a farm of Wave Energy Converters (WECs) in a numerical wave propagation model. A case study is performed to examine the wave height reduction behind offshore Wave Dragon WECs at a specific site where good potential is observed for combining electricity production from wave energy converters with coastal protection.

Additionally, a case study is performed on the use of a multipurpose storm surge barrier for dampening of storm surge water levels and for improvement of water exchange in estuaries where also a good potential is observed.

10.1.4 Specific Finding in Papers

Specific objectives and findings from the nine research papers in appendix are summarized in the following. It is advised to read the papers to obtain an in-depth description of the findings and their contribution to the research within the field of coastal engineering.

Paper 1: Based on scaled physical model tests a sensitivity analysis is performed on the wave transmission from a floating wave energy converter for various stiffness in the mooring system and for various wave steepness. It is concluded, that the mooring stiffness and wave steepness have a big influence on the wave transmission.

Paper 2: A new method is suggested for providing rough estimates on the wave transmission from floating wave energy converters. Moreover, it is concluded that a depth-integrated wave propagation model is well suited for modelling wave transmission from floating wave energy converters if the devices are implemented in the model as frequency dependent porous structures.

Paper 3: A case study is performed to evaluate the potential of using wave energy converters for coastal protection. A good potential is observed from the study where it is found that the wave power is reduced by approximately 50% at the shoreline in Santander bay, Spain.

Paper 4: A case study is performed in the Limfjord estuary, Denmark, where a three-dimensional hydrodynamic model is used for simulation of the dampening of storm surges and improvement of water exchange by controlling the opening and closing of a storm surge barrier. It is concluded that the storm surge barrier can significantly reduce the storm surges and improve the water exchange in the Limfjord.

Paper 5: Formulae for estimation of overtopping flow parameters on sea dikes are extended to include the effects of oblique and short-crested waves. Additionally, the flow directions and distribution of overtopping flow parameters on sea dike crests are evaluated.

Paper 6: A new method is suggested for measuring and detecting flow velocities and flow directions of overtopping wave volumes on sea dikes.

Paper 7: Formulae for estimation of low-exceedance single overtopping wave volumes on rubble mound breakwaters are extended to include the effects of shallow-water wave conditions.

Paper 8: Design formulae for estimation of low-exceedance horizontal wave loads on rubble mound breakwater crown walls are extended to include the effects of shallow-water wave conditions. Additionally, a re-calibration of the original formulae by Pedersen (1996) is performed to provide better estimations of wave loads on un-protected crown wall faces and new formulae are suggested for more precise estimations of horizontal overturning moments.

Paper 9: The performance of a simple tool for estimation of sliding distances of crown wall superstructures on rubble mound breakwaters is considered. Load reduction factors are suggested for better description of wave loads on sliding crown walls compared to fixed crown walls.

10.2 Discussion of Findings in Thesis

Influences from climate changes makes it necessary to evaluate the needs for upgrading or re-designing existing coastal protection structures to maintain their initial design performance criteria. An evaluation like that requires reliable tools, guidelines, and design methodologies.

From the research in this thesis, it is observed that some existing design formulae are too conservative and are unable to describe the impact from climate changes with sufficient accuracy. It is seen, that if more details are included in the design formulae (such as e.g. the influence from oblique and short-crested waves or the influence from depth limitation effects in shallow-water wave conditions) they become more accurate and less conservative.

Conservative estimates on wave actions can lead to unnecessarily expensive designs of new coastal protection structures or un-necessarily expensive upgrades of existing structures. On the other hand, since many existing structures are based on conservative estimates of wave actions in the design conditions, they may be less vulnerable to climate changes in the future than initially expected. As an example, from the evaluated case studies in the present thesis on rubble mound breakwaters and a sea dike it is seen that notable increases in SWL can be accepted to retain the initial performance criteria of the structures if they are initially designed based on conservative scenarios, such as deep water or long-crested head-on wave conditions.

Instead of e.g. upgrading existing structures, another strategy can be to allow for periodical damage, which however, will require periodical maintenance of the structures. As an example, for crown walls on rubble mound breakwaters an un-conventional strategy can be to allow for small displacements in the design conditions, which will significantly decrease the required crown wall dimensions compared to the case where no displacements are accepted. Off course, total failures of the structures should be avoided.

Additionally, little erosion on crests and landward slopes of sea dikes can be accepted in the design conditions, as long as the resilience of the dike cover layers is sufficient to ensure sufficient safety against total dike breaching. Such strategy can significantly reduce the costs of upgrading the dikes to withstand the influences from climate changes compared to e.g. heightening the structures.

If upgrading existing coastal protection structures to withstand the impact from climate changes or if constructing new defenses, an unconventional method can be to combine e.g. electricity production with coastal protection. This can be done by e.g. installing wave energy converters in breakwaters, such as in (Vicinanza, 2012*a*, 2012*b*, 2013), or by installing offshore floating WECs to dampen the waves, such as described in the present thesis. Additionally, storm surge barriers can be used to control and improve the water exchange in estuaries, such as in the example with the storm surge barrier in the Limfjord, presented in the present thesis.

Good potential is observed for sharing costs between e.g. renewable energy and coastal protection. It is believed that the cost-sharing can help introducing the wave energy devices as cost-effective and “green” alternatives to other types of coastal protection structures. Moreover, it is believed that the secondary coastal protection function can help to reduce the costs of produced electricity from the WECs and thus help the devices to compete against other renewable energy sources (wind, solar, etc.).

10.3 Recommendations for Supplementary Studies

This thesis has studied the vulnerability of only a few types of coastal protection structures to climate changes and has evaluated the performance of only a few selected design formulae for estimation of the impact from climate changes. However, it is highly relevant to assess the vulnerability of additional types of coastal protection structures to climate changes.

To the author’s opinion, special attention should be applied to coastal protection structures in shallow waters, since these are seen in the present thesis to be especially vulnerable to SWL-rise. This also require attention to the performance of existing design tools in shallow waters - including the methods for estimation of design waves in depth-limited conditions, which at present are seen to provide very different estimates in some conditions. Additionally, many design formulae are conservatively based on two-dimensional wave conditions with long-crested head-on waves (such as the case with the Pedersen (1996)

formulae), whereas many coastal protections structures are placed in three-dimensional wave conditions (short-crested oblique waves). These effects should thus be incorporated in the existing formulae to avoid conservative estimates.

Since many existing design formula (such as for estimation of wave run-up levels and wave loads on crown walls) are presently based on model tests in small scale more attention should be paid to influences from scale effects and model effects in the future. A great amount of research already exists on the topic but design guidelines should be developed for practical use.

Regarding multipurpose structures for coastal protection, more research is still needed on the subject. An idea could e.g. be to perform case studies with cost-analysis on the use of multipurpose wave energy converters for coastal protection at specific sites compared to using more traditional coastal defenses.

Bibliography

Andersen, T. L., Martinelli, L., Zanuttigh, B., Nørgaard, J. ., Silva, R., & Roul, P. (2010). *"Barriers for wave energy conversion: Part B. I: THESEUS Deliverable OD 2.1: Integrated Inventory of Data and Prototype Experience on Coastal Defenses and Technologies"*. (p. 7-22). European Commission.

Andersen, T. L., Burcharth, H. F., & Gironella, X. (2011). *"Comparison of New Large and Small Scale Overtopping Tests for Rubble Mound Breakwaters."* Coastal Engineering, 58(4).

Battjes, J.A., and Groenendijk H.W. (2000). *"Wave height distributions on shallow foreshores."*, Coastal Engineering, 40, 161-182.

Beels, C., Troch, P., Visch, K.D., Kofoed, J.P. and Backer, G.D. (2010)*, "Application of the Time-Dependent Mild-Slope Equations for the Simulation of Wake Effects in the Lee of a Farm of Wave Dragon Wave Energy Converters".*, Renewable Energy, vol 35, nr. 8.

Besley P. (1999). *"Wave overtopping of Seawalls"*. Design and Assessment Manual. HR Wallingford. R&D Technical Report W178

Bosman, G., Van der Meer, J.W., Hoffmans, G., Schüttrumpf, H., Verhagen, H.J., (2008). *"Individual overtopping events at dikes".* World Scientific, Proc. ICCE 2008, Hamburg, Germany, pp. 2944–2956.

Briganti, R. Bellotti, G., Franco, L., De Rouck, J. Geeraerts, J. (2005). *"Field measurements of wave overtopping at the rubble mound breakwater of Rome–Ostia yacht harbor".* Coastal Engineering, Volume 52, Issue 12, December 2005, Pages 1155-1174, ISSN 0378-3839, 10.1016/j.coastaleng.2005.07.001.

Bruun, P. (1962). *"Sea-level Rise as a Cause of Shore Erosion"*, Journal of Waterways Harbors Division, American Society of Civil Engineers, 88, 117–130.

Bryan, K.R., P.S. Kench, and D.E. Hart, (2008). *"Multi-decadal coastal change in New Zealand: Evidence, mechanisms and implications".* New Zealand Geographer, 64(2), 117-128.

Burcharth, H. F., Liu, Z., & Troch, P. (1999). *"Scaling of Core Material in Rubble Mound Breakwater Model Tests".* Proc. of the Fifth International Conference on Coastal and Port Engineering in Developing Countries, Cape Town, South Africa(s. 1518-1528).

Burcharth, H. F. & Andersen, T. L. (2007). *"Scale Effects Related to Small Physical Modelling of Overtopping of Rubble Mound Breakwaters."* Coastal Structures 2007. (s. 1532-1541). World Scientific Publishing Co Pte Ltd. doi: 10.1142/9789814282024_0135

Burcharth, H. F., Andersen, L. & Lykke Andersen, T. (2008): *Analyzes of Stability of Caisson Breakwaters on Rubble Foundation Exposed to Impulsive Loads.* Proc. of the 31st Int. Conf. on Coastal Eng.: Hamburg, Germany, pp. 3606-3618.

Caires, S., & Van Gent, M. (2012). *"Wave Height Distribution in Constant and Finite Depths".* Coastal Engineering Proceedings, (33)

Chini, N., Stansby, P.K, Leake, J., Wolf, J., Jones, J.R., Lowe, J. (2010). *"The impact of sea level rise and climate change on inshore wave climate: A case study for East Anglia (UK)"*., Coastal Engineering, Volume 57, Issues 11–12, November–December 2010, Pages 973-984, ISSN 0378-3839, 10.1016/j.coastaleng.2010.05.009.

Chini, N. & Stansby, P.K. (2012). *"Extreme values of coastal wave overtopping accounting for climate change and sea level rise"*. Coastal Engineering, Volume 65, July 2012, Pages 27-37, ISSN 0378-3839, 10.1016/j.coastaleng.2012.02.009.

Church, J.A., Gregory, J.M., White, N.J., Platten, S.M., and Mitrovica, J.X. (2011). *"Understanding and projecting sea level change"*. Oceanography, 24(2), 130-143.

CIRIA, CUR, CETMEF, (2007). *"The Rock Manual: The Use of Rock in Hydraulic Engineering"*. 2nd edition. CIRIA C683, London.

Clavero, M., Vílchez, M., Pérez, D., Benedicto, M. I., Losada, M.A. (2012) *"An Unified Design Method of Maritime Works against Waves*. Proceedings of 33rd Conference on Coastal Engineering, Santander, Spain, 2012

De Rouck, J. D., Troch, P., Walle, B. V. D., Meer, J. V. D., Damme, L. V., Medina, J. R., Willems, M., Frigaard, P., & Kofoed, J. P. (2001). *"Wave Run-Up on a Rubble Mound Breakwater: prototype measurements versus scale model tests."* Proceedings of the 5th Int. Conf. on the Mediteranean Coastal Environment. National Institute for Marine Science and Technology Coastal Management and Protection Agency.

De Rouck, J., Van de Walle, B., Troch, P., van de Meer, J., Van Damme, L., Medina, J. R., Willems, M., & Frigaard, P. (2007). *"Wave Run-up on the Zeebrugge Rubble Mound Breakwater: Full-Scale Measurement Results Versus Laboratory Results."* Journal of Coastal Research, 23(3), 584-591doi: 10.2112/04-0157A.1

De Waal, J.P. and van der Meer, J.W (1992). *"Wave run-up and overtopping on coastal structures."* ASCE, proc. 23rd ICCE, Venice, Italy, pp. 1758-1771.

Debernard, J., Røed, L. (2008). *"Future wind, wave and storm surge climate in the Northern Seas: a revisit"*. Tellus 60:427–438. doi: 10.1111/j.1600–0870.2008.00312.x

DEXA, (2013). DEXAWAVE A/S., www.dexawave.com, (Website visited May 23, 2013)

DNV (Det Norske Veritas) (2010). *"DNV-OS-J101: Offshore standard: design of offshore wind turbine Structures"*. DNV, Oslo, Norway.

Falcão, A. F. de O. (2010). *"Wave energy utilization: A review of the technologies"*., Renewable and Sustainable Energy Reviews, Volume 14, Issue 3, April 2010, Pages 899-918, ISSN 1364-0321.

Franco, L., de Gerloni, M., van der Meer, J.W., (1994). *"Wave overtopping on vertical and composite breakwaters"*. Proc. 24th International Conference on Coastal Engineering. ASCE, New York, pp. 1030–1044.

Fitzgerald, D.M., Fenster, M.S., Argow, B.A., and Buynevich, I.V. (2008). *"Coastal impacts due to sea level rise"*. Annu. Rev. Earth Planet. Sci. 36:601-647.

Grabemann, I. and Weisse, R. (2008). *"Climate change impact on extreme wave conditions in the North Sea: an ensemble study"*. Ocean Dynamics (2008) 58:199–212

Grinsted, A., Moore, A.J. and Jevrejeva, S. (2010). *"Reconstructing sea level from paleo and projected temperatures 200 to 2100 AD".* Climate Dynamics, 34(4), 461-472.

Glukhovsky, B. H. (1966) *"Issledovanie morskogo vetrovogo volnenia (Study of sea wind waves)"*., Leningrad, Gidrometeoizdat (in Russian).

Goda, Y., (2010). *"Random Seas and Design of Maritime Structures".*, 3rd Edition. World Scientific, Singapore

Goda, Y. (2012). *"Design wave height selection in intermediate-depth waters".* Coastal Engineering, Volume 66, August 2012, Pages 3-7.

Gravelle, G. and N. Mimura, (2008). *"Vulnerability assessment of sea-level rise in Viti Levu, Fiji Islands".* Sustainability Science, 3(2), 171-180.

Günback, A.R., Ergin, A. (1983) *"Damage and repair of Antalya harbor breakwater"*. Proc. Conf. on Coastal Structures, Alexandria, Egypt.

Hald, T. and Frigaard, P.: (2001), *"Forces and Overtopping on 2. Generation Wave Dragon for Nissum Bredning, Phase 3 project, Danish Energy Agency."* Project no: ENS-51191/00 - 0067. AAU

Hamm, L., Pernnard, C., (1997). *"Wave parameters in the nearshore. A clarification."* Coastal Engineering 32, 119–135.

Haugen, J. E. & Iversen, T. (2008). *"Response in extremes of daily precipitation and wind from a downscaled multi-model ensemble of anthropogenic global climate change scenarios".* Tellus A, doi:10.1111/j.1600-0870.2008.00315.x.

Horton, R., Herweijer, C., Rosenzweig, C., Liu, J., Gornitz, V., and Ruane, A.C. (2008). *"Sea level rise projections for current generation CGCMs based on the semi-empirical method".* Geophysical Research Letters, 35, L02715.

IPCC, (2000), Nebojsa Nakicenovic and Rob Swart, *"Emission Scenarios."* Special Report on Emissions Scenarios. Cambridge University Press, UK. pp 570

IPCC, **(**2007). "*Climate Change 2007: The Physical Science Basis. Contribution of Working Group II to the Fourth Assessment Report of the IPCC*." [Solomon, S., D. Qin, M. Manning, Z. Chen, M. Marquis, K.B. Averyt, M. Tignor and H.L. Miller (eds.)]. Cambridge University Press, Cambridge, United Kingdom and New York, NY, USA, 996 pp.

IPCC, (2012), Field, C.B., Barros, V., Stocker, T.F., Qin, D., Dokken, D.J., Ebi, K.L., Mastrandrea, M.D., Mach, K.J., Plattner, G.-K., Allen, S.K., Tignor, M. and Midgley P.M. *"Managing the Risks of Extreme Events and Disasters to Advance Climate Change Adaptation."* Special Report of the Intergovernmental Panel on Climate Change. Cambridge University Press

Isobe, M., (2013) *"Impact of global warming on coastal structures in shallow water."* Ocean Engineering, http://dx.doi. org/10.1016/j.oceaneng.2012.12.032i

Kobayashi, N., de los Santos, F.J. and Kearney, P.G. (2008). *"Time-Averaged Probabilistic Model for Irregular Wave Runup on Permeable Slopes,"* Journal of Waterway, Port, Coastal and Ocean Engineering, ASCE, 134(2), 88-96.

Kont, A., J. Jaagus, R. Aunap, U. Ratas, and R. Rivis, (2008). *"Implications of sea-level rise for Estonia."* Journal of Coastal Research, 24(2), 423-431.

Lander, V., van der Meer, J.W., and Troch, P. (2012). *"Probability distribution of individual wave overtopping volumes for smooth impermeable steep slopes with low crest freeboards"*, Coastal Engineering, Volume 64, June 2012, Pages 87-101, ISSN 0378-3839, 10.1016.

Lambeck, K., C.D. Woodroffe, F. Antonioli, M. Anzidei, W.R. Gehrels, J. Laborel, and A.J. Wright, (2010). *"Paleoenvironmental records, geophysical modeling, and reconstruction of sea-level trends and variability on centennial and longer timescales".* In: Understanding Sea-Level Rise and Variability [Church, J.A., P.L. Woodworth, T. Aarup, and W.S. Wilson (eds.)]. Wiley-Blackwell, Chichester, UK, pp. 61-121.

Larsen, T. (1985). *"Styring af Limfjordens Hydrografi. Konference om Miljø og Produktion, Limfjorden som eksempel"*. Dansk Ingeniørforening. Aalborg 20.-22. maj 1985. (Danish conference paper).

Larsen, T. (2007). *"Climate Change and Closure of Thyborøn Channel"*. Paper presented at Seminar on Coastal Zone Management, Blåvand, Danmark.

Larsen, T., and Beck, J. B. (2009). *"Stormflodsvandstande i Limfjorden ved lukning af Thyborøn Kanal"*. *Stads og Havneingenioeren*, (1), 54-57

Lee, C.E., Kim, S.W., Park, D.H, Suh, K.D. (2013) *"Risk assessment of wave run-up height and armor stability of inclined coastal structures subject to long-term sea level rise"*. Ocean Engineering, ISSN 0029-8018

Longuet-Higgins, M. S. (1952). *"On the Statistical Distribution of the Heights of Sea Waves"*. Journal of Marine Research, 11(3), PP. 245-266.

Mai, S., Wilhelmi, J., and Barjenbruch, U. (2011). *"Wave Height Distributions in Shallow Waters". Coastal Engineering Proceedings, 1* (32)
Margheritini, L., Vicinanza, D., Frigaard, P. (2009). *"SSG wave energy converter: Design, reliability and hydraulic performance of an innovative overtopping device"*. Renewable Energy, 34 (5), pp. 1371-1380.

Margheritini, L., and Nørgaard, J. H. (2012). *"Key Aspects of Wave Energy".* Proceedings of Sustainable Energy and Environmental Sciences (SEES 2012). Singapore.

Martin F. L., Losada, M. A., Medina, R. (1999), *"Wave loads on rubble mound breakwater crown walls"*, Coastal Engineering, Vol. 37, Issue 2, July 1999, p. 149-174

McCowan, J. (1891). *"On the Solitary Wave"*. Philosophical Magazine, 5th Series, Vol 36, pp 430-437

Medina, J. (1998). *"WIND EFFECTS ON RUNUP AND BREAKWATER CREST DESIGN".* Coastal Engineering Proceedings, 1(26). doi:10.9753/icce.v26.

Miche, R. (1944). *"Mouvement ondulatoires de la mer en profondeur constante ou decroissante.",* Annales des Ponts et Chaussees.

Ministeriet for Offentlige Arbejder (1942), *"Foranstaltninger til sikring af Limfjordstangerne og Thyborøn havn og kanal"*. Betænkning fra kommission af 16. april 1937. (Report from commission – in danish).

Mitrovica, J.X., M.E. Tamisiea, E.R. Ivins, L.L.A. Vermeersen, G.A. Milne, and K. Lambeck, (2010). *"Surface mass loading on a dynamic earth: complexity and contamination in the geodetic analysis of global sea-level trends."* In: Understanding Sea-Level Rise and Variability [Church, J.A., P.L. Woodworth, T. Aarup, and W.S. Wilson (eds.)]. Wiley-Blackwell, Chichester, UK, pp. 285-325.

Monk, K., Zou, Q., Conley, D. (2013). "An approximate solution for the wave energy shadow in the lee of an array of overtopping type wave energy converters". Coastal Engineering, Volume 73, March 2013, Pages 115-132

Nicholls, R., Cazenave, A. (2010). *"Sea-level rise and its impact on coastal zones"*. Science 328:1517–1520.

Oumeraci, H., H. Schüttrumpf, J. Möller and M. Kudella (2000). *"Large scale model tests on wave overtopping with natural sea states."* LWI-Bericht Nr. 852.

Oyster, (2013). Aquamarine Power., www.aquamarinepower.com, (Website visited May 23, 2013)

Palha, A. Mendes L., Fortes C.J, Melo A.B, and Sarmento A. (2010). *"The impact of wave energy farms in the shoreline wave climate: Portuguese pilot zone case study using Pelamis energy wave devices."* Renewable Energy, 35(1), p.62-77.

Pedersen, J. (1996). *"Wave Forces and Overtopping on Crown Walls of Rubble Mound Breakwaters".* PhD thesis, Series paper 12, ISBN 0909-4296, *Hydraulics & Coastal Engineering Lab.*, Dept. of Civil Engineering, Aalborg University, Denmark.

Pelamis, (2013). Pelamis Wave Power Ltd., www.pelamiswave.com, (Website visited May 23, 2013)

Pérez, D., M. Correa, M. Ortega-Sánchez, M. Clavero, M. A. Losada. (2010). *"Pressure distributions on a vertical breakwater: experimental study and scale effects*. Proceedings of 32nd Conference on Coastal Engineering, Shanghai, China.

Pullen, T., Allsop, W., Bruce, T., Kortenhaus, A., Schuttrumpf, H. & van der Meer, J. (2007). *"Wave overtopping of sea defenses and related structure: Assessment manual". www.overtopping-manual.com*

Putz, R., R. (1952). *"Statistical distributions of sea waves"*. Trans. Amer. Geophys. Union 33, pp. 685-692

Rahmstorf, S., (2007). *"A semi-empirical approach to projecting future sea-level rise".* Science, 315(5810), 368-370.

Ranasinghe, R., R. McLoughlin, A. Short, and G. Symonds, (2004). *"The Southern Oscillation Index, wave climate, and beach rotation".* Marine Geology, 204(3-4), 273-287.

Riedel, H., & Byrne, A. (1986). *"RANDOM BREAKING WAVES HORIZONTAL SEABED"*. Coastal Engineering Proceedings, 1(20).

Ruol, P., Zanuttigh, B., Martinelli, L., Kofoed, J. P., and Frigaard, P. (2011). *"Near-Shore Floating Wave Energy Converters: applications for coastal protection."* I Smith, J. M., & Lynett, P. (red.), Coastal Engineering 2010: Proceedings of the 32nd International Conference on Coastal Engineering.

Schüttrumpf, H.F.R., (2001). *"Wellenüberlaufströmung bei See-deichen"*, PhD-thesis, Technical University Braunschweig.
Schüttrumpf, H., Van Gent, M.R.A., (2003). *"Wave overtopping at seadikes"*. ASCE, Proc. Coastal Structures 2003, pp. 431–443.

Sheppard, C., D.J. Dixon, M. Gourlay, A. Sheppard, and R. Payet, (2005). *"Coral mortality increases wave energy reaching shores protected by reef flats: Examples from the Seychelles".* Estuarine Coastal and Shelf Science, 64(2-3), 223-234.

Steendam, G.J., Zanuttigh, B., Prinos, P., Lopez Lara, J., Andersen, T.L. (2010). *Overtopping resistant and overwashed dikes: Part E. I: THESEUS Deliverable OD 2.1: Integrated Inventory of Data and Prototype Experience on Coastal Defenses and Technologies"*. European Commission.

Steendam, G.J., Peeters, P., van der Meer, J.W., Van Doorslaer, K., Trouw, K. (2011). *"Destructive wave overtopping tests on Flemish dikes."* ASCE, Proc. Coastal Structures 2011, Yokohama, Japan

STOWASUS-project (1998). *"Regional storm, wave and surge scenarios for the 2100 century"*. Project year 1997 – 1998. Funded by the European commision. Contract no. ENV4-CT97-0498. Coordinator, Eigil Kaas, DMI

Stratigaki, V., P. Troch, J. Degroote (2011). *"Numerical modelling of wake effects of a farm of Wave Energy Converters: computational performance evaluation".* In proceeding of: Fifth International Conference on Advanced COmputational Methods in ENgineering (ACOMEN 2011), At Liège, Belgium

Tamura, T., K. Horaguchi, Y. Saito, L.N. Van, M. Tateishi, K.O.T. Thi, F. Nanayama, and K. Watanabe, (2010). *"Monsoon-influenced variations in morphology and sediment of a mesotidal beach on the Mekong River delta coast."* Geomorphology, 116(1-2), 11-23.

Technical Advisory Committee for Water Retaining Structures (TAW) (2002) (May). *"Technical Report—Wave Run-up and Overtopping at Dikes."* The Netherlands.

Tedd, J. (2007). *"Testing, Analysis and Control of Wave Dragon, Wave Energy Converter"*, PhD-Thesis defended in public at Aalborg University.

THESEUS, (2013). "*Innovative technologies for safer European coasts in a changing climate*", www.theseusproject.eu, funded by the European Commission within FP7-THEME 6 - Environment, including climate, grant 244104

Troch, P., De Somer, M., De Rouck, J., Van Damme, L., Vermeir, D., Martens, J.P., and Van Hove, C. (1996). *"Full Scale Measurements of Wave Attenuation Inside a Rubble Mound Breakwater."* Proc. ICCE'96, ASCE, 1916-1929.

Trung, L.H. van der Meer, J.W., Verhagen, H.J. (2012). *"Wave overtopping simulator tests on sea dikes in Viet Nam"*. ASCE, Proc. ICCE 2012, Santander, Spain.

U.S. Army Corps of Engineers. (2002). *"Coastal Engineering Manual"*. Engineer Manual 1110-2-1100, U.S. Army Corps of Engineers, Washington, D.C. (in 6 volumes).

Vandermeerconsulting (2013). www.vandermeerconsulting.com. Van der Meer Consulting B.V., Coastal Engineering Consultancy & Research. (Website visited May 17, 2013)

Van der Meer, J.W. (1988). *"Rock slopes and Gravel Beach under Wave Attack".* PhD Thesis. Graficheverzoging Waterlookpkundig Laboratorium, 1988, 162 pages.

Van der Meer, J.W. and Stam, C.J.M (1992). *"Wave run-up on smooth and rock slopes".* ASCE, Journal of WPC and OE, Vol. 188, No. 5, pp. 534-550, New York. Also Delft Hydraulics Publication No. 454

Van der Meer, J.W., Janssen, J.P.F.M., (1994). *"Wave run-up and wave overtopping at dikes".* Wave Forces on Inclined and Vertical Wall Structures. ASCE, pp. 1–27 (Also Delft Hydraulics Publication number 485).

Van der Meer, J.W., (1995). *"Conceptual design of rubble mound breakwaters. World Scientific".* In: Advances in Coastal and Ocean Engineering, Volume 1. Ed. P.L.F. Liu, pp. 221-315

Van der Meer, J.W., Snijders, W., Regeling, E., (2006). *"The wave overtopping simulator."* ASCE, Proc. ICCE 2006, San Diego, pp. 4654–4666.

Van der Meer, J.W, Verhaeg, H., Steendam, G.J., (2009). *"The new wave overtopping database for coastal structures."* Coastal Engineering 56 (2), pp. 108-120.

Van der Meer, J.W., Hardeman, B., Steendam, G.J., Schttrumpf, H., Verheij, H., (2010). *"Flow depths and velocities at crest and inner slope of a dike, in theory and with the wave overtopping simulator."* ASCE, Proc. ICCE 2010, Shanghai.

Van der Meer, J.W., Provoost, Y. and Steendam, G.J. (2012). *"The wave run-up simulator, theory and first pilot test."* ASCE, Proc. ICCE 2012, Santander, Spain

Van Gent, M.R.A., (2001). *"Wave Runup on Dikes with Shallow Foreshores".* Journal of Waterway, Port, Coastal, and Ocean Engineering 2001 127:5, 254-262

Van Gent, M.R.A., (2002). *"Wave overtopping events at dikes".* World Scientific, Proc. ICCE 2002, Cardif, Vol.2, pp. 2203–2215

Van Gent, M.R.A, Smale, A., Kuiper, C. (2003). *"Stability of rock with shallow foreshores"*. Proc. Of fourth international coastal structure conference. Portland, ASCE, Reston, 2003

Van Gent, M.R.A., van den Boogaard, H.F.P., Pozueta, B., Medina, J. R. (2007), *"Neural network modelling of wave overtopping at coastal structures".* Coastal Engineering, Volume 54, Issue 8, August 2007, Pages 586-593.

Venugopal, V. and Smith, G., (2007). *"Wave climate investigation for an array of wave power devices."* In Proceedings of the 7th European Wave and Tidal Energy Conference. IST/IDMEC.

Verhaeghe, J., Van der Meer, J.W, Steendam, G.J, Besley, P., Franco, L., Van Gent, M.R.A., (2003). *"Wave overtopping database as the starting point for a neural network prediction method."* Proceedings of Coastal Structures 2003. ASCE, pp. 418-430.

Verhagen, H.J., Van Vledder, G.P., Eslami Arab, S. (2008). *"A practical method for design of coastal structures in shallow water"*. Coastal Engineering 2008: Proceedings of the 31th International Conference, Hamburg, Germany, 31 August - 5 September 2008

Vermeer, M. and Rahmstorf, S. (2009): *"Global sea level linked to global temperature"*. Proceedings of the National Academy of Science of the USA, 106, 21527-21532.

Vicinanza, D., Contestabile, P., Ferrante, V., Stagonas, D., Müller, G., Lykke Andersen, T., Nørgaard, J. H., & Frigaard, P. (2012*a*). *"Innovative Seawalls and Rubble Mound Breakwater Design for Wave Energy Conversion."* 33 Conference of Hydraulics and Hydraulic Engineering, Brescia, Italy, 2012.

Vicinanza, D., Stagonas, D., Müller, G., Nørgaard, J. H., & Lykke Andersen, T. (2012*b*). *"Innovative Breakwaters Design for Wave Energy Conversion."* Coastal Engineering conference, Santander, Spain, 2012. American Society of Civil Engineers. (Proceedings of the International Conference on Coastal Engineering; 33).

Vicinanza, D., Nørgaard, J. H., Contestabile, P., & Lykke Andersen, T. (2013). *"Wave loadings acting on Overtopping Breakwater for Energy Conversion."* Proceedings of the 12th international coastal symposium, Plymouth, Great Britain.

Vining, J.G. and Muetze, A. (2007), *"Governmental Regulation of Ocean Wave Energy Converter Installations,"* Industry Applications Conference, 2007. 42nd IAS Annual Meeting. Conference Record of the 2007 IEEE , vol., no., pp.749,755, 23-27 Sept. 2007

Ward, D. L., Wibner, C. G., Zhang, J., and Edge, B. (1994). *"Wind Effects on Run-up and Overtopping." Proc. ICCE'94,* ASCE, 1687-1699.

Ward, D. L., Zhang, J.,Wibner, C. G. and Cinotto, CM. (1996). *"Wind Effects on Run-up and Overtopping of Coastal Structures."* Proc. ICCE'96, ASCE, 2206-2215.

WaveDragon, (2013). Wave Dragon ApS., www.wavedragon.net, (Website visited May 23, 2013).

WAVEPLAM, (2009). *"State of the Art Analysis - A Cautiously Optimistic Review of the Technical Status of Wave Energy Technology"*. Funded under the Intelligent Energy Europe Programme. Contract number: EIE/07/038/SI2.466832

WAVESTAR, (2013). Wave Star A/S., www.wavestarenergy.com, (Website visited May 23, 2013).

Winter, R. C*.,* A. Sterl*, and* B. G. Ruessink (2013). "*Wind extremes in the North Sea Basin under climate change: An ensemble study of 12 CMIP5 GCMs".* J. Geophys. Res. Atmos*.,* 118*,* 1601–1612.

Zanuttigh, B., Martinelli, L., Castagnetti, M., Ruol, P., Kofoed, J. P., & Frigaard, P. (2010). *"Integration of Wave Energy Converters into Coastal Protection Schemes."* In Proceedings of the 3rd International Conference and Exhibition on Ocean Energy: ICOE 2010

Zanuttigh, B. (2011). *"Coastal flood protection: What perspective in a changing climate? The THESEUS approach"*. Environmental Science & Policy, Volume 14, Issue 7, November 2011, pp. 845-863

Zanuttigh, B., and Angelelli, E. (2012). *"Experimental investigation of floating wave energy converters for coastal protection purpose"*. Coastal Engineering. December 2012.

Zhang, K., Douglas, B.C. and Leatherman, S. P. (2004). *"Global warming and coastal erosion".* Climatic Change, 64(1-2), 41-58.